Structure - Function

Relationship of Viral Coat Proteins

A Site-Directed Spectroscopic Study

of M13 Coat Protein

David Stopar

Structure-Function

Relationship of Viral Coat Proteins

A Site-Directed Spectroscopic Study
of M13 Coat Protein

David Stopar

Proefschrift

Statements

1. The fact that virtually all the protein side-chain interactions are between different subunits in the coat protein array, rather than within subunits, makes M13 major coat protein a useful model system for studies of interactions between α-helix subunits in a macromolecular assembly.

Marvin, D.A., Hale, R. D., Nave, C., & Citterich, M. H.(1994) *J. Mol. Biol. 235*, 260-286.

2. The process by which filamentous phages are concomitantly assembled and secreted across the cell membranes is likely to involve a series of protein-protein interactions that are accessible to genetic analysis.

Russel, M. (1993) *J. Mol. Biol. 231*, 689-697.

3. Because our knowledge of physical and chemical systems is based on statistical analysis of models derived from repeatable experiments, all insignificant results are ignored. Thus, a single random DNA mutation would be regarded as unrepetable and insignificant, although it has all the potentials to be amplified to an extent that determines the fate of the entire system.

Eigen, M., & McCaskill, J. (1988) *J. Phys. Chem. 92*, 6881-6891.

4. Experimental work should be guided and directed by the writing, inasmuch as; the more you write, the more you know what are you looking for, and the better you understand the significance and relevance of what you find.

5. Physicists tend to strive for simplicity and quantitative predictions, while biologists are more intent on synthesizing many interrelated phenomena in order to understand complex systems.

Glanz, J. (1996) *Science 272*, 646-648.

6. To the trained eye, protein patterns are as pleasing as the lines of a Mondrian painting or the Verranzo-Narrows Bridge.

7. All historical facts come to us as a result of interpretative choices made by historians, influenced by the moral standards of their environment.

8. It is always pleasant to retire in the realm of poetry.

9. Statements taken out of the context are prone to lead to a misconception.

Statements are part of the PhD Thesis entitled: "Structure-function relationship of viral coat proteins; a site-directed spectroscopic study".

David Stopar,

Wageningen, August 1997

Prologue

In this thesis the results are discussed of research carried out at the Department of Molecular Physics at the Wageningen Agricultural University . This research was to a great extent improved by a cordial assistance of many different people involved. My very special thanks go to promoter Prof. dr. T. J. Schaafsma, co-promotor dr. Marcus A. Hemminga, Prof. dr. France Megusar, Ruud Spruijt, and Cor Wolfs for their tireless tutorial help during PhD learning period.

Part of the research presented in this thesis has been done together with the group of Derek Marsh at the Max-Planck-Institut für biophysikalische Chemie, Göttingen. I have appreciated very much their genuine scientific spirit. I would also like to acknowledge the stimulating contributions of the colleagues and students at the Department of Molecular Physics (at the Wageningen Agricultural University).

Finally, I wish to record my deep gratitude to my wife Majda for her understanding and generous assistance she has provided at all stages of the challenging task of producing this thesis.

Contents

Abbreviations

A25C	major coat protein mutant; alanine 25 was replaced with cysteine
A49C	major coat protein mutant; alanine 49 was replaced with cysteine
A_{280}	absorption at 280 nm
ANS	1-anilino-napthalene-8-sulfonate
$2A_{max}$	outer hyperfine splitting
B_1	microwave amplitude
CD	circular dichroism
CL	cardiolipin
cmc	critical micellar concentration
CTAB	cetyltrimethylammonium-bromide
DDM	n-dodecyl β-D-maltoside
DLPC	L-α-phosphatidylcholine dilauroyl
DOPC	1,2-dioleoyl-*sn*-glycero-3-phosphocholine
DOPG	1,2-dioleoyl-*sn*-glycero-3-phosphoglycerol
DTNB	5,5'-dithio-bis-(2-nitrobenzoic acid)
EDC	1-Ethyl-3-[3-(dimethylamino)propyl]carbodiimide·HCl
EDTA	ethylene-diamine-tetraacetic acid
ESR	electron spin resonance
γ	electron gyromagnetic ratio
G38C	major coat protein mutant; glycine 38 was replaced with cysteine
HPSEC	high-performance size exclusion chromatography
IAEDANS	N-[[(iodoacetyl)amino]ethyl]-1-sulfonaphthylamine
L/P	lipid to protein molar ratio
MML	L-α-monomyristoyl lecithin
5-MSL	3-maleimido-2,2,5,5-tetramethylpyrrolidine-*N*-oxyl
Mw	molecular weight
NMR	nuclear magnetic resonance
n-PCSL	1-acyl-2-[n-(4,4-dimethyloxazolidine-*N*-oxyl)stearoyl]-*sn*-glycero-3-phosphocholine
n-SASL	n-(4,4-dimethyloxazolidine-*N*-oxyl)stearic acid
RPM	rotations per minute
S	order parameter
S50C	major coat protein mutant; serine 50 was replaced with cysteine
SDS	sodium dodecyl sulphate
SDS-PAGE	sodium dodecyl sulfate poly acrylamide gel electrophoresis

SL	spin label
ST-ESR	saturation transfer electron spin resonance
T36C	major coat protein mutant; threonine 36 was replaced with cysteine
T46C	major coat protein mutant; threonine 46 was replaced with cysteine
τ_c	rotational correlation time
Tris HCl	tris(hydroxymethyl)aminomethane
TS	4-octadecanoyl-2,2,6,6-tetramethylpiperidine-N-oxyl
T_1	spin-lattice relaxation time
T_2	spin-spin relaxation time
UV	ultra violet

Key words in the PhD Thesis: bacteriophage M13, coat protein environment, coat protein local structure, site-directed mutagenesis, ESR spectroscopy, paramagnetic relaxation, fluorescence spectroscopy, CD spectroscopy, protein-lipid interactions, membrane-mimicking systems, protein membrane location, S-form phage, virus disassembly, virus assembly.

Chapter 1

Introduction

General Introduction

A challenging question in bacteriophage biology is how bacteriophages utilize the biophysical properties of the host plasma membrane to pass this cell barrier. In general, bacteriophages use the receptor properties of the membrane, and trigger a sequence of processes enabling them to transfer their genetic information into a host cell. The large number of possible mechanisms of how bacteriophages surpass membrane barrier has been only partly elucidated on a detailed biophysical level. Filamentous bacteriophages are particularly exciting in this respect, because they can enter and leave the plasma membrane without lysis of the host cell. How they carry out this on the molecular level, and what kind of protein-protein or protein-lipid interactions play an initial or catalytic role, is not known. Among the proteins of bacteriophages, the major coat protein of bacteriophage M13 has been used extensively to address the questions above. In this thesis, the structural properties of the major coat protein of the bacteriophage M13, that can have a stable association with different model membrane systems, will be discussed.

Bacteriophage M13

M13 is a small filamentous *Escerichia coli* specific bacteriophage that consists of approximately 2800 copies of coat protein molecules protecting the circular single-stranded DNA (Marvin & Hohn, 1969; Newman et al., 1977; Banner et al., 1981; Rasched & Oberer, 1986). The virus particle is about 6.5 nm in diameter with a length dependent on the length of the enclosed genome (Marvin, 1990). A large fraction (98%) of the virus coat is made up of gene 8 product (gp8) that forms a 1.5-2.0 nm thick, flexible cylinder around the virus genome (Makowski, 1994). Since, gp8 is the most abundant product of the small virus genome, it is often referred to as the major coat protein. On the distal end of the virus particle, that is assembled first, there are five copies each of gp7 and gp9 minor coat proteins. At the proximal end of the virus, which enters the host cell, there are five copies each of gp3 and gp6 minor coat proteins (Simons et al., 1981; Lopez & Webster, 1983). The gp3 protein is involved in binding to the F-pilus of the host cell, which is the first step

1

① outer membrane ②

periplasm
inner membrane gp4 gp4 gp7 + gp9 gp8 gp4 gp4 gp8

cytoplasm
thioredoxin phage DNA packaging signal

DNA + V

initiation

③ ④

gp3
gp6

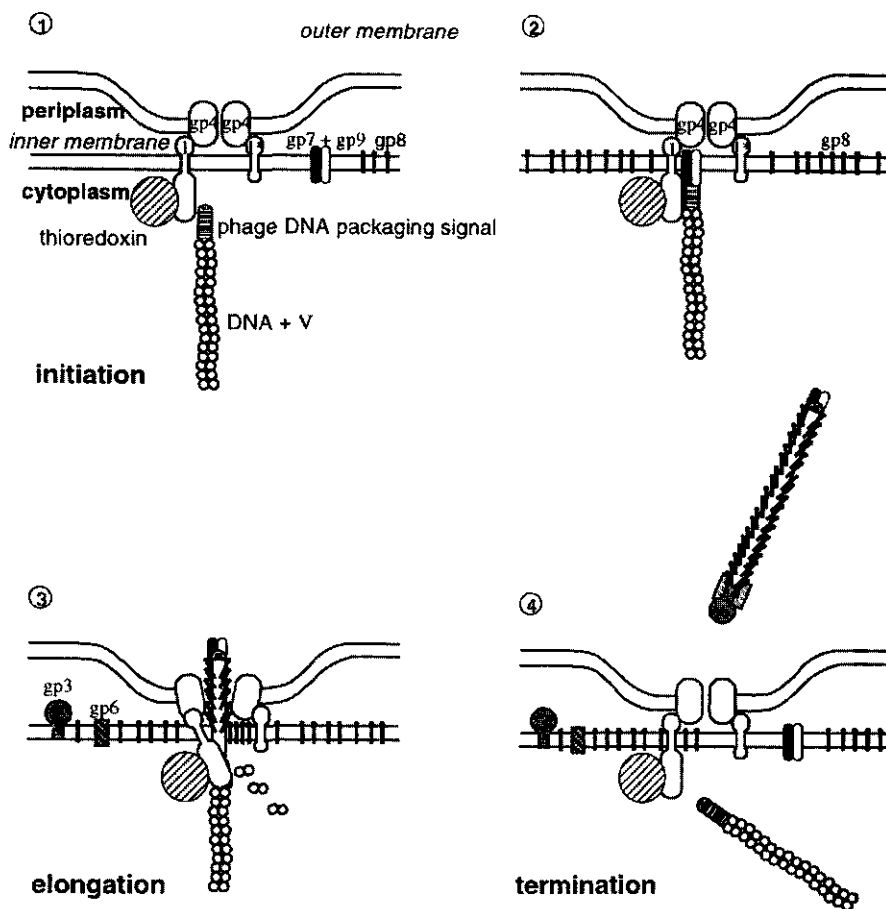**elongation** **termination**

FIGURE 1: Schematic illustration of the assembly of bacteriophage M13. At the assembly site the gp4 proteins constitute an extrusion channel through the outer *E. coli* membrane. The gp1 and gp1* proteins are assumed to form an extrusion channel in the cytoplasmic membrane. The viral proteins gp7, gp9 and at least one host protein (thioredoxin) are necessary for the initation of the virus assembly process. During assembly the major coat protein gp8 first interacts with the gp1 protein and then interacts with the viral DNA and previously added major coat protein on the extruding particle. The gp5 protein is released as a dimer in the cytoplasm. Assembly is terminated when gp6 and gp3 are added. Steps 1 and 2 depict initial interactions of the assembly of the new phage, in step 3 elongation and extrusion takes place, in step 4 the assembly is completed and new cycle can begin. After Russel (1991) and Hemminga et al. (1993).

2

in the infection process (Gläser-Wüttke et al., 1989). During virus disassembly, gp6 and gp3 are released from the entering virus particle exposing the major coat proteins to the host cytoplasmic membrane (Webster & Lopez, 1985). The major coat proteins are subsequently dissolved in the cytoplasmic membrane, while the DNA is released in the cytoplasm where it is replicated using the host cell machinery (Pratt et al., 1969). Newly replicated DNA is coated with gp5 protein, and synthesis of new virus proteins exploiting the existing host protein producing machinery begins (Webster & Lopez, 1985; Rasched & Oberer, 1986; Model & Russel, 1988). The newly synthesized coat proteins are inserted in the cytoplasmic membrane, where they are stored before used in the assembly process (Mandel & Wickner, 1979). Assembly of a new virus is taking place in the host membrane, where both host and virus proteins are involved (Bayer & Bayer, 1986; Brissette & Russel, 1990; Russel, 1991). As depicted in Fig. 1, assembly is initiated by gp7 and gp9 proteins, which interact with the viral DNA. However, the main process during assembly of the new virus particle is replacement of gp5 protein that protects the viral DNA in the host cytoplasm with the major coat protein, which protects viral DNA outside the cell. Assembly of the virus is terminated with addition of the gp3 and gp6 proteins (Makowski, 1992). The newly formed virus is extruded from the *E. coli* without lysis of the host (Hofschneider & Preuss, 1963).

M13 bacteriophage, as well as the closely related fd and f1 phages, have an important role in molecular biology and molecular physics that extends far beyond their own life cycle. There are a number of practical reasons why M13 is so widely used as part of protocols for DNA sequencing, generating radiolabeled DNA probes for hybridization, site-directed mutagenesis (Kuhn et al., 1986; Sambrook et al., 1989), foreign peptide display on the phage particle (Smith, 1993), model system for protein-lipid interactions, model system for protein translocation, and model system for macromolecular assembly (Russel, 1991; Hemminga et al., 1993; McDonnell et al., 1993). The main reason, however, is ability of the bacteriophage to produce large numbers of progeny, providing an ample amount of biological material. This is possible, because the replication of the bacteriophages occurs in harmony with the host. The infected cells are not lysed, but continue to grow (albeit at one half to three quarters of the normal rate), while producing up to 1000 viruses per cell (Marvin & Hohn, 1969). Together with the relative ease of DNA and major coat protein isolation, this makes M13 a very interesting biophysical model system. Many of the above mentioned applications of the M13 bacteriophage are a direct consequence of the architecture of the virus particle, and in particular the structure and function of the M13 major coat protein.

3

M13 Major Coat Protein

In this thesis, interactions of the M13 major coat protein with membrane-mimicking model systems are studied in more detail. The major coat protein is a small multi-functional protein, composed of 50 amino acids (Van Wezenbeek et al., 1980). Its primary structure is given in Fig. 2, and must be such to allow stable protein-protein and protein-DNA interactions in the virus particle, but fast solubilization in the host membrane during phage disassembly. It should also provide a stable thermodynamical association with the host membrane, where the proteins are stored before the assembly in the new virus particle.

In addition, the protein sequence should have information for insertion of all newly synthesized major coat proteins in the host cytoplasmic membrane. For this later purpose, the major coat protein has an extra leader sequence consisting of 23 amino acid, which is cleaved off after insertion of the protein in the membrane (Chang et al., 1978; Mandel & Wickner, 1979). Finally, the parental and the newly synthesized major coat protein should leave the membrane during assembly in the new virus particle (Trenkner et al., 1967; Smilowitz, 1974).

For all the molecular interaction mentioned above, the primary sequence of the major coat protein is surprisingly small (Mw = 5238 Da). It represents a very efficient structural compromise, which is capable of protein-DNA, protein-protein and protein-lipid interactions (Hemminga et al., 1993). To accomplish all this, the major coat protein has three domains: a positively charged C-terminal domain, which primarily is responsible for the interaction with DNA; a hydrophobic central part of the protein which stabilize protein-protein interactions in the virus particle as well as maintains a stable thermodynamic association with the host membrane during replication; and an amphiphatic N-terminal domain, which probably is important in docking of the protein to the virus assembly site, as well as in keeping a low isoelectric point of the virus particle in the solution (Marvin et al., 1994).

To accompany an extreme change in environment and different structural functions during the replication cycle, the secondary structure of the major coat protein is almost certain to change. The protein secondary structure in the phage particle is characteristic for a single continuos, slightly curved α-helix extending from the N-terminus to the C-terminus (Cross & Opella, 1985; Marvinet al., 1994; Griffith et al., 1981) have found that upon addition of chloroform, the long filament structure contracts to a spherical form (S-form). Since the protein conformation in the S-form was very unstable in contrast to a very stable phage structure, and also part of the viral DNA was ejected outside the

4

Predicted domains   Primary structure   Secondary structure

	1	N-Ala
		Glu -
		Gly
		Asp -
Acidic	5	Asp -
		Pro
		Ala
		Lys +
		Ala
N-terminal	10	Ala
		Phe
		Asn
		Ser
		Leu
Domain	15	Gln
		Ala
		Ser
		Ala
		Thr
	20	Glu -
		Tyr
		Ile
		Gly
		Tyr
	25	Ala
		Trp
Hydrophobic		Ala
		Met
		Val
	30	Val
		Val
Domain		Ile
		Val
		Gly
	35	Ala
		Thr
		Ile
		Gly
		Ile
	40	Lys +
		Leu
Basic		Phe
		Lys +
		Lys +
C-terminal	45	Phe
		Thr
		Ser
Domain		Lys +
		Ala
	50	Ser-C

Amphi-

pathic
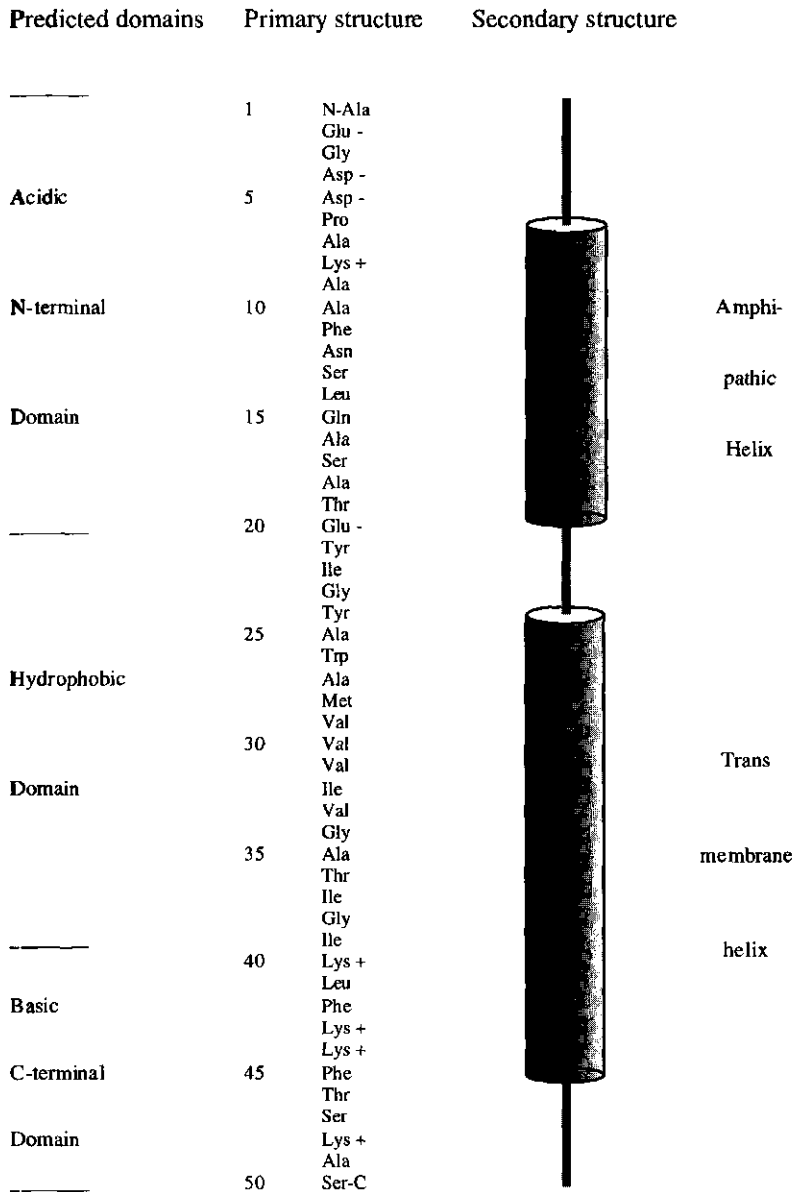
Helix

Trans

membrane

helix

FIGURE 2: Primary structure of the bacteriophage M13 major coat protein (Van Wezenbeek et al., 1980). The secondary structure of the major coat protein solubilized in SDS (Van de Ven et al., 1993; McDonnell et al., 1993). Two boxed regions represent a transmembrane and amphiphatic helix. The hydrophobic calculation and domain assignment is according to the prediction method of Kyte and Doolite (1982)

5

structure, these authors suggested that the S-form might be involved in the phage disassembly (Griffith et al., 1981; Manning & Griffith, 1985). There is relatively little structural information about protein in the S-form (Roberts & Dunker, 1993; Khan et al., 1995). During phage disassembly, however, the major coat protein is incorporated into the host membrane (Smilowitz, 1974). The secondary structure in the membrane has been determined in different micellar model systems (Nozaki et al., 1976; Nozaki et al., 1978; Spruijt et al., 1989; Spruijt & Hemminga, 1991; McDonnell et al., 1993; Van de Ven et al., 1993; Papavoine et al., 1994). In these model systems, the major coat protein has two well-defined states; an α-helical conformation, where the major coat protein has an ability to undergo a reversible aggregation, and a β-polymeric state, where the major coat protein is irreversibly aggregated (Fodor et al., 1981; Hemminga et al., 1992; Sanders et al., 1993; Wolkers et al., 1995). The *in vivo* state of the membrane-bound major coat protein has not been elucidated yet. However, based on the reversibility of the processes, where the major coat protein is involved during phage replication cycle, it is likely that an α-helical conformation is the functional membrane-bound state (Hemminga et al., 1993). The α-helical conformation has been characterised with NMR in SDS micelles, where the major coat protein has two helices; an amphiphatic N-terminal helix from residue 6-20 which is connected by a flexible loop to the transmembrene helix from residue 24-45 (see also Fig. 2) (McDonnell et al., 1993; Van de Ven et al., 1993; Papavoine et al., 1997). Although, the secondary structure of the major coat protein in the micelles is well characterised, the protein structure and topography in lipid bilayers is poorly identified.

Protein-Lipid Interactions

The protein-lipid interface is characterized by the configuration of the lipid chains, interaction of the polar head groups of the lipids with protein residues, secondary structure of the protein, overall conformation of the protein, and the state of oligomerization in the membrane (Marsh, 1990; Stubbs & Williams, 1992). The interactions of the bacteriophage M13 major coat protein with lipids can have a pronounced effect on the structure and function of the protein (Spruijt & Hemminga, 1991). Some of these effects arise from general physiochemical properties of the lipid environment such as, lipid composition, fluidity, membrane curvature, protein to lipid molar ratio, while others may be induced by protein-lipid selectivity and specificity, or by protein-lipid hydrophobic mismatch (Hemminga et al., 1993). Although the small single transmembrane spanning helix of the M13 major coat protein has been extensively used as a model system for protein-lipid

6

interactions, many of the important questions about the protein structure in the membrane-like environment remain unsolved.

Because of the inherent complexity of the *E. coli* cytoplasmic membrane, simplified membrane model systems have to be used to study molecular details of the major coat protein-lipid interactions. Two widely accepted membrane model systems for biophysical studies are detergent micelles and lipid bilayers (Tanford & Reynolds, 1976). Bilayers, generally are constructed from double-chain amphiphiles, that is from molecules which have two hydrocarbon chains attached to a single polar head group (Cantor & Schimmel, 1980). On the other hand, single-chain amphiphiles do not make bilayers but form micelles instead, which are globular aggregates with polar groups exposed to the surface and hydrocarbon part in the micelle interior (Helenius & Simons, 1975; Helenius et al., 1979). The micellar systems generally provide a favourable hydrophobic environment for the membrane proteins that in addition can be relatively easy experimentally studied (Tanford, 1972). However, lipid bilayers are more appropriate to mimic the typical structure of a biological membrane, due to its well characterised structure-function relationship (Cantor & Schimmel, 1980).

The experimental approach used to study the molecular details of protein-lipid interactions usually involves different magnetic resonance and optical spectroscopy techniques (Hemminga et al., 1992). The choice of the spectroscopic method to be employed in the study of protein-lipid interactions is dominated by: rates and amplitudes of the molecular motion in question; time-scale of the motion being investigated; and type or nature of the sample available (Watts, 1987). The sample preparation and nature of the sample may often restrict the choice of the spectroscopic method. For example, magnetic resonance experiments require rather large amounts of protein, typically 1-50 mg, which is very high as compared to some types of biochemistry, molecular biology, or optical spectroscopic experiments (Watts, 1993).

In any case little useful biochemical information will be gained from studies of protein-lipid interactions that involve a denatured or inactive protein. The only real criterion that the information being obtained is of direct relevance to the physiological situations, is to show that the protein is active (Watts, 1993). This may be simple to test in the case of proteins that posses a chromatophore, where the absorption spectrum is a sensitive measure of the protein conformation and activity. However, it is very difficult with structural proteins such as M13 major coat protein, which have no measurable biochemical activity. In the case of the major coat protein-lipid system, the samples should be checked for structural features such as α-helix or β-sheet content, and protein aggregational properties (Hemminga et al., 1993). Since the β-polymeric state of the major coat protein is considered as a denatured

7

form, samples with the β-polymeric state present were not used in this thesis, unless otherwise stated.

Most of what we know about molecular details of protein-lipid interactions comes from the study of labeled lipids (Marsh, 1981; Devaux & Seigneuret, 1985). This is mainly due to the fact that reporter lipid molecules are relatively easy to synthesize and manipulate for the purpose of different spectroscopic techniques, as compared to membrane proteins. For example, the bacteriophage M13 major coat protein was used in these type of studies mainly as a factor influencing lipid conformation and dynamics (Datema et al., 1987; Wolfs et al., 1989; De Jongh et al., 1990). On the other hand, much less information is available about the major coat protein structure changes induced by different lipids. With the new developments in the membrane molecular biology, site-directed labeling is now available which allows one to probe protein structure very specifically (Altenbach et al., 1990; Hubbell & Altenbach, 1994; Wolkers et al., 1997). This is expected to significantly increase our understanding of the protein behaviour in the lipid environment, and will give us a new insight in the protein-lipid interactions, because the main emphasis in the protein-lipid interaction can now be focused on the protein. In the following, this is discussed in more detail. Information on the production of the major coat protein mutants for site-directed labeling is given first, and then the different spectroscopic techniques used in this thesis are considered.

Site-Directed Major Coat Protein Labeling

It is well established that the composition of biological macromolecules defines its structure and ultimately, through the motion of specific groups its function. Information gained from site-directed labeling of membrane proteins, for example, may provide such a direct link between structure and function (Watts, 1993). The M13 coat protein does not contain a suitable site for site-specific labeling of the protein molecule for either ESR or fluorescence purposes. Therefore the approach of site-directed mutagenesis was followed in this thesis (Sambrook et al., 1989). A desired amino acid in the major coat protein primary sequence was replaced for a cysteine residue which was labeled with either a maleimido spin label for the purpose of ESR spectroscopy, or IAEDANS for the purpose of fluorescence spectroscopy. Care was required, however, in the design of the mutations to avoid non-functional proteins. Selection for viable mutant bacteriophage in the absence of any protein biochemical activity ensured the choice of functional mutant major coat proteins. Mutations of the M13 major coat protein did not include replacements of any charged or aromatic amino acid residues which apparently cause lethal mutations (Marvin et al., 1994).

8

Mutants were located in different topological domains of the coat protein, i.e., membrane-embedded positions as compared to positions in the aqueous phase. Since ESR experiments require rather large amounts of protein, typically 1-5 mg per sample, only mutants which could be grown to milligram quantities were selected.

Electron Spin Resonance (ESR)

ESR employing spin labels is an extremely specific magnetic resonance technique in its application, because it looks only to those systems that contain the unpaired electron. (Knowles et al., 1976). In the absence of any intrinsic ESR signal, labeling of the major coat protein cysteine mutants with a maleimido spin label enables one to use spin label ESR spectroscopy to study specific environments of the proteins within membranes and at the water-membrane interface. The spin-labeled proteins are sensitive to molecular motions on the time scale determined by the ^{14}N hyperfine splitting anisotropy of the nitroxide radical, typically in the nano second domain. It is this spectral anisotropy which has made spin label ESR such a powerful tool in the study of protein molecular motions (Marsh, 1981). The hyperfine splittings of the nitroxide spin labels are partially averaged by the anisotropic motion of the protein side chain, which gives a measure of the motional amplitude. The line widths in the spectrum are differentially broadened by an extent, which depends on the rate of molecular motion. Other important features of spin label spectra are the broadening by intermolecular spin label interactions, and the ability to detect compartementation of the spin label by accessibility to different relaxation agents (Berliner, 1976). A detailed description of the quantum mechanical basis of electron spin resonance can be found in many comprehensive review articles (Marsh, 1982; Hemminga, 1983; Marsh, 1985) and excellent books (Berliner, 1976; Knowles et al., 1976; Berliner, 1979; Berliner & Reuben, 1981; Poole, 1983).

With the recent progress in molecular biology, relatively versatile schemes are now available for spin label attachments to the protein. Analysis of the dynamics of the spin-labeled proteins can be used to determine the topography of the polypeptide chain and the electrostatic potential at any surface site. Such an analysis can also identify regular secondary structure elements and determine their orientation in the protein, measure the distance between two sites bearing a spin label, identify sites of tertiary interactions, and investigate structural changes through the time-dependence of the above parameters (Hubbell & Altenbach, 1994; Marsh, 1994).

9

In this thesis, spin-labeled major coat protein mutants were used for the identification of interactions between neighbouring proteins in the phage particle, and when reconstituted in different membrane-mimicking systems. The steric constraints sensed by the spin label were used to evaluate the protein local conformation, or the extent of protein-protein interactions at spin-labeled residues of the major coat protein mutants. Furthermore, the position of the spin label on the protein in the membrane bound form was determined from the interaction of the nitroxide label with paramagnetic relaxation agents by using progressive saturation ESR spectroscopy. In this case, changes in the nitroxide spin-lattice relaxation rates on interaction with fast-relaxing paramagnetic species were a measure of their accessibility or distance of closest approach to the nitroxide group. The membrane location of the spin-labeled major coat protein was determined with molecular oxygen and Ni^{2+} as paramagnetic relaxation agents preferentially confined to the hydrophobic and aqueous region, respectively. In the later case, a decreasing distance-dependent relaxation enhancement is expected for spin-labeled residues that are embedded in the membrane.

Circular Dichroism Spectroscopy (CD)

CD spectra are the result of a difference in absorption of left and right circulary polarized light by optically active molecules such as proteins and nucleic acids (Schellman, 1974). The CD spectrum of the protein in the far UV region (190-290 nm) can be used to determine the overall secondary structure of the polypeptide chain. The observed signal can be considered as a linear combination of CD signals which originate from various secondary structure elements present in the protein structure: α-helix, β-sheet, and random coil as given in Figure 3 (Greenfield & Fasman, 1969).

The accuracy of secondary structure depends on the determination of the protein concentration, optical aberrations, light scattering, aromatic amino acids contributions in far UV and the relative amount of secondary structure elements (Wallace & Mao, 1984; Wallace & Teeters, 1987). This has to be taken into an account when interpreting the CD spectra. The CD spectrum of an optically active molecule is very sensitive to the micro environment (Cantor & Schimmel, 1980). Therefore CD was used in this thesis for the preparative purpose to detect the presence of β-sheet, as well as to determine the overall conformational changes in the major coat protein resulting from a change in pH, solubilization in different membrane mimicking systems, or phage coat disruption.
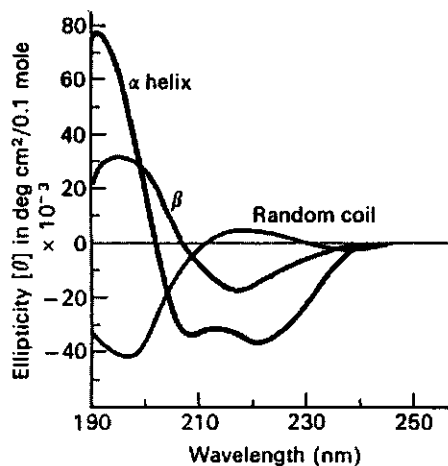
FIGURE 2: Circular dichroism (CD) spectra of a polypeptide, poly-1-lysine in various conformations (from Greenfield & Fasman, 1969).

Fluorescence Spectroscopy

When a photon of sufficient energy is absorbed by a molecule, a valence electron is promoted from the ground state to some vibrational level in the excitation singlet state. After ultra rapid relaxation (in the order of ps) to the lowest excited singlet state, the molecules decay to the ground state via several competing relaxation processes: a spontaneous radiative emission (fluorescence), radiationless decay to the ground state (internal conversion), transition to the lowest triplet state (inter system crossing), and transfer of the energy to the acceptor molecules (energy transfer) (Atkins, 1995). The occurrence of these extra nonradiative processes accelerates the decay of the excited state and therefore fluorescence measurements can yield information about the mobility and local environment of fluorophores in protein-lipid systems (Stubbs & Williams, 1992).

Some of the main areas of interest concerning protein-lipid interactions using fluorescence spectroscopy were: lipid and protein rotational diffusion, lateral diffusion, lateral phase separation, protein membrane location, polarity, surface charge density, membrane fusion, lipid-lipid and protein-protein associations (Sanders et al., 1992; Stubbs & Williams, 1992). In this thesis, the location and polarity of fluorescence-labeled major

11

coat protein mutants was probed. The location of the fluorophore was detected by changes in the fluorescence emission maximum. This is possible because the fluorescence emission maximum is dependent on the dielectric constant and molecular polarizability of the medium in which the fluorophore reside (Bakhshiev & Piterskaya, 1965). Typically, red shifts are observed for the more hydrophilic environment, while blue shifts are indicative for a more hydrophobic fluorophore environment. In addition, the surface accessibility of fluorophores was probed by addition of external quenchers, such as iodide or acrylamide. Fluorescence quenching refers to any of the above mentioned processes that results in a decreased fluorescence intensity of the fluorophore (Stubbs & Williams, 1992). Since quenching is a bimolecular process, it was used also to obtain information about the degree of the protein steric hindrance for the interaction with the quencher (London & Feigenson, 1981; Spruijt et al., 1996).

Bacteriophage M13 in Relation to Other Viruses

The work presented in this thesis was carried out within the research theme "Plant-Pathogen Interactions" of the Graduate School "Experimental Plant Sciences". Although bacteriophage M13 is not directly related to plant viruses and other plant pathogens, the methods and techniques discussed in this thesis offer a basic endeavour at fundamental virus research. If one assumes that the underlying physical and chemical principles of biological processes and interactions will be similar, the information gained about bacteriophage M13 disassembly and assembly can be translated ultimately to other viral systems. The study of the relatively small and simple bacteriophage M13 and its major coat protein therefore provides a basic approach and strategy towards understanding virus replication processes. In addition, bacteriophage M13 is an interesting model system for studying protein assemblies, because virtually all the protein side-chains are between different subunits in the coat protein array, rather than within the subunits. Thus the biophysical studies, such as carried out in this thesis, will give new insights in the atomic details responsible for protein complex formation, disruption, and stability.

Outline of the Thesis

The essential question in this thesis is how different membrane-mimicking systems influence the major coat protein structure. This problem is approached by studying the molecular details of the major coat protein reconstituted in lipid bilayers, and solubilized in

12

detergents using electron spin resonance, circular dichroism, and fluorescence spectroscopy. These spectroscopic techniques are particularly suitable for comparison of protein structural changes in different membrane systems. For this purpose a set of viable cysteine mutants was produced for site-directed labeling of the major coat protein.

In the first part of the thesis (chapters 2 and 3), the molecular details during membrane-assisted phage disassembly will be presented. In chapter 2 the process of phage disassembly, where the tight phage coat is disrupted and incorporated in the host membrane, is addressed. Valuable structural information was obtained about the initial molecular events during disassembly by following the spin label mobility and environment changes of the fluorescence labeled major coat protein in the membrane model systems. The results show that the major coat protein can be very quickly and efficiently solubilized in the membrane, provided the hydrophobic part of the protein is in direct contact with an amphiphilic solvent. In addition, molecular interactions responsible for the interlocking of the major coat protein in the phage particle are revealed in chapter 3. The results also suggest that the major coat protein is in the monomeric form in the host membrane after disruption of the phage coat, and before assembly in a new virus particle.

In the second part of the thesis (chapters 4 and 5) protein-lipid interactions were characterised in detail with the major coat protein already incorporated in different membrane-mimicking systems. In chapter 4, the conformational state of the major coat protein in lipids is compared with the well-described state of the protein in micellar systems. The major coat protein mutants were spin-labeled and reconstituted in different micellar and lipid systems. Analysis of the ESR line shapes provided a direct comparison of the protein structure and topology in different micelles and lipids. The detailed topology of the major coat protein in lipid bilayers will be further characterised in chapter 5 by progressive-saturation electron spin resonance spectroscopy. This technique is possible because the cysteine mutants are evenly distributed along the hydrophobic domain, and therefore their relative depth to the lipid molecules in the lipid vesicles can be determined by spin label quenching experiments. By combining the effect of oxygen and Ni^{2+} quenchers on the spin-labeled mutants, the relative position of the major coat protein in the membrane can be deduced.

In the concluding chapter the observed results are summarised, and the possible biological relevance of the protein-lipid interactions studied in this thesis is indicated.

References

Altenbach, C., Marti, T., Khorana, H.G., & Hubbell, W.L. (1990) *Science 248*, 1088-1092.

Atkins, P.W. (1995) *Physical Chemistry. Fifth Edition*, Oxford University Press, Oxford.

Bakhshiev, N.G., & Piterskaya, I.V. (1965) *Opt. Spectrosk. 19*, 390-395.

Banner, D.W., Nave, C., & Marvin, D.A. (1981) *Nature 289*, 814-816.

Bayer, M.E., & Bayer, M.H. (1986) *J. Virol. 57*, 258-266.

Berliner, L.J. editor (1976). *Molecular Biology: Spin Labeling. Theory and Applications*, Academic Press, New York.

Berliner, L.J. editor (1979) *Spin Labeling II: Theory and Applications*, Academic Press, New York.

Berliner, L.J., & Reuben, J. (1981) *Biological Magnetic Resonance*, Plenum, New York.

Brissette, J.L., & Russel, M. (1990) *J. Mol. Biol. 211*, 565-580.

Cantor, C.R., & Schimmel, P.R. (1980). *Biophysical chemistry Part I: The conformation of biological macromolecules*, Freeman, W. H. & Company, New York.

Cantor, C.R., & Schimmel, P.R. (1980) *Biophysical Chemistry Part II: Techniques for the Study of Biological Structure and Function*, Freeman, W. H. & Company, San Francisco.

Chang, C.N., Blobel, G., & Model, P. (1978) *Proc. Natl. Acad. Sci. U. S. A. 75*, 361-365.

Cross, T.A., & Opella, S.J. (1985) *J. Mol. Biol. 182*, 367-381.

Datema, K.P., Wolfs, C.J.A.M., Marsh, D., Watts, A., & Hemminga, M.A. (1987) *Biochemistry 26*, 7571-7574.

De Jongh, H.H.J., Hemminga, M.A., & Marsh, D. (1990) *Biochim. Biophys. Acta 1024*, 82-88.

Devaux, P.F., & Seigneuret, M. (1985) *Biochim. Biophys. Acta 822*, 63-125.

Fodor, S.P.A., Dunker, A.K., Carsten, D., & Williams, R.W. (1981) *Prog. Clin. Biol. Res. 64*, 441-455.

Gläser-Wüttke, G., Keppner, J., & Rasched, I. (1989) *Biochim. Biophys. Acta 985*, 239-247.

Greenfield, N.J., & Fasman, G.D. (1969) *Biochemistry 8*, 4108-4116.

Griffith, J., Manning, M., & Dunn, K. (1981) *Cell 23*, 747-753.

Helenius, A., McCaslin, D.R., Fries, E., & Tanford, C. (1979) in *Methods in Enzymol.* Vol. 56 (Fleischer, S., Packer, L., Eds.) pp 734-749, Academic Press, New York, San Francisco, London.

Helenius, A., & Simons, K. (1975) *Biochim. Biophys. Acta 415*, 29-79.

Hemminga, M.A. (1983) *Chem. Phys. Lipids 32*, 323-383.

Hemminga, M.A., Sanders, J.C., & Spruijt, R.B. (1992) in *Progress in Lipid Research* (Sprecher, H., Ed.) ed. 301-333, Pergamon Press, Oxford.

Hemminga, M.A., Sanders, J.C., Wolfs, C.J.A.M., & Spruijt, R.B. (1993) in *Protein-Lipid Interactions, New Comprehensive Biochemistry* (Watts, A., Ed.) pp 191-212, Elsevier, Amsterdam.

Hofschneider, P.H., & Preuss, A. (1963) *J. Mol. Biol. 7*, 450.

Hubbell, W.L., & Altenbach, C. (1994) *Curr. Opinion Struct. Biol. 4*, 566-573.

Khan, A.R., Williams, K.A., Boggs, J.M., & Deber, C.M. (1995) *Biochemistry 34*, 12388-12397.

Knowles, P.F., Marsh, D., & Rattle, H.W.E. (1976). *Magnetic Resonance of Biomolecules*, John Wiley & Sons, London, New York, Sydney, Toronto.

Kuhn, A., Wickner, W., & Kreil, G. (1986) *Nature 322*, 335-339.

Kyte, J., & Doolittle, R.F. (1982) *J. Mol. Biol. 157*, 105-132.

London, E., & Feigenson, G.W. (1981) *Biochemistry 20*, 1939-1948.

Lopez, J., & Webster, R.E. (1983) *Virology 127*, 177-193.

Makowski, L. (1992) *J. Mol. Biol. 228*, 885-892.

Makowski, L. (1994) *Curr. Opin. Struct. Biol. 4*, 225-230.

Mandel, G., & Wickner, W. (1979) *Proc. Natl. Acad. Sci. U. S. A. 76*, 236-240.

Manning, M., & Griffith, J. (1985) *Archives of Biochemistry and Biophysics* 236, 297-303.

Marsh, D. (1981) in *Membrane Spectroscopy. Molecular Biology, Biochemistry and Biophysics* (Grell, E. Ed.) Vol. 31, pp 51-142, Springer-Verlag, Berlin, Heidelberg, New York.

Marsh, D. (1982) *Tech. Life Sci.: Biochem. B4/2*, 44 pp.

Marsh, D. (1985) *Prog. Protein-Lipid Interact. 1*, 143-72.

Marsh, D. (1990) *FEBS Lett. 268*, 371-375.

Marsh, D. (1994) in *Electron Spin Resonance* (Atherton, N. M., Davies, M. J.,

Gilbert, B. C., Eds.) pp 166-202, The Royal Society of Chemistry, Cambridge.

Marvin, D.A. (1990) *Int. J. Biol. Macromol. 12*, 125-138; 335.

Marvin, D.A., Hale, R.D., Nave, C., & Citterich, M.H. (1994) *J. Mol. Biol. 235*, 260-286.

Marvin, D.A., & Hohn, B. (1969) *Bacteriol. Rev. 33*, 172-209.

McDonnell, P.A., Shon, K., Kim, Y., & Opella, S.J. (1993) *J. Mol. Biol. 233*, 447-463.

Model, P., & Russel, M. (1988) in *The Bacteriophages* (Calendar, R. Eds.) pp 375-456, Plenum Press, New York.

15

Newman, J., Swinney, H., & Day, L. (1977) *J. Mol. Biol. 116*, 593-606.

Nozaki, Y., Chamberlain, B.K., Webster, R.E., & Tanford, C. (1976) *Nature 259*, 335-337.

Nozaki, Y., Reynolds, J.A., & Tanford, C. (1978) *Biochemistry 17*, 1239-1246.

Papavoine, C.H.M., Konings, R.N.H., Hilbers, C.W., & Van de Ven, F.J.M. (1994) *Biochemistry 33*, 12990-12997.

Papavoine, C.H.M., Remerowski, L.M., Horstink, L.M., Konings, R.N.H., Hilbers, C.W., & Van de Ven, F.J.M. (1997) *Biochemistry 36*, 4015-4026.

Poole, C. (1983) *Electron Spin Resonance a Comprehensive Treatise on Experimental Techniques*, Intersience Publishers, New York.

Pratt, D., Tzagoloff, H., & Beaudoin, J. (1969) *Virology 39*, 42-53.

Rasched, I., & Oberer, E. (1986) *Microbiol. Rev. 50*, 401-427.

Roberts, L.M., & Dunker, K.A. (1993) *Biochemistry 32*, 10479-10488.

Russel, M. (1991) *Mol. Microbiol. 5*, 1607-1613.

Sambrook, J., Fritsch, E.F., & Maniatis, T. (1989). *Molecular Cloning: A laboratory manual*, Cold Spring Harbor Laboratory Press, Cold Spring Harbor, New York,

Sanders, J.C., Haris, P.I., Chapman, D., Otto, C., & Hemminga, M.A. (1993) *Biochemistry 32*, 12446-12454.

Sanders, J.C., Ottaviani, M.F., van Hoek, A., Visser, A.J.W.G., & Hemminga, M.A. (1992) *Eur. Biophys. J. 20*, 305-311.

Schellman, J.A. (1974) *Chem. Rev. 75*, 323-331.

Simons, G. F. M., Veeneman, H. H., Konings R. N. H., Van Boom, J. H. (1981) *Proc. Natl. Acad. Sci. USA 78*, 4194-4198.

Smilowitz, H. (1974) *J. Virol. 13*, 94-99.

Smith, G.P. (1993) *Gene 128*, 1-2.

Spruijt, R.B., & Hemminga, M.A. (1991) *Biochemistry 30*, 11147-11154.

Spruijt, R.B., Wolfs, C.J.A.M., & Hemminga, M.A. (1989) *Biochemistry 28*, 9158-9165.

Spruijt, R.B., Wolfs, C.A.J.M., Verver, J.W.G., & Hemminga, M.A. (1996) *Biochemistry 35*, 10383-10391.

Stubbs, C.D., & Williams, B.W. (1992) in *Topics in Fluorescence Spectroscopy* (Lakovicz, J.R. Ed.) pp 231-271, Plenum Press, New York.

Tanford, C. (1972) *J. Mol. Biol. 67*, 59-74.

Tanford, C., & Reynolds, J.A. (1976) *Biochim. Biophys. Acta 457*, 133-170.

Trenkner, E., Bonhoeffer, F., & Gierer, A. (1967) *Biochem. Biophys. Res. Commun. 28*, 932-939.

Van de Ven, F.J.M., Van Os, J.W.M., Aelen, J.M.A., Wymenga, S.S., Remerowski, M.L., Konings, R.N.H., & Hilbers, C.W. (1993) *Biochemistry 32*, 8322-8328.

Van Wezenbeek, P.M.G.F., Hulsebos, T.J.M., & Schoenmakers, J.G.G. (1980) *Gene 11*, 129-148.

Wallace, B.A., & Mao, D. (1984) *Anal. Biochem. 142*, 317-328.

Wallace, B.A., & Teeters, C.L. (1987) *Biochemistry 26*, 65-70.

Watts, A. (1987) *J. Bioenerg. Biomembr. 19*, 625-653.

Watts, A. (1993) in *Phospholipids Handbook* (Cevc, G. Ed.) pp 687-741, Marcel Dekker, Inc, New York.

Webster, R.E., & Lopez, J. (1985). in *Virus Structure and Assembly* (Casjens, S. Eds.) pp. 235-267, Jones and Bartelett Publishers Inc., Boston.

Wolfs, C.J.A.M., Horváth, L.I., Marsh, D., Watts, A., & Hemminga, M.A. (1989) *Biochemistry 28*, 9995-10001.

Wolkers, W.F., Haris, P.I., Pistorius, A.M.A., Chapman, D., & Hemminga, M.A. (1995) *Biochemistry 34*, 7825-7833.

Wolkers, W.F., Spruijt, R.B., Kaan, A., Konings, R.N.H., & Hemminga, M.A. (1997) *Biochim. Biophys. Acta 1327*, 5-16.

Chapter 2

Mimicking Initial Interactions of Bacteriophage M13 Coat Protein Disassembly in Model Membrane Systems

David Stopar, Ruud B. Spruijt, Cor J.A.M. Wolfs, and Marcus A. Hemminga

Abstract

The structure and changes in environment of the M13 major coat protein were studied in model systems, mimicking the initial molecular process of the phage disassembly. For this purpose we have systematically studied protein associations with various detergents and lipids in two different coat protein assemblies: phage particles and S-forms. It is remarkable that the major coat protein can change its conformation to accommodate three distinctly different environments: phage filament, S-form, and membrane-bound form. The structural and environmental changes during this protein transformations were studied by site-directed spin labeling, fluorescence labeling, and CD spectroscopy in different membrane model systems. The phage particles were disrupted only by strong ionic detergents (SDS and CTAB), but were not affected by sodium cholate and sodium deoxycholate, non-ionic detergents, and DLPC lipid bilayers. Conversion of the phage particles into S-forms by addition of chloroform, rendered the coat protein accessible for the association with different ionic and non-ionic detergents, as well as DLPC lipids. The disruption of the S-form by all detergents studied was instantaneous, but was slower with DLPC vesicles. Only small unilamellar vesicles effectively solubilized the S-form. The data suggest that the viral protein coat is inherently unstable when the major coat protein is exposed to amphiphilic molecules. During conversion from the phage to the S-form, and subsequently to the membrane-bound form, the coat protein undergoes pronounced changes in environment, and in response the α-helix content decreases and the local protein structure changes dramatically. This adaptation of the protein conformation enables a stable association of the protein with the membrane.

Introduction

Bacteriophage M13 coat is a filamentous phage composed of approximately 2800 copies of the major coat protein and a few copies of the minor coat proteins located at both ends of the phage (Rasched & Oberer, 1986). During phage disassembly the virus leaves its coat proteins in the *Escherichia coli* cytoplasmic membrane, while DNA is ejected in the cytoplasm (Pratt et al., 1969). An intriguing question about phage disassembly is how the major coat protein is incorporated into the host membrane from a very tightly packed and stable phage coat.

M13 is a very stable virus, and it is hardly affected by lipid bilayers and detergents (Griffith et al., 1981; Manning & Griffith, 1985). The only well-documented exception is SDS, a strong anionic detergent, which easily disrupts the phage particle (Dunker et al., 1991a; McDonnell et al., 1993). Also, the phage particle is stable at high temperature (up to 90 °C), it is not sensitive to protease activity, high or low values of pH, and different salt concentrations (Griffith et al., 1981; Marvin et al., 1994). The phage particle, however, is sensitive to the mechanic stress, ultrasonication, and it is highly sensitive for addition of chloroform, which in turn makes it susceptible for different detergents (Rasched & Oberer, 1986). The strong native architecture of the phage coat seems to be maintained primarily by hydrophobic interactions between the individual coat proteins (Ikehara & Utiyama, 1975; Marvin et al., 1994). The coat proteins form a tube around the viral DNA, with a flexible amphiphatic N-terminus located at the outside of the coat, and the basic C-terminus interacting with the DNA at the inside of the coat. The hydrophobic domain of the major coat protein is located in the central section of the protein sequence, and it interlocks the coat protein with its neighbouring subunits. The packing of the coat protein subunits is very tight as can be seen from the X-ray structure (Marvin et al., 1994) and solid state NMR data (Cross & Opella, 1985).

Upon disassembly of the virus particle this tight coat structure, however, must be released. It has been speculated by Makowski (1992), that the major coat protein in the phage particle is stable only when surrounded by copies of other major coat proteins. It was also suggested that the stability of the virus particle can be compromised at the unprotected ends of the filament, where addition of solvent may affects the major coat protein conformation and its affinity for other proteins (Makowski, 1992). This seems to be supported to some extent by the observation that phage particles with an amber mutation in the minor coat protein gp6 and gp3 at the host entering end of the phage particle are less stable (Rossomando & Zinder, 1968; Lopez & Webster, 1983). However, it is very difficult to monitor disassembly *in vivo*. The first events in the phage infection have been mimicked

in vitro by Griffith and co-authors (1981, 1985) using a chloroform-water interface. They found that upon addition of chloroform, the long filamentous phage structure contracted in an ordered way to a spheroid form (the so-called S-form) without loss of coat proteins, and with approximately two thirds of the DNA ejected outside the S-form. It was also suggested by Manning and Griffith (1985), based on sucrose density gradient centrifugation, that the S-form interacts with preformed phospholipid vesicles. Since the major coat protein from the S-form associated with the lipids, they suggested that the S-form might be involved in the phage disassembly process as an intermediate step. Formation of the S-form may provide a mechanism for a release of the viral DNA, and coat protein association with the lipid bilayers. However, there is no evidence that chloroform or chloroform-like molecules participate in the phage disassembly, as well as there is no evidence of S-form formation *in vivo* (Manning et al., 1981; Roberts & Dunker, 1993).

Despite a disagreement about the significant role of the S-form during the infection process, it is very interesting to note that the major coat protein has the ability to change its conformation, which allows the protein to exist in distinctly different environments: phage filament, S-form, and membrane-bound form. During conversion from one form to another, the coat protein undergoes an extreme change in environment, and in response its structure is almost certain to change.

Since, ultimately the major coat protein-lipid interactions in the host membrane are responsible for the solubilization of the protein coat and concomitant DNA release, we mimicked possible changes of the protein structure and changes in its local environment during the initial interactions of the phage disassembly in membrane model systems. Because hydrophobic interactions are expected to play an important role in this process, a V31C major coat protein mutant, located in the centre of the hydrophobic part of the protein, was produced. This mutant was labeled using a nitroxide spin label for studies with ESR spectroscopy, and a fluorescence label for fluorescence spectroscopy. Associations of different detergents and phospholipids with the coat protein were systematically studied with two well-defined protein associations: phage particles and S-forms. Changes in the overall secondary structure of the major coat protein upon phage disruption were followed by CD spectroscopy. The local structural changes in the hydrophobic part of the protein, responsible for the coat stabilization, were determined by site specific spin labeling of the V31C major coat protein mutant using ESR spectroscopy. The polarity of the protein in different environments during phage disruption was followed by site specific fluorescence AEDANS labeling of the V31C major coat protein, and exposure to the polar quencher acrylamide. The information obtained allowed us to determine structural and environmental

changes of the coat protein during conversion from filamentous form to S-form, and subsequent association with the membrane.

Materials and Methods

Phage labeling. The major coat protein mutant V31C was grown and purified as described previously (Spruijt et al., 1996; Stopar et al., 1996). The concentrated phage solution was spin labeled with 3-maleimido proxyl at a spin label to phage ratio 5/1 (mol/mol) in a 150 mM NaCl, 10 mM Tris-HCl buffer, pH 8.0 at 37 °C for 2 hours. The labeling reaction was stopped by adding an excess cysteine to the reaction mixture. Free spin label was removed by dialyses at room temperature against a 100-fold excess of 150 mM NaCl, 10 mM Tris-HCl buffer, pH 8.0. The dialysis buffer was changed four times every 12 hours. The major coat protein mutant V31C was also labeled with the IAEDANS fluorescence label as described above for the spin-labeled phage, but with labeling and dialysis carried out in the dark to prevent photodegradation of the AEDANS.

Phage disruption in detergents and lipids. Spin-labeled or fluorescence-labeled phage solution (8-16 mg/ml) was mixed with an equal volume of concentrated detergent solution to obtain the final detergent concentration well above the critical micellar concentration (cmc). The detergents used in this paper are shown in Figure 1. Final detergent concentrations were: 30 mM SDS, 100 mM sodium cholate, 100 mM sodium deoxycholate, 20 mM cetyltrimethylammonium-bromide (CTAB), 100 mM dodecyl β-D-maltoside (DDM), 100 mM monomyristoyl lecithin (MML), and 3 % Triton X-100. The detergent solutions were prepared in 150 mM NaCl, 10 mM Tris-HCl, pH 8.0 buffer. The phage-detergent mixtures were vigorously vortexed before applying to either ESR, fluorescence, or CD experiments. The samples for the CD measurements were diluted in 50 mM phosphate buffer, pH 8.0. Small unilamellar vesicles of DLPC and DOPC were prepared as follows. The lipids were dissolved in chloroform, evaporated onto the surface of the glass tube by nitrogen gas, and dried under vacuum for at least 2 hours to remove traces of chloroform. The lipids were resuspended in 150 mM NaCl, 10 mM Tris-HCl buffer, pH 8.0, and sonicated on a Branson B15 cell disrupter for 20 min, until a clear opalescent solution was obtained. Large lipid vesicles were removed by centrifugation at 12000 RPM for 30 min in a Sigma-220MC centrifuge. Small unilamellar vesicles were incubated with phage (20 mg lipids per mg phage) at 37 °C for two hours with occasional mixing.

S-form preparation. The S-form was prepared by gently vortexing a mixture of equal volumes of filamentous phage and chloroform for 5 s per minute at least 5 times at room
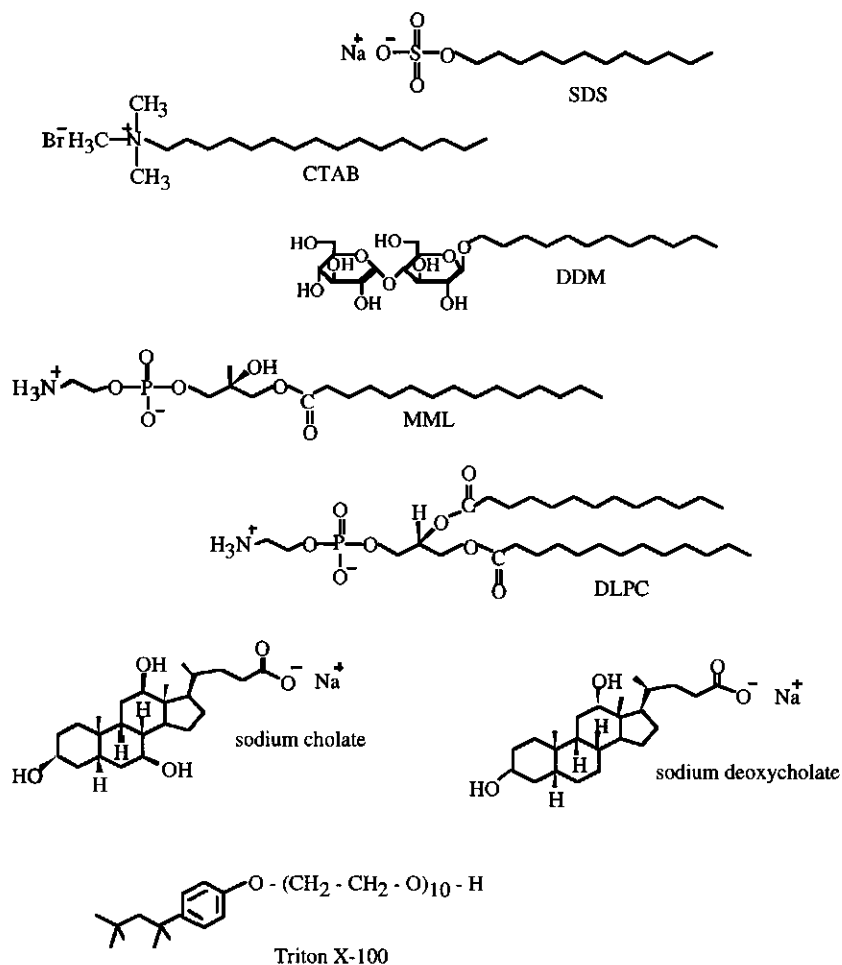
FIGURE 1: Structural formulas of sodium dodecyl sulfate (SDS), cetyltrimethylammonium-bromide (CTAB), dodecyl β-D-maltoside (DDM), monomyristoyl lecithin (MML), L-α-phosphatidylcholine dilauroyl (DLPC), sodium cholate, sodium deoxycholate, and Triton X-100.

temperature as described by Griffith et al. (1981). After phase separation the aqueous supernatant containing the S-form was collected and the remaining chloroform was removed under a flow of nitrogen. The filamentous phages were transformed completely to uniform spherical morphology (S-form) as checked by electron microscopy (data not shown). Since S-form is not stable over a prolonged period of time, fresh S-form were prepared for each set of experiments.

S-form disruption in detergents and lipids. The S-form was disrupted in 30 mM SDS, 100 mM sodium cholate, 100 mM sodium deoxycholate, 20 mM CTAB, 100 mM DDM, 100 mM MML, and 3 % Triton X-100 final concentration. The detergent solutions were prepared in 150 mM NaCl, 10 mM Tris-HCl buffer, pH 8.0. The S-form was incubated with small unilamellar DLPC or DOPC vesicles as described above for the disruption of phage particles.

ESR spectroscopy. ESR spectra were recorded on a Bruker ESP 300E spectrometer equipped with a 108TMH/9103 microwave cavity at room temperature as described previously (Stopar et al., 1996).

Fluorescence spectroscopy. Fluorescence spectroscopy was performed using a Perkin-Elmer LS-5 luminescence spectrophotometer at room temperature. The emission spectra of AEDANS-labeled major coat protein mixed with different detergents were collected using an excitation wavelength of 340 nm, and an excitation and emission bandwidth of 5 nm. The emission spectra were recorded from 400 to 550 nm. The background intensity from the labeled wild type phage in the same buffer was recorded under the same experimental conditions and was subtracted from the corresponding spectral intensity. Steady-state quenching studies were performed by addition of acrylamide as described by Spruijt et al. (1996).

CD spectroscopy. CD measurements were performed at room temperature on a Jasco J-715 spectrometer in the wavelength range 190 to 290 nm using a 10 mm path length. The CD settings were: 100 s scan time, 1 nm bandwidth, 0.1 nm resolution, 125 ms response time. Up to 20 spectra were accumulated to improve the signal to noise ratio. Background spectra, consisting of the same buffer, were recorded under the same experimental conditions. Difference spectra were generated by subtracting the background spectra from the corresponding spectra. For CD spectroscopy both wild type and labeled phage particles were used.

Results

The CD spectra of the wild type M13 phage filament, S-form, and cholate-associated coat protein are given in Figure 2. The CD spectra of the S-form and cholate-associated coat protein have significantly different lineshapes and spectral intensities as compared to the filamentous phage particles. The intensity of the CD spectrum of the phage filaments is consistent with a high α-helix content of the major coat protein, although the lineshape is anomalous around 222 nm (Arnold et al., 1992). Conversion of the filamentous phage to
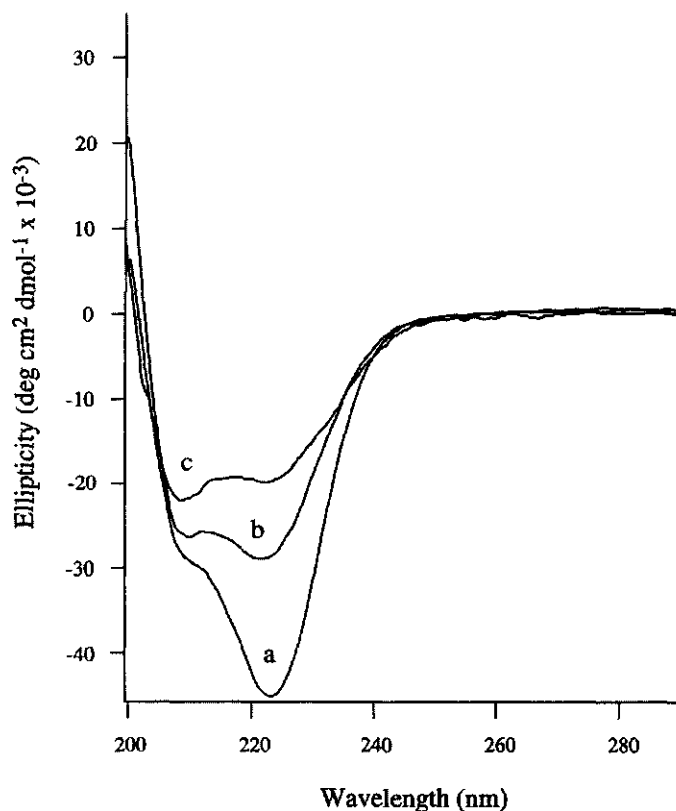
24

FIGURE 2: CD spectra at room temperature of the major coat protein in: (a) filamentous phage, (b) intact S-form, and (c) solubilized from the S-form in sodium cholate.

the S-form dramatically decreases the ellipticity at 222 nm, and to a smaller extent at 208 nm. Association of the S-form with sodium cholate further decreases the ellipticity throughout the 208-240 nm region. The CD spectra of the major coat protein associated with other detergents (data not shown) are similar to those of the coat protein in sodium cholate and are consistent with previous reports in the literature (Spruijt et al., 1989; Dunker et al., 1991a; Roberts & Dunker, 1993). The higher CD intensity of the coat protein in the S-form indicates that the α-helical content is higher as compared to the coat protein associated with detergents. The CD spectra for the spin-labeled and fluorescence-labeled coat protein were indistinguishable from the wild type coat protein (data not shown).

25

TABLE 1: Fluorescence emission wavelength maximum (nm) of the AEDANS-labeled V31C mutant coat protein in filamentous phage and in the S-form after solubilization in different detergents. The final detergent concentrations were: 30 mM SDS, 20 mM CTAB, 3% Triton X-100, 100 mM sodium cholate, 100 mM sodium deoxycholate, 100 mM DDM, and 100 mM MML. The AEDANS-labeled coat protein in filamentous phage and solubilized from S-form in different detergents was quenched by a 125 mM final concentration of acrylamide. The maximum decrease in fluorescence intensity is given as F/F_0, where F_0 is the fluorescence intensity of the non-quenched sample. The cmc values of the detergents were obtained from Helenius and Simons (1975) and Helenius et al. (1981), taking into account the sample salt concentration in the case of ionic detergents.

treatment	filaments	F/F_o	S-form	F/F_o	cmc
	491	0.60	462	0.90	
DLPC	491	0.60	471	0.93	< 0.01
sodium cholate	489	0.64	463	0.81	15.00
sodium deoxycholate	491	0.63	465	0.79	6.00
CTAB	475	0.75	473	0.74	0.92
Triton	488	0.64	480	0.68	0.24
DDM	490	0.63	481	0.72	0.60
MML	490	0.62	486	0.71	0.01
SDS	500	0.55	502	0.54	0.90

The wavelengths of the fluorescence emission maximum of the AEDANS-labeled V31C coat protein in filamentous phage, and in the S-form in the presence of different detergents are given in Table 1. The wavelength of the fluorescence emission maximum of the coat protein in the filamentous phage in the absence of amphiphiles was 491 nm, and was not changed significantly upon addition of the detergents sodium cholate, sodium deoxycholate, DDM, MML, and Triton, respectively. However, in the presence of SDS and CTAB, the fluorescence emission maximum increased to 500 and 475 nm, respectively. Conversion of phage filaments to the S-form shifted the wavelength of the fluorescence emission maximum to 462 nm in the absence of amphiphiles. When the S-form was mixed with detergents, the
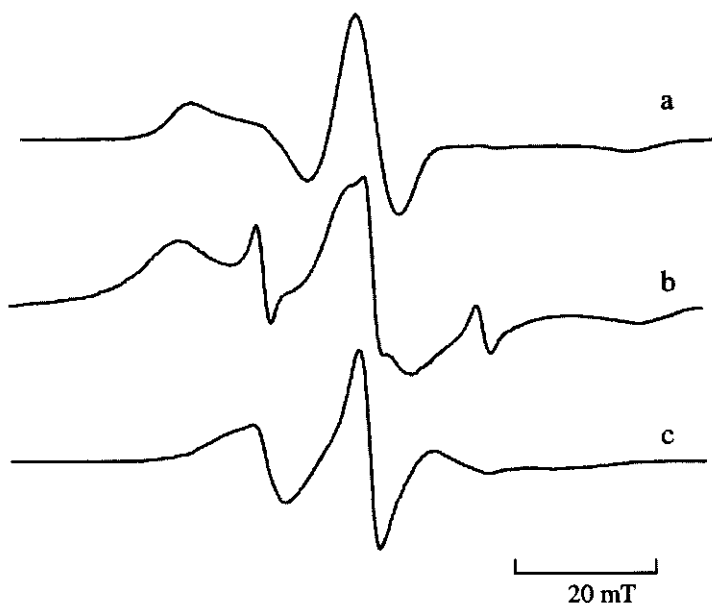
26

FIGURE 3: ESR spectra of spin-labeled V31C major coat protein in: (a) filamentous phage, (b) intact S-form, and (c) solubilized from the S-form in CTAB. Spectra were recorded at room temperature and were normalised to the same central lineheight.

fluorescence emission wavelength maximum increased again. The influence of acrylamide, a water-soluble quencher, on the fluorescence intensity of the AEDANS-labeled V31C major coat protein is given in Table 1. The fluorescence of detergent-associated fluorescence-labeled coat proteins with higher emission wavelength maximum was quenched more efficiently than detergent-associated coat proteins with a lower fluorescence emission wavelength maximum.

The ESR spectra of spin-labeled V31C coat protein in the filamentous phage, converted to S-form, and mixed with CTAB at room temperature are given in Figure 3. The spectrum of the spin-labeled filamentous phage is characteristic for a strongly immobilised spin label with an outer splitting $2A_{max}$ of 6.44 mT, as given in Table 2. The spectrum of the filamentous phage was not affected by addition of 100 mM sodium cholate, 100 mM sodium deoxycholate, 100 mM DDM, 100 mM MML, or 3 % Triton X-100. The mobility of the spin probe, however, dramatically increased upon mixing with 30 mM SDS and 20 mM CTAB, giving values for $2A_{max}$ of 4.85 and 5.16 mT, respectively. Conversion of the spin-labeled filamentous phage to the S-form in the absence of amphiphiles resulted in an

TABLE 2: The outer splitting ($2A_{max}$) in mT of the ESR spectra of phage filaments and the S-form solubilized with different detergents and lipids. The final detergent concentrations are the same as in Table 1.

treatment	filaments	S-form
	6.44	6.68
DLPC	6.44	5.89
sodium cholate	6.44	5.71
sodium deoxycholate	6.44	5.73
CTAB	5.16	5.16
Triton	6.44	5.94
DDM	6.44	5.80
MML	6.44	5.35
SDS	4.85	4.85

immobilization of the spin label, giving a value of $2A_{max}$ of 6.68 mT, and a substantial linebroadening of the spectrum. An additional mobile component appeared in the spectrum. As shown in Figure 3, association of the spin-labeled S-form with CTAB detergent significantly reduced the outer hyperfine splitting. This ESR spectrum is characteristic for an intermediate motion with an outer splitting $2A_{max}$ of 5.16 mT. The spectrum was indistinguishable from the spin-labeled filamentous phage after mixing with CTAB (data not shown). The outer hyperfine splitting after mixing spin-labeled S-form with sodium cholate, sodium deoxycholate, Triton, DDM, MML, and SDS is given in Table 2. The outer hyperfine splitting of spin labeled S-form decreased significantly with all detergent studied.

To study the type of association of DLPC and DOPC with the S-form, small unilamellar vesicles were incubated with either phage particles or S-forms. There was no interaction between DLPC or DOPC bilayers and phage filaments. The S-form, however, was disrupted when incubated with DLPC bilayers. The disruption was much slower than with detergents, and was possible only with small unilamellar vesicles. The fluorescence emission wavelength maximum of the AEDANS-labeled coat protein associated with DLPC bilayers was 471 nm. This is somewhat higher than found for the S-form, and the

28

fluorescence intensity was only slightly quenched by acrylamide (see Table 1). The CD spectrum of the major coat protein associated with lipids was similar to the spectra obtained with detergent-associated forms of the coat protein, indicative for an α-helix secondary structure. The ESR spectrum of the spin-labeled coat protein associated with lipids was characteristic for an immobilized spin label with an outer splitting of $2A_{max}$ of 5.89 mT. Small unilamelar DOPC vesicles could also disrupt the S-form, however, the results were not well reproducible. Furthermore, small unilamelar DOPC vesicles were not stable during incubation, and tend to form larger vesicles (data not shown).

Discussion

Bacteriophage M13 major proteins form a very stable protective coat around the viral DNA, which is not easily disrupted by various chaotropic reagents (Griffith et al., 1981). The stability of the coat, however, must be compromised during uncoating of the phage particle, when DNA enters into the host cell, and coat proteins are incorporated into the host cytoplasmic membrane. The data in this paper clearly indicate that it is possible to disrupt the protein coat with different detergents and lipids. The latter, however, is a special case, and we will first discuss the more general case of phage disruption by detergents.

Phage filament. The accessibility, mobility, and polarity of the V31C mutant of the major coat protein in the phage are all consistent with the known X-ray structure of the phage particle, and the proposed tight protein subunit packing (Marvin et al., 1994). Amino acid residue Val 31 of the mutant protein is located in the middle of the protein hydrophobic domain. In the phage structure, however, this residue is consistently located in a more hydrophilic environment, because it is easily accessible to either spin label or the more bulky IAEDANS label, which has a relatively high fluorescence emission maximum (491 nm) and a good exposure for acrylamide quencher (see Table 1). Although, located in a more hydrophilic environment, the spin label is considerably immobilised by surrounding amino acids in the filamentous phage structure, as can be inferred from the large values of the outer splitting in the ESR spectrum.

In order to solubilize the phage coat, the detergent has to bind to the protein aggregate and penetrate into the hydrophobic interior (Helenius & Simons, 1975; Tanford & Reynolds, 1976). As deduced from the spin-label ESR studies, fluorescence-labeling experiments, CD spectroscopy, and electron microscopy experiments, the filamentous phage particle after mixing with detergents were disrupted only with the detergents SDS and CTAB. All other detergents and lipids used did not change ESR, CD, or fluorescence spectral parameters (see

29

Table 1 and 2). This is consistent with an undisrupted filament structure, as seen by electron microscopy (data not shown). There was no influence of the labeling of the mutant on the disruption properties of the phage particle, as deduced from CD experiments of the wild type and fluorescence or spin labeled protein. This shows that the labeled V31C mutant coat protein is a good reporter for the behaviour of the native coat protein.

The two detergents that disrupt filamentous particles, the anionic SDS and the cationic CTAB have in common a flexible monoacyl chain 12 or 16 carbons long, attached to a charged head group. From geometry consideration there are two possible reasons for the ability of these two detergents to disrupt the phage particle. First, they have a single charge, and second they both have a flexible hydrophobic tail. It has been suggested by Roberts and Dunker (1993) that the non rigidly packed hydrophobic tails of the SDS molecules readily penetrate and dissolve hydrophobic protein aggregates. This also applies for CTAB. In contrast, the rigid and flat negatively charged sodium cholate and sodium deoxycholate detergents are unable to disrupt the phage particle. This indicate that tightly packed protein coat does not allow the penetration of rigid and relatively bulky molecules to the hydrophobic interior of the protein coat. Although, a flexible hydrophobic tail is clearly important in phage disruption, its presence alone is not sufficient. For example, DDM, Triton X-100, and MML all have a comparable single flexible hydrophobic chain, but they are unable to disrupt the phage particle. DDM and Triton X-100 are non-ionic detergents, which suggests that charge is important in phage disruption. It is, however, interesting to note that also the zwitterionic MML is not able to disrupt the phage particle. This would indicate that in addition to a single flexible acyl chain a net detergent charge is needed for phage disruption.

S-form phage. Conversion of the filamentous phage particle to the S-form is accompanied by a significant structural and environmental change. The fluorescence blue shift of the AEDANS-labeled V31C major coat protein (see Table 1), and a decreased accessibility to acrylamide quencher, indicate a more hydrophobic environment of the fluorescence label in the S-form (Spruijt et al., 1996). In addition, the conversion to the S-form removes the anomalous high negative ellipticity at 222 nm in the CD spectrum of the phage (see Figure 2). This anomaly in the CD spectrum has been tentatively attributed to a strong absorption of chromophore oscillator coupling between Trp26 and Phe45 of the two neighbouring proteins in the phage particle labeled as 0 and 11 in the index notation used by Marvin (Marvin et al., 1994). This coupled oscillator breaks down during conversion into the S-form, whereby neighbouring proteins slide along their length relative to each other (Roberts & Dunker, 1993). The conversion to the S-form also significantly decreases the side-chain mobility of the spin-labeled part of the protein (see Figure 3). This reduced side chain

mobility of the spin-labeled V31C contradicts to the idea introduced by Dunker et al. (1991b) that the S-form resembles molten globules. The principal feature of molten globules is the nonrigid side chain packing (Ohgushi & Wada, 1983). In addition, Dunker et al. (1991b) showed that the S-form but not filamentous phage binds ANS (1-anilino-napthalene-8-sulfonate). ANS binds either to the exposed hydrophobic groups on the protein, or to the nonrigid side chains packed in the protein aggregate (Dunker et al., 1991b). An appearance of the sharp ESR component upon conversion to the S-form suggests that a small fraction of the spin labels (5 - 10 %) has a nonrigid side chain packing, which may explain at least part of the ANS binding to the S-form. Based on the observed changes it must be concluded that the initial protein-protein interactions in the filamentous phage are broken during the conversion to the S-form.

It is interesting to note that chloroform, which is hydrophobic, significantly changes the hydrophobic protein-protein interactions of the filamentous phage particle allowing protein sliding, and a change of morphology. However, chloroform is essentially unable to solubilize the major coat protein. On the other hand, all amphiphilic molecules studied were able to disrupt the S-form. The data also show that the spatial constrains preventing phage solubilization are no longer present in the S-form, because also the bulky detergents sodium cholate, sodium deoxycholate, and Triton X-100 are able to disrupt the spherical particles. Inspection of electron microscopy pictures of our S-forms and already published S-forms clearly indicates the presence of at least one relatively large aperture in the spheroid structure at the place where DNA is emerging (Griffith et al., 1981; Manning et al., 1981; Lopez & Webster, 1982; Dunker et al., 1991b; Roberts & Dunker, 1993). The appearance of the additional small mobile component in the ESR spectrum upon conversion to the S-form is consistent with part of the labels being in a different environment, presumably provided by this aperture. The apertures in the S-form structure will permit an enhanced accessibility of the major coat proteins in the S-form for interaction with detergents. Once the detergent has a direct access to the hydrophobic part of the major coat protein, the disruption proceeds very rapidly towards a complete solubilization of the protein aggregate. The solubilization of the S-form upon addition of the detergents was practically instant on the time scale of our experiments.

Although, all detergents studied solubilize the S-form, the state of the protein after association with various detergents was not the same (see Table 1 and 2). Since protein solubilization is an equilibrium between protein-protein and protein-amphiphile interactions, it is not surprising that protein association with the different detergents is not the same. For instance, sodium cholate is a weak detergent with a high cmc. It has a relatively low aggregation tendency, and it has a weak interaction with the protein, because it can be easy

removed by dialysis. It has been shown previously that sodium cholate is unable to completely disrupt protein-protein interactions (Spruijt et al., 1989). This is consistent with our results, whereby disruption of the fluorescence labeled S-form in sodium cholate the hydrophobic environment is preserved to a great extent. In addition, a relatively low mobility of the spin-labeled protein in small sodium cholate micelles also suggests protein aggregation. The detergent SDS represents the other extreme. SDS is a strong anionic detergent, with a low cmc. It is relatively insoluble in an aqueous environment, it has a high aggregation tendency, and it has a strong interaction with the protein. In addition, it has a strong ability to disrupt noncovalent protein-protein interactions. During disruption of the S-form in SDS, the polarity of the fluorescence-labeled part of the protein is changed dramatically from the situation in the S-form, and the mobility of the spin-labeled part of the protein was increased significantly. This is in agreement with a monomeric state of the protein in SDS (McDonnell et al., 1993). The fluorescence and spin label characteristics of the labeled coat protein associated with other detergents used in this study are intermediate to the states of the protein described for sodium cholate and SDS.

S-form interaction with phospholipids. Manning and Griffith (1985) suggested that the major coat protein from the S-form was able to interact with lipids, however, they could not exclude nonspecific aggregation of the protein in the presence of lipids. In our experiments, the CD spectra of the S-form associated with DLPC lipid bilayers showed no sign of β-sheet secondary structure. It was shown by other groups that nonspecific protein aggregation of the major coat protein causes an irreversible β-sheet polymeric state (Williams & Dunker, 1977; Nozaki et al., 1978; Wilson & Dahlquist, 1985). The CD results furthermore indicate that the secondary structure of the lipid-associated protein is comparable with a very well-characterised protein secondary structure in SDS. (McDonnell et al., 1993). It is also interesting to note that the α-helix content of the coat protein decreases during disruption of the S-form (see Fig. 2), which could indicate that the coat protein has an extended helical conformation in the S-form, in contrast to an L-shaped conformation suggested in lipid bilayers (McDonnell et al., 1993; Wolkers et al., 1997). The decrease in α-helical content is consistent with the formation of a loop connecting the two helices in L-form and absence of secondary structure in the C-terminus after the protein has dissociated from the viral DNA in the S-form.

In addition, the fluorescence data strongly suggest that the hydrophobic part of the protein is incorporated in the hydrophobic core of the lipid, because of the low fluorescence emission maximum and almost complete exclusion from acrylamide quencher. Finally, it must be emphasised that all the experimental data for the S-form major coat protein associated with lipids compare very well with the data of the major coat protein reconstituted

32

into lipids from sodium cholate by dialysis (Spruijt et al., 1996; Stopar et al., 1996). Although, the two mechanisms of protein reconstitution into lipid bilayers, S-form solubilization and reconstitution from the cholate, differ markedly, the end results agree well. In both cases the major coat protein is reconstituted into the membrane.

Effective solubilization of the S-form was only achieved when small unilamellar DLPC vesicles were used. Since the lipid monomer concentration in the solution is low, and the majority of the lipids form vesicles, it is unlikely that saturation of the S-form, and subsequent solubilization can be achieved. The demand for small vesicles, on the other hand, suggests that vesicles must be able to come in close proximity to the hydrophobic part of the protein in order to obtain protein solubilization. This is only possible near to the aperture in the S-form, where the DNA is emerging. Taken into an account the dimensions of the aperture, estimated to be 5-15 nm, this is possible with small, but not with large vesicles. This may also explain why disruption with DOPC vesicles was not well reproducible. In the case of DOPC it was difficult to maintain small vesicles during relatively long incubation (2 hours) with S-forms. The instability of small DOPC vesicles is in agreement with the finding that small highly curved DOPC vesicles are thermodynamically unstable (Marsh, 1996). Since the requirement of small vesicles for S-form disruption also implies a stressed bilayer situation, it is conceivable that solubilization of the protein decreases the curvature and consequently the internal lipid stress. A similar situation may occur during phage disassembly in the cytoplasmic membrane, where locally around the disassembly site, the lipids are expected to be in a stressed state.

References

Arnold, G.E., Day, L.A., & Dunker, K.A. (1992) *Biochemistry 31*, 7948-7956.

Cross, T.A., & Opella, S.J. (1985) *J. Mol. Biol. 182*, 367-381.

Dunker, K.A., Ensign, L.D., Arnold, G.E., & Roberts, L.M. (1991a) *FEBS Lett. 292*, 271-274.

Dunker, K.A., Ensign, L.D., Arnold, G.E., & Roberts, L.M. (1991b) *FEBS Lett. 292*, 275-278.

Gläser-Wüttke, G., Keppner, J., & Rasched, I. (1989) *Biochim. Biophys. Acta 985*, 239-247.

Griffith, J., Manning, M., & Dunn, K. (1981) *Cell 23*, 747-753.

Helenius, A., McCaslin, D.R., Fries, E., & Tanford, C. (1979) in *Methods in Enzymology* (Fleischer, S., & Packer, L., Eds) Vol. 56, pp 734-749, Academic Press, New York.

Helenius, A., & Simons, K. (1975) *Biochim. Biophys. Acta 415*, 29-79.

Hemminga, M.A., Sanders, J.C., Wolfs, C.J.A.M., & Spruijt, R.B. (1993) in *Protein-Lipid Interactions* (Watts, A., Ed.) New Comprehensive Biochemistry 25, pp 191-212, Elsevier, Amsterdam.

Ikehara, K., & Utiyama, H. (1975) *Virology 66*, 306-.

Lopez, J., & Webster, R.E. (1982) *J.Virol.42*, 1099-1107.

Lopez, J., & Webster, R.E. (1983) *Virology 127*, 177-193.

Makowski, L. (1992) *J. Mol. Biol. 228*, 885-892.

Manning, M., Chrysogelos, S., & Griffith, J. (1981) *J.Virol.40*, 912-919.

Manning, M., & Griffith, J. (1985) *Archives of Biochemistry and Biophysics* 236, 297-303.

Marsh, D. (1996) *Biophys. J.* 70, 2248-2255.

Marvin, D.A., Hale, R.D., Nave, C., & Citterich, M.H. (1994) *J. Mol. Biol. 235*, 260-286.

McDonnell, P.A., Shon, K., Kim, Y., & Opella, S.J. (1993) *J. Mol. Biol. 233*, 447-463.

Nozaki, Y., Reynolds, J.A., & Tanford, C. (1978) *Biochemistry 17*, 1239-1246.

Ohgushi, M., & Wada, A. (1983) *FEBS Lett.164*, 21-24.

Pratt, D., Tzagoloff, H., & Beaudoin, J. (1969) *Virology 39*, 42-53.

Rasched, I., & Oberer, E. (1986) *Microbiol. Rev. 50*, 401-427.

Roberts, L.M., & Dunker, K.A. (1993) *Biochemistry 32*, 10479-10488.

Robinson, N.C., & Tanford, C. (1975) *Biochemistry 14*, 369-378.

Rossomando, E.F., & Zinder, N.D. (1968) *J. Mol. Biol.* 36, 387-399.

Spruijt, R.B., Wolfs, C.J.A.M., & Hemminga, M.A. (1989) *Biochemistry 28*, 9158-9165.

Spruijt, R.B., Wolfs, C.J.A.M., Verver, J.W.G., & Hemminga, M.A. (1996) *Biochemistry 35*, 10383-10391.

Stopar, D., Spruijt, R.B., Wolfs, C.J.A.M., & Hemminga, M.A. (1996) *Biochemistry 35*, 15467-15473.

Tanford, C. (1972) *J. Mol. Biol. 67*, 59-74.

Tanford, C., & Reynolds, J.A. (1976) *Biochim. Biophys. Acta 457*, 133-170.

Williams, R.W., & Dunker, A.K. (1977) *J. Biol. Chem. 252*, 6253-6255.

Wilson, M.L., & Dahlquist, F.W. (1985) *Biochemistry 24*, 1920-1928.

Wolkers, W.F., Spruijt, R.B., Kaan, A., Konings, R. N. H, & Hemminga, M.A. (1997) *Biochim. Biophys. Acta 1327*, 5-16.

Chapter 3

In Situ Aggregational State of M13 Bacteriophage Major Coat Protein in Sodium Cholate and Lipid Bilayers

David Stopar, Ruud B.Spruijt, Cor J.A.M.Wolfs, and Marcus A. Hemminga

Abstract

The *in situ* aggregational behaviour of the bacteriophage M13 major coat protein was determined for the protein isolated in sodium cholate and reconstituted into DOPC lipid bilayers. For this purpose, the cysteine mutants A49C and T36C of the major coat protein were labeled with either a maleimido spin label or a fluorescence label (IAEDANS). The steric restrictions sensed by the spin label were used to evaluate the local protein conformation and the extent of protein-protein interactions at the position of the labeled residue. In addition, fluorescent labels covalently attached to the protein were used to determine the polarity of the local environment. The labeled coat protein mutants were examined under different conditions of protein association (amphiphile environment, ionic strength, temperature, and pH). The aggregational state of the major coat protein solubilized from the phage particle in sodium cholate was not dependent on the ionic strength, but was strongly dependent on cholate concentration and pH during sample preparation. At pH 7.0 and high sodium cholate concentration, the protein was in a dimeric form. The unusually strong association properties of the protein dimer in sodium cholate at pH 7.0 were attributed to the inability of sodium cholate to disrupt the strong hydrophobic forces between neighbouring protein subunits in the phage particle. Such a "structural protein dimer" was, however, completely and irreversibly disrupted at pH 10.0. Qualitatively the same aggregational tendency was found upon changing the pH for the coat protein reconstituted in DOPC lipid bilayers. This reveals that the dimer disruption process is primarily a protein property, because there are no titratable groups on DOPC in the experimental pH range. The results are interpreted in terms of a model relating the protein aggregational state in the assembled phage to the protein aggregational behaviour in sodium cholate and lipid bilayers.

Introduction

The major coat protein of the bacteriophage M13 is a multi-functional protein. It forms a polymeric protective coat around the viral DNA (Marvin et al., 1994). Alternatively, it inserts into the cytoplasmic membrane of the host *Escherichia coli* during virus disassembly, and it leaves the membrane in a virus assembly-extrusion process (Russel, 1991). The conformational and aggregational state of the coat protein are believed to change from a polymeric form in the virus particle to a monomeric form in the membrane, and back to the polymeric form in a newly assembled phage (Hemminga et al., 1993). Versatility as well as reversibility of these processes are remarkable characteristics of the major coat protein.

The conformational and aggregational states of the major coat protein, as studied in various amphiphatic environments, are strongly dependent on the protein history and method of sample preparation. The amphiphile composition, ionic strength, temperature, and pH are the most important factors that shift the chemical equilibrium between different coat protein aggregate sizes (Hemminga et al., 1993). Depending on the sample preparation, two specific conformations of the coat protein were suggested: a predominantly α-helical conformation, where the coat protein has an ability to undergo a reversible aggregation; and a predominantly β-polymeric state, where the coat protein is irreversibly aggregated into large β-sheet complexes (Nozaki et al., 1978). It should be mentioned that the β-polymeric state is considered as an artifact, a denatured form of the coat protein, because it is formed in an irreversible way, unable to convert into an α-helical conformation as found in the virus particle (Spruijt & Hemminga, 1991).

Sodium cholate is able to preserve the coat protein in a predominantly α-helical conformation. Sodium cholate is a weak detergent and has been used extensively as an intermediate hydrophobic environment for protein labeling and subsequent reconstitution in the phospholipid bilayers (Woolford et al., 1974; Makino et al., 1975; Stopar et al., 1996). The smallest protein aggregate in sodium cholate is assumed to be an α-helical coat protein dimer (Knippers & Hoffmann-Berling, 1966; Makino et al., 1975). Therefore, coat protein oligomerization in sodium cholate is thought to be a process in which coat protein dimers are joined together (Spruijt et al., 1989). Although, dimers appear to be stable in sodium cholate, it was demonstrated that in the strong detergent SDS, they dissociate into monomers (McDonnell et al., 1993). This suggests that the coat protein dimers in sodium cholate are stabilized primarily by non-covalent interactions.

On the other hand, the *in situ* aggregational state of the coat protein reconstituted in phospholipid bilayers is very difficult to determine. Size-exclusion chromatography, HPSEC, has been employed previously (Makino et al., 1975; Spruijt et al., 1989; Spruijt &

Hemminga, 1991). However, in the absence of detergents, only the size distribution of the entire lipid-protein complex can be determined, but no information about the size of the protein aggregate can be obtained (Tanford & Reynolds, 1976). In contrast, HPSEC in the presence of detergents disrupts the lipid-protein complexes and extracts the coat protein, thereby probably changing the protein-protein interactions and the original aggregational state of the coat protein in the bilayer (Spruijt et al., 1989). The same applies for SDS-PAGE gel electrophoresis, because it disrupts all the non-covalent interactions between proteins. The oligomeric state of the coat protein in lipid bilayers, as determined by sodium cholate-HPSEC, is characterized by weak protein-protein interactions that can be readily disrupted, because SDS-HPSEC elution profiles indicate the presence of only monomers (Spruijt & Hemminga, 1991).

Analysis of the dynamics of the spin-labeled proteins was used earlier to identify sites of interaction between neighbouring protein units in the lipid bilayers (Bittman et al., 1984; Hubbell & Altenbach, 1994). When the spin-labeled part of the protein makes contacts with other structures in the protein, or between neighbouring proteins, its motion is highly constrained. The steric restrictions sensed by the spin label can thus be used to evaluate the local protein conformation (Wolkers et al., 1997), or the extent of protein-protein interactions at any residue (Hubbell & Altenbach, 1994). In addition, fluorescent labels covalently attached to the protein have been a valuable tool in determining information about the polarity of the environment. For example, the wavelength emission maximum gives information about the polarity of the fluorophore environment in different aggregational states of the protein (Spruijt et al., 1996).

In this paper we describe the *in situ* aggregational behaviour of the major coat protein isolated in sodium cholate and reconstituted in lipid bilayers. For this purpose, cysteine mutants of the coat protein were labeled with either a spin label or a fluorescence label. The labeled coat protein mutants were examined under different conditions of protein association (by variation of ionic strength, temperature, and pH). This has enabled us to obtain detailed information about the protein-protein interactions in a membrane environment.

Materials and Methods

Coat Protein Isolation and Spin Labeling. The major coat protein mutants A49C and T36C were grown and purified from the phage as described previously (Spruijt et al., 1996). The major coat protein mutants were checked for their conformation and aggregational properties with HPSEC and CD as described previously (Stopar et al., 1996).

The phage was disrupted in a mixture of 2.5% (v/v) chloroform, 100 mM sodium cholate, 150 mM NaCl, and 10 mM Tris-HCl at 37 °C, pH 7.0, with subsequent spin labeling of the major coat protein mutants as described previously (Stopar et al., 1996). The spin label 3-maleimido proxyl was obtained from Aldrich Chemical Co. To separate the spin-labeled protein from the free spin label and DNA, the mixture was applied to a Superose 12 prepgrad HR 25/60 column (Pharmacia) and eluted with 25 mM sodium cholate, 150 mM NaCl, and 10 mM Tris-HCl equilibrated to pH 7.0, pH 8.0, or pH 10.0. Fractions with an A_{280}/A_{260} absorbance ratio higher than 1.5 were collected and concentrated by Amicon filtration. The aggregational state of the protein at each pH value was checked by SDS-HPSEC and sodium cholate-HPSEC as described previously (Spruijt et al., 1989).

Coat Protein Reconstitution in Lipid Vesicles. The spin-labeled protein mutants were reconstituted in DOPC and DOPC/DOPG vesicles (80/20 mol/mol) as described earlier (Stopar et al., 1996) with the following modifications. Lipid vesicles were prepared by evaporating chloroform from the desired amount of DOPC or DOPC/DOPG mixture. The residual traces of chloroform were removed under vacuum overnight. The lipids were solubilized in 50 mM sodium cholate buffer (150 mM NaCl, 10 mM Tris-HCl) at the desired pH: pH 7.0, 8.0, or 10.0 by brief sonication (Branson B15 cell disrupter) in ice-cold water until a clear opalescent solution was obtained. The desired amount of spin-labeled mutant major coat protein isolated in 50 mM sodium cholate at pH 7.0, 8.0, and/or 10.0 was added to give a molar lipid/protein ratio of 200 (L/P 200). Dialysis was performed at room temperature against a 100-fold excess of 50 mM NaCl, 10 mM Tris-HCl buffer at pH 7.0 for the protein isolated in sodium cholate at pH 7.0; pH 8.0 for the protein isolated in sodium cholate at pH 8.0; or pH 10.0 for the protein isolated in sodium cholate at pH 10.0. The dialysis buffer was changed four times every 12 hours. After dialysis, the proteoliposome suspension of the spin-labeled coat protein reconstituted at either pH 7.0, 8.0, or 10.0 in DOPC was divided into five aliquots and adjusted to the desired pH by a second dialysis against a 100-fold excess of 150 mM NaCl, 10 mM Tris-HCl buffer to obtain a final proteoliposome suspension at pH 6.0, 7.0, 8.0, 9.0, and 10.0. The dialysis buffer for the second dialysis was also changed four times every 12 hours.

For ESR measurements, the samples were freeze-dried, resuspended in a volume of distilled water equal to the original volume, and then concentrated by centrifugation (Beckman XL-90 ultracentrifuge, 45000 rpm, 1 hour, 10 °C). During the second dialysis, samples with high and low salt concentration were prepared by dialysis against a 100-fold excess of 1000 mM NaCl (high salt), 10 mM Tris-HCl buffer, or 25 mM NaCl (low salt), 10 mM Tris-HCl buffer at the desired pH value. The aggregational state of the protein was

checked by SDS-HPSEC and sodium cholate-HPSEC as described previously (Spruijt et al., 1989).

Chemical cross-linking experiments. Spin-labeled major coat protein isolated in sodium cholate at pH 7.0 and pH 10 was cross-linked with 100 mM 1-ethyl-3-[3-(dymethylamino)propyl]carbodiimide (EDC), at room temperature for 2 min. The cross-linking reaction was stopped by adding an excess of concentrated Tris-HCl buffer up to 0.8 M. The aggregational state of the sample was analyzed with Tricine sodium dodecylsulfate polyacrylamide gel electrophoresis (Schägger & von Jagow, 1987). Molecular weight markers from horse-heart globin were obtained from Pharmacia in the range from 2.5 to 16.9 kD.

ESR Spectroscopy. Samples containing spin-labeled coat protein isolated in sodium cholate or reconstituted into DOPC or DOPC/DOPG bilayers were filled up to 5 mm in 100 µl glass capillaries. These capillaries were accommodated within standard 4 mm diameter quartz tubes. ESR spectra were recorded on a Bruker ESP 300E ESR spectrometer equipped with a 108TMH/9103 microwave cavity and with a nitrogen gas flow temperature regulation system. The ESR settings were 6.38 mW microwave power, 0.1 mT modulation amplitude, 40 ms time constant, 80 s scan time, 10 mT scan width, and 338.9 mT centre field. Up to 20 spectra were accumulated to improve the signal to noise ratio. The first and second integrals of the ESR spectra were determined after base line correction. The effective rotational correlation times were determined from the line height ratios as described previously (Marsh, 1981).

Evaluation of the Immobilized Component. To estimate the fraction of the immobilized component in ESR spectra, only spectra recorded at low temperature (5 ± 0.5 °C) were used. In these spectra, the mobile and immobile components were clearly separated on the composed spectrum. To obtain the percentage of immobilized component, a pairwise subtraction method was used (Devaux & Seigneuret, 1985). The basic assumption of this method is that, to a first approximation, over a limited range of temperature only the ratio of the two components varies substantially, while the line shape of the components is affected only to a small extent (Andersen et al., 1981). Typically, spectra of the spin-labeled protein isolated in sodium cholate at pH 10.0 and reconstituted in DOPC bilayers at pH 10.0 were subtracted from the ESR spectra until an undistorted line shape, with no spikes, was generated. Double integration of the original spectra and the generated immobilized component spectra gives the relative amount of the immobilized spin labels.

CD Spectroscopy. Circular dichroism measurements were performed on a Jasco J-715 spectrometer in the wavelength range from 190 to 290 nm at room temperature. Samples were prepared as described previously by Sanders et al. (1993).

Fluorescence Spectroscopy. For the purpose of steady-state fluorescence experiments, the A49C coat protein mutant was labeled with IAEDANS (Molecular Probes) directly after phage disruption, as described previously (Spruijt et al., 1996). Fluorescence-labeled protein was reconstituted into DOPC bilayers, similar to as described above for the spin-labeled coat protein, but with dialysis carried out in the dark to prevent photodegradation of the AEDANS. Steady-state fluorescence was performed on a Perkin-Elmer LS-5 luminescence spectrophotometer at room temperature. The absorbance of the samples was kept below 0.1 at the excitation wavelength. The excitation wavelength was 340 nm and emission scans were recorded from 400 to 640 nm with an excitation and an emission bandwidth of 5 nm. Steady-state quenching studies of AEDANS-labeled A49C coat protein mutant were performed by addition of the same amount of spin-labeled A49C coat protein mutant (mol/mol) and acrylamide in the concentration range from 0 to 125 mM at room temperature.

Results

The ESR spectra of the spin-labeled A49C coat protein mutant isolated in 25 mM sodium cholate at pH 7.0 and subsequently reconstituted at high lipid to protein ratio (L/P 200) in DOPC bilayers at pH 6.0, 8.0, and 10.0 are given in Figure 1. The spectra display two well-resolved components: a sharp, three-line component corresponding to spin labels undergoing fast isotropic motion, and a second broad component resolved in the outer wings of the spectrum, representing spin labels undergoing restricted motion. The fraction of the immobile component dominates in the composite spectrum at pH 6.0, but it is dramatically reduced in the ESR spectrum at pH 10.0.

The fraction of motionally restricted labels was quantitated by spectral subtraction of the mobile component. (Devaux & Seigneuret, 1985). This enabled us to obtain a line shape of the immobilized component. This procedure works best at low temperatures (5 °C), where the two components are well resolved. The mobile component used in the spectral subtraction is taken from the spin-labeled A49C coat protein isolated in 25 mM sodium cholate at pH 10.0 and subsequently reconstituted at L/P 200 in DOPC bilayers at pH 10.0. This component is characteristic for a single component with a fast isotropic motion with a rotational correlation time, τ_c, of 0.59 ns, and an isotropic splitting of 1.59 mT. The immobilised component obtained from spectral subtraction is characteristic for a slow mobility with an outer splitting of $2A_{max} = 5.93$ mT at 5 °C. The choice of the mobile component for the spectral subtractions is justified by the observation that several non-base line isoclinic points are observed in the spectra in Figure 1, normalized to the same double
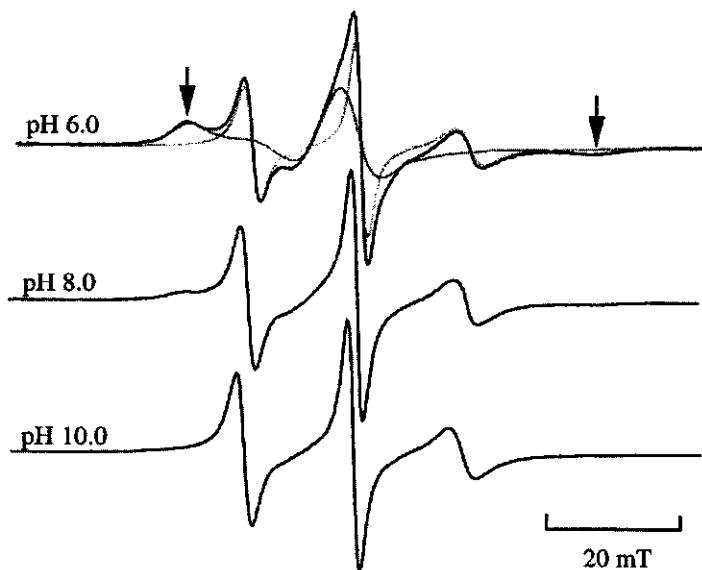
40

FIGURE 1: Conventional ESR spectra of the spin-labeled A49C major coat protein mutant in DOPC bilayers at a lipid/protein ratio of 200 (mol/mol). Samples were isolated in 25 mM sodium cholate at pH 7.0 and reconstituted into DOPC at the desired pH; from top to bottom, pH 6.0, 8.0, and 10.0, respectively. Spectra are normalized to the same central line height. The temperature of the samples was 5 °C. Total scan width is 10 mT. The outermost peaks of the immobilised component in the ESR spectra are indicated with arrows in the pH 6.0 spectrum. The two component fit to the experimental spectrum is indicated in the pH 6.0 spectrum.

integral (data not shown). These non-base line isoclinic points indicate that the ESR spectra are a linear combination of the mobile and immobile spectra (Marriott & Griffith, 1974).The subtraction procedure leads to a reliable quantitation (the estimated error is ± 5 %) of the fraction of the immobilized component.

The fraction of motionally restricted component of the spin-labeled A49C coat protein mutant reconstituted in DOPC bilayers at L/P 200 is given in Fig. 2. The fraction of the immobilized component of the coat protein isolated in 25 mM sodium cholate at pH 7.0 and subsequently reconstituted in DOPC bilayers at pH 6.0 is 70%. This fraction decreases dramatically to 5% if the protein was reconstituted in DOPC bilayers at pH 10.0 (Fig. 2A).
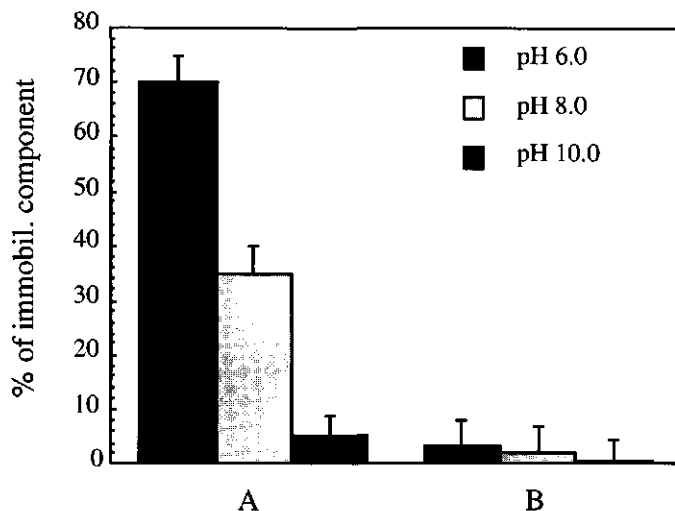
41

FIGURE 2: Fraction of the immobilised component of the spin-labeled A49C coat protein mutant in DOPC bilayers. The fraction of the immobilised component was estimated as described under Materials and Methods. The temperature of the samples was 5 °C. (A) The spin-labeled A49C coat protein mutant was isolated in 25 mM sodium cholate at pH 7.0 and reconstituted in DOPC at the desired pH; pH 6.0 (black bar), pH 8.0 (light gray bar), and pH 10.0 (dark gray bar). (B) The spin-labeled A49C coat protein mutant was isolated in 25 mM sodium cholate at pH 10.0 and reconstituted in DOPC at the desired pH; pH 6.0 (black bar), pH 8.0 (light gray bar), and pH 10.0 (dark gray bar).

In contrast, the fraction of the immobilised component for the protein isolated in 25 mM sodium cholate at pH 10 and subsequently reconstituted in DOPC bilayers at pH 10.0 is low (< 5%), and is not significantly influenced by different pH values (Fig. 2B). It should be noted, that the fraction of the immobile component was strongly dependent on pH during protein isolation in sodium cholate. The disappearance of the immobile component is completely irreversible.

The fraction of the immobilized component was also dependent on the concentration of sodium cholate during protein isolation. When the concentration of sodium cholate at pH 7.0 isolation was increased from 25 to 100 mM, the fraction of the immobilised component decreased from 63 to 49%. If both the concentration of sodium cholate and the pH were increased, the immobilized component was completely removed from the ESR spectra. There was no immobilised component and no sodium cholate concentration dependence for the protein isolated in 25 mM sodium cholate at pH 10.0. If the pH of such samples was

TABLE 1: Fraction of immobilised component of spin-labeled A49C coat protein mutant isolated in 25 mM sodium cholate, pH 8.0 and reconstituted into DOPC bilayers, lipid/protein ratio 200 (mol/mol) at the desired pH; a) DOPC: 150 mM NaCl, 10 mM Tris-HCl, b) DOPC low salt: 25 mM NaCl, 10 mM Tris-HCl, c) DOPC high salt: 1000 mM NaCl, 10 mM Tris-HCl, and d) DOPC/DOPG (80/20 mol/mol): 150 mM NaCl, 10 mM Tris-HCl. The estimated errors are ± 5%.

pH	DOPC	DOPC low salt	DOPC high salt	DOPC/DOPG (80/20 mol/mol)
6.0	18	19	24	20
8.0	6	7	10	7
10.0	1	2	3	2

lowered at either high or low sodium cholate concentration, there was no increase in the fraction of the immobilised component, which indicates that the process is irreversible. Experiments with addition of wild type protein to the spin-labeled protein isolated at either pH 7.0 or pH 10.0 were also performed. The fraction of the immobilized component and the spectral line shape were not changed upon titration of spin-labeled mutant with wild type protein up to 10 times mol/mol excess.

The effect on the fraction of the immobilised component to high salt, and low salt concentrations, and to negatively charged lipids for the protein isolated in 25 mM sodium cholate at pH 8.0 and reconstituted in DOPC or DOPC/DOPG bilayers (L/P 200) at pH 6.0, 8.0, and 10.0 is given in Table 1. The fraction of the immobilised component was pH dependent in all systems studied, but was generally lower as compared to the protein isolated in sodium cholate at pH 7.0 and subsequently reconstituted in DOPC bilayers. There was again no significant immobilised component at pH 10.0. The fraction of the immobilised component at a given pH was not significantly dependent on different model systems, except for the case of high salt concentration, which shows a slight increase at pH 6.0.

The temperature dependence of the immobilised component of the spin-labeled A49C coat protein mutant isolated in 25 mM sodium cholate at pH 7.0 and reconstituted in DOPC bilayers (L/P 200) at pH 6.0 is represented by the outer hyperfine splitting $2A_{max}$, as given by Fig. 3. The line shape of the two components was temperature dependent. This makes it
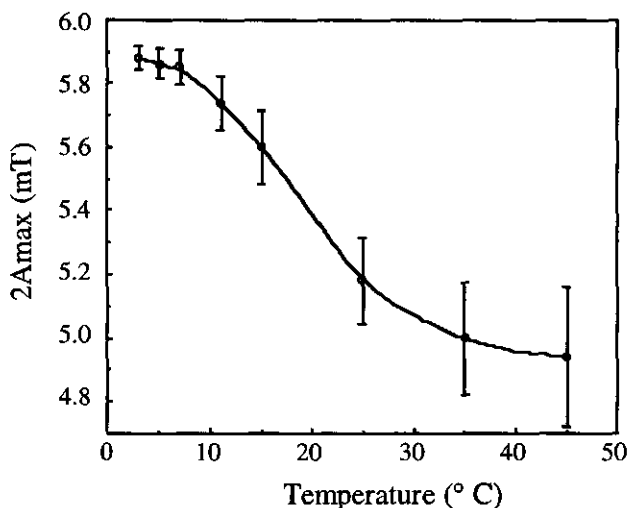
43

FIGURE 3: Outer hyperfine splitting, $2A_{max}$ of the immobilised component in the spin-labeled A49C coat protein mutant isolated in 25 mM sodium cholate and reconstituted in DOPC L/P 200 at pH 6.0, as a function of the temperature.

very difficult to determine the fraction of the immobilised component at higher temperatures. However, the outer hyperfine splitting $2A_{max}$, which could be identified up to about 45 °C, was used instead in Fig. 3 to characterize the motional freedom of the motionally restricted spin probes. The temperature effect was fully reversible upon decreasing the temperature, indicating that no irreversible conformational change occurred during the temperature scan.

In all cases, the secondary structure of the coat protein in micellar samples was determined with CD. Within experimental error, no change in the spectral intensity or in the line shape was found between samples containing the coat protein isolated in sodium cholate at pH 7.0 and 10.0. The aggregational state of the protein was checked by sodium cholate-HPSEC. The protein cholate complex at 100 mM sodium cholate was eluted from the column as a protein dimer peak for both pH 7.0 and pH 10.0 samples (data not shown). The aggregational states of the EDC cross-linked major coat protein isolated in sodium cholate at pH 7.0, and pH 10.0 and analysed with SDS-PAGE are given in Figure 4. After EDC cross-linking, the major coat protein isolated at pH 7.0 was a mixture of monomers and dimers; at pH 10.0, it was monomeric.
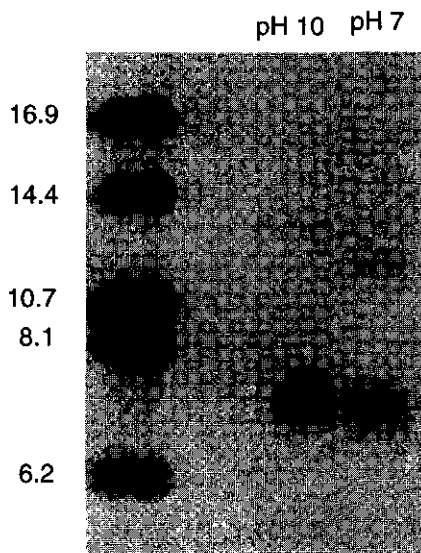
44

FIGURE 4: EDC-dependent cross-linking of the spin labeled A49C major coat protein mutant isolated in 25 mM sodium cholate at pH 7.0 and 10.0 at room temperature. The aggregational state was analyzed by Tricine-SDS-PAGE.

Additional experiments were carried out with spin-labeled T36C coat protein mutant isolated in 25 mM sodium cholate at pH 7.0 and 10.0. The spin label at position 36 is located in the transmembrane α-helical domain of the protein, and has a powder-like appearance with little segmental motion, as discussed previously (Stopar et al., 1996). The spectra of spin-labeled T36C mutant isolated in 25 mM sodium cholate at pH 7 and 10 are given in Figure 5. The high and low field peaks in the spectrum of the spin-labeled T36C mutant isolated at pH 10 are slightly line broadened as compared to the spectrum at pH 7. To characterise the mobility of the spin label, the outer hyperfine splitting $2A_{max}$ was measured from the ESR spectra. The motion of the spin-labeled coat protein was slightly reduced when the protein was isolated in sodium cholate at pH 7.0, giving a value for $2A_{max}$ of 6.30 mT, as compared to 6.12 mT for the protein isolated at pH 10.0 (data not shown).

To further characterize the properties of the coat protein isolated in sodium cholate at pH 7.0 and 10.0, the A49C coat protein mutant was labeled with the fluorescence label IAEDANS. The fluorescence wavelength emission maximum of IAEDANS is indicative for
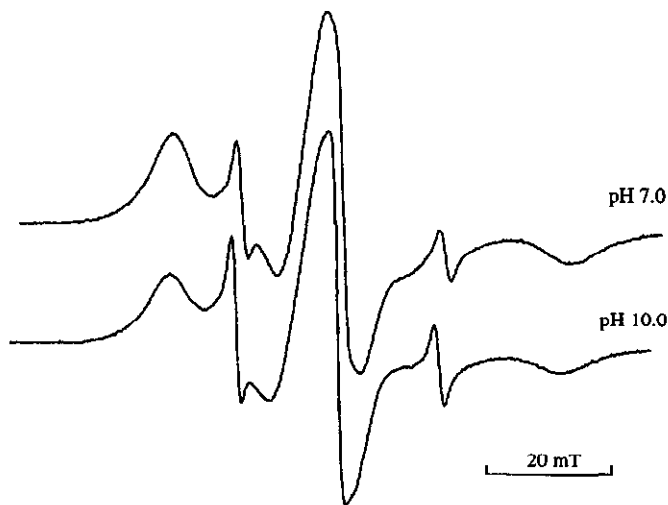
45

FIGURE 5: ESR spectra of spin-labeled T36C major coat protein isolated in 25 mM sodium cholate at pH
7.0 and 10.0. Spectra were recorded at room temperature and normalized to the same central line height.

the environment of the fluorophore (*i.e.* hydrophobic vs aqueous) as discussed previously
for M13 coat protein mutants (Spruijt et al., 1996). The wavelengths of emission maximum
for the coat protein isolated in 50 mM sodium cholate at pH 7.0 and pH 10.0 are given in
Table 2.

The accessibility of the AEDANS-labeled coat protein to a quencher depends on the
polarity of the fluorophore environment as well as steric effects (Mandal & Chakrabarti,
1988). To assess the steric effects imposed on the AEDANS-labeled coat protein isolated in
sodium cholate at pH 7.0 (more hydrophobic environment) and at pH 10.0 (more
hydrophilic environment), quenching studies were performed with acrylamide, which is a
neutral quencher molecule. The accessibilities of fluorescence-labeled coat protein at both
pH values are given in the Stern-Volmer plot shown in Fig. 6. The quenching of the
AEDANS-labeled coat protein at pH 7 by acrylamide was very low which is consistent with
AEDANS labels being substantially protected from the solvent. In contrast, the quenching
by acrylamide at pH 10.0 indicates that AEDANS labels are more accessible for the
acrylamide, providing additional evidence for a change in the environment of the
fluorescence label at increased pH.

46

TABLE 2: Wavelength emission maximum of AEDANS-labeled A49C coat protein mutant isolated in 50 mM sodium cholate at pH 7.0 and/or pH 10.0, and subsequently reconstituted in DOPC bilayers (L/P 200) at pH 6.0 and/or pH 10.0.

coat protein	wavelength max. (nm)		
isolation	sodium cholate	DOPC, pH 6.0	DOPC, pH 10.0
pH 7.0	484	489	492
pH 10.0	497	491	491
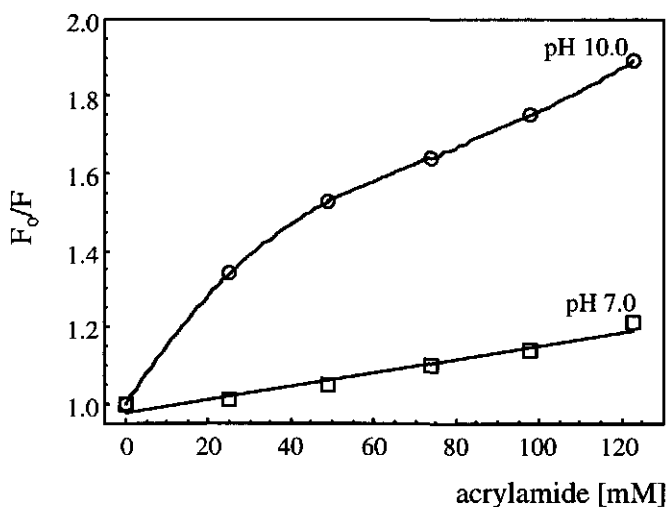
FIGURE 6: Quenching of the AEDANS-labeled A49C coat protein mutant with acrylamide in 50 mM sodium cholate at pH 7.0 and 10.0.

In addition, ADEANS-labeled coat protein isolated in 50 mM sodium cholate at pH 7.0 and 10.0 was also quenched with spin-labeled A49C coat protein mutant isolated in sodium cholate at pH 7.0 or 10.0. The fluorescence intensity after mixing at a molar ratio of spin-labeled to fluorescence-labeled coat protein of 1/1 (mol/mol) was reduced by 12% for the coat protein isolated in sodium cholate at pH 7.0. In contrast, the fluorescence intensity was reduced by 5% in the case coat protein was isolated in sodium cholate at pH 10.0 (data not shown).

Discussion

The aggregational state of the major coat protein in micellar model systems has been investigated previously (Makino et al., 1975; Nozaki et al., 1976; Spruijt et al., 1989; Henry & Sykes, 1990; Sanders et al., 1991; Spruijt & Hemminga, 1991). It was also shown that mutant M13 coat proteins can exist in a range of conformational and aggregational states depending uniquely upon mutation type and locus [for a review see Li et al. (1993) and Williams et al. (1995)]. In this paper, we report the *in situ* aggregational states of labeled mutant coat protein, as a model for wild type coat protein, solubilized in sodium cholate and reconstituted in lipid bilayers. This requires that the mutation and labeling do not significantly change the properties of the protein. Previously we have demonstrated that, concerning the conformational and aggregational properties, the mutant coat proteins are indistinguishable from the wild type M13 coat protein (Stopar et al., 1996). This means that labeled mutant coat protein can thus be used as a model system to characterize the aggregational behaviour of the coat protein in a membrane environment.

The ESR spectra of the spin-labeled A49C major coat protein mutant in DOPC bilayers isolated in 25 mM sodium cholate at pH 7.0 and reconstituted into DOPC at various pH values are shown in Fig. 1. The two components in the ESR spectra that are seen at pH values below about 8.0 are typical for a mixture of immobilized and mobile spin labels. The two spectral components are clearly separated, and the line shape of the immobile component indicates that there is no fast exchange between the components at a time scale of about 10^{-7} s (Horváth et al., 1988). Further evidence for this observation follows from the multiple non-baseline isoclinic points in the ESR spectra. These points indicate that the spectra are composed of a pH-dependent linear combination of the two components (Marriott & Griffith, 1974). Although the spin labels in the immobilised component are significantly restricted in motion, they still have some anisotropic motion on the ESR time scale. This is deduced from the value of the outer hyperfine splitting $2A_{max}$ of 5.93 mT, which is significantly less than the rigid limit value of nitroxide radicals, which is about 6.7 mT in an aqueous environment. This relatively fast anisotropic motion probably arises from the local motion of the spin label and the cysteine side chain on which it is attached, whereas the segmental mobility of the C-terminal polypeptide chain is restricted. The mobile, isotropic component in the spectrum suggests a large segmental flexibility of the C-terminal part of the coat protein mutant, which will additionally lead to an increased local side chain motion of the spin-labeled cysteine.

Similar effects are found for the spin-labeled A49C coat protein mutant solubilized in sodium cholate: on increasing the pH from 6.0 to 10.0, the immobile component completely

disappears. A very striking observation is that the disappearance of the immobile component in bilayers as well as in sodium cholate is completely irreversible: on decreasing the pH from 10.0 to 6.0, the immobile component does not reappear. In contrast, the temperature dependence of the immobilised component of the spin-labeled A49C coat protein mutant at pH 6.0, as represented by the outer hyperfine splitting $2A_{max}$ (see Fig. 3), is fully reversible.

The following questions now arise: what limits the motion of the spin label in samples at low pH, and what causes this irreversible pH effect? To solve these questions, it is most helpful to consider first the situation of the coat protein solubilized in sodium cholate. According to HPSEC experiments in 100 mM sodium cholate at pH 7.0, it is found that the protein at most has a dimeric state (Spruijt et al., 1989). Cross-linking experiments for the protein isolated at pH 7.0 (see Figure 4) further indicate that the protein has more tendency to cross-link, due to a closer proximity of the two proteins in the sodium cholate micelle. From the spin label experiments, it follows that under these conditions the spin label senses two different states of motion. This indicates that the two protein monomers in the dimer are asymmetric with respect to each other, and have different states of the C-termini: one monomer has a C-terminal part with a large amplitude of motion, whereas the C-terminus of the other monomer is strongly reduced in motion. This reduced motion roughly reflects the overall motion of a sodium cholate micelle containing two protein molecules (the rotational correlation time τ_c is estimated to be about 10 ns in pure water). These two states are consistent with a model where the proteins are dissolved from the phage particle as parallel dimers slide with respect to each other for about 1.6 nm. This dimer will be labeled as "structural dimer". In this state, the C-terminus of one monomer is sticking out in the aqueous phase and reflects a large motion, whereas the C-terminus of the other protein must be strongly limited in motion by very specific interactions with the neighbouring protein molecule. This protein-protein interaction will limit the segmental flexibility of the C-terminus and result in the immobile component in the ESR spectrum. This model is depicted in Fig. 7A. The distance between axes of nearest neighbours in the phage particle, in the index notation used by Marvin et al. (1994), is similar in both the 0 to 6 and 0 to 11 directions. However, in the 0 to 11 direction, the α-helices make an angle with respect to each other (-18 °), whereas in the 0 to 6 direction the α-helices are nearly parallel (-5 °). Also in the 0 to 6 direction strong interlocking of the apolar side chains of the coat protein molecules occurs. Therefore, it is hypothesized that during the sodium cholate solubilization at pH 7.0, the coat protein dissolves from the phage particle as 0-6 dimers with the same orientation as in the phage. This also explains the unusually strong association properties of the "structural dimer" in sodium cholate. This furthermore indicates that at pH 7.0 the
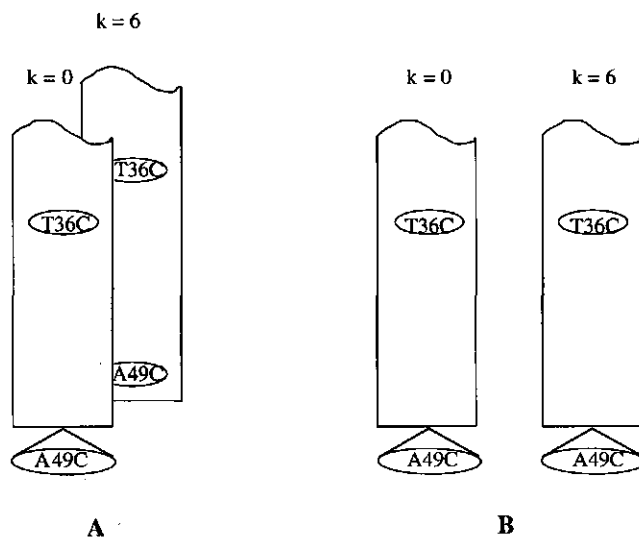
49

FIGURE 7: Schematic representation of a part of the transmembrane helix and C-terminus of the coat protein. (A) "Structural dimer" in sodium cholate micelles at pH 7.0. The two proteins are shifted relative to each other about 1.6 nm, similar to that found in the phage. (B) Disrupted structural dimer in sodium cholate micelles at pH 10.0. In this case, the two proteins are symmetric and in line with each other. The residues that are immobilised in the ESR spectra are indicated by numbered ellipses. The residues that are mobile are indicated by cones. The index k refers to the coat protein numbering in the phage as given by Marvin et al. (1994).

solubilization power of sodium cholate is not strong enough to disrupt the 0-6 dimer interactions in the phage.

The situation described above at pH 7.0 reflects the state of the coat protein at high sodium cholate concentration (100 mM). From the ESR results, it is found that the fraction of the immobilised component increases at lower cholate concentrations. This can be explained by the formation of tetramers of the coat protein in the micelle as shown previously (Spruijt et al., 1989). The increased fluorescence quenching with spin-labeled coat protein at pH 7.0 is consistent with such an increased protein aggregation.

At pH 10, the immobile component is absent from the spectra. This is consistent with the absence of the specific dimer protein-protein interaction in cross-linked samples at pH 10.0 (see Figure 4). Nevertheless, sodium cholate micelles still contain two protein monomers,

50

as deduced from HPSEC elution profiles of non cross-linked samples. In this case, the dissociated dimer exists as two protein molecules within the same micelle, and the two spin labels in the monomers must experience an identical environment, because there is no second component present. However, there are many orientations of the two proteins in the micelle, which would satisfy this condition. One of the possible orientations, which may be of relevance for the lipid bilayer situation is depicted in Figure 7B.

Although the two proteins in Figure 7B are relatively close to each other, the spectra of spin-labeled A49C coat protein isolated in sodium cholate at pH 10.0 do not indicate extensive spin-spin broadening. This is consistent with a high mobility of the spin-labeled A49C protein, which effectively averages out the dipolar spin-spin interactions. In addition, different possible orientations of the two proteins in the micelle would further reduce spin-spin exchange by reducing the spin collision frequency. The outer splitting of the spin-labeled T36C protein isolated in sodium cholate at pH 10.0 has decreased as compared to the protein isolated in sodium cholate at pH 7.0 (see Figure 5). In addition, the outer lines in the spectrum at pH 10.0 are slightly broadened. The reduction of the outer splitting and the broadening effect may arise from an incomplete averaging of the powder components in the line shape, due to an increase of molecular motion after disruption of the "structural dimer". Part of the observed broadening may also arise from spin-spin interactions, but in the absence of any effect of dilution with wild type protein on the ESR line shape, this effect is probably small.

The mobility and hydrophilic environment of the spin-labeled and fluorescence-labeled A49C coat protein mutant isolated in sodium cholate at pH 10.0 are consistent with an aqueous environment. In sharp contrast, the reduced C-terminal flexibility, the increased hydrophobicity of the AEDANS-labeled A49C coat protein mutant, and AEDANS protection from acrylamide quencher of the coat protein isolated in sodium cholate at pH 7.0 indicate that a significant number of the C-termini are in a different environment (see Table 2). Such an environment can easily be found in the structural protein dimer as discussed above.

The coat protein solubilized in sodium cholate and subsequently reconstituted into lipid bilayers has qualitatively the same aggregational tendency, suggesting that the aggregational states of the protein in two model systems are comparable. Moreover, structural dimers reconstituted into lipid bilayers at low pH show a tendency to form tetramers (increased immobilised component), and can be solubilized by the surrounding lipids only when the pH is increased. In the absence of titratable groups of DOPC in the experimental pH range, this indicates that the solubilization process is induced primarily by changing titratable groups of the major coat protein. It is a remarkable finding that the lipid membrane can

51

accommodate the structural dimers, as shown in Fig. 7A. This indicates that the coat protein in the structural dimer has the unique ability to change its conformation and topology to adapt to the water-membrane interface, and to cope with the hydrophobic forces within the membrane. In the case of the coat protein solubilized in sodium cholate micelles at pH 10.0, the structural dimers have been disrupted, and two identical protein monomers are observed, that stay together in the micelles (Fig. 7B), probably because of the relatively weak solubilizing properties of sodium cholate. When the coat protein is reconstituted in lipid bilayers at pH 10.0, these disrupted dimers no longer exist, and the protein behaves as separate monomers, as has been found in previous work (Spruijt & Hemminga, 1991).

From the experiments shown in Table 1, it is found that the fraction of the immobilised component of the spin-labeled A49C coat protein mutant is not strongly dependent upon the ionic strength and the presence of DOPG in mixed DOPC/DOPG bilayers. This result further indicates that the reduction of spin label motion is not caused by a specific lipid effect. At pH 7.0, the coat protein has net charge of +1. By increasing the pH, the net charge of the protein will eventually become negative, for example, by deprotonating the lysine residues ($pK_a \approx 10.0$). This will give an increase in the net electrostatic repulsion between the protein molecules in the dimers, in competition with the hydrophobic interactions. At pH 10.0, this explains the complete dissociation of the structural protein dimer, in favour of protein-amphiphile interactions. However, the molecular details of this process are still missing.

The results in this paper illustrate the sequence of events during phage disruption with sodium cholate. Sodium cholate is a flat hydrophobic molecule with a weak solubilizing power. It can disrupt the phage particle only when the rigid phage structure is "loosened" with chloroform (Makino et al., 1975). Upon disruption of the loosened phage particle, it may be expected that sodium cholate disrupts the weak hydrophobic forces between the coat proteins by removing patches of parallel oriented coat protein, which turn up as "structural dimers" in sodium cholate at a low pH value. It may be expected that the "structural dimers" can reversibly aggregate, depending upon the sodium cholate concentration (Spruijt et al., 1989). At high sodium cholate concentration, however, the "structural dimer" is the smallest possible protein aggregate. The last step in coat protein solubilization is a disruption of the "structural dimer". In sodium cholate, this process only takes place at an increased pH. This also implies that the pH should be increased to at least pH 10.0 during sodium cholate protein isolation or in lipid bilayer reconstitution, if one wants to study the monomeric form of the major coat protein in lipid bilayers.

Our data suggest that during disruption of the phage particle in sodium cholate at pH 7.0, the protein is solubilized as a "structural dimer", and that after increasing the pH to 10.0 this

dimer is further disrupted. Clearly, at pH 7.0 phage disruption is not complete. There are, however, no experimental data available about the conformational state of the protein, or local pH values in the cytoplasmic membrane during phage disassembly. Apparently, *in vivo* complete dissociation of the coat protein can be achieved, because parental coat proteins can be reutilized in the assembly process (Smilowitz, 1974). This is believed to be a monomeric process (Russel, 1991). Furthermore, prior to assembly of the coat protein in the virus particle, neighbouring α-helix units cannot have the same side-chain interlocking as in the assembled phage, because the formation of the original "structural dimer" in micelles and lipid bilayers turns out to be impossible. As suggested by Russel (1993), the interaction with the gene I product is likely to play a key role in bringing the major coat protein to the phage assembly site. At the assembly site, coat proteins are extruded from the membrane lipids in a controlled fashion by the virus assembly machinery, preventing aspecific protein aggregation in the membrane. Such a lipid-free monomer could then interact with the protein coat previously added to the elongating phage particle. To obtain the final side-chain interlocking in the virus particle, extrusion of the new phage through the membrane and addition of the coat protein must be correlated in such a way that the extruding phage moves 1.6 nm out of the plane of the membrane before the next coat protein is added.

References

Andersen, J. P., Fellmann, P., Møller, J. V., & Devaux, P. F. (1981) *Biochemistry 20*, 4928-4936.

Bittman, R., Sakaki, T., Tsuji, A., Devaux, P. F., & Ohnishi, S.-I. (1984) *Biochim. Biophys. Acta 769*, 85-95.

Devaux, P. F., & Seigneuret, M. (1985) *Biochim. Biophys. Acta 822*, 63-125.

Hemminga, M. A., Sanders, J. C., Wolfs, C. J. A. M., & Spruijt, R. B. (1993) in *Protein-Lipid Interactions*, New Comprehensive Biochemistry, 25 (Watts, A., ed.) pp. 191-212. Elsevier, Amsterdam.

Henry, G. D., & Sykes, B. D. (1990) *J. Mol. Biol. 212*, 11-14.

Horváth, L. I., Brophy, P. J., & Marsh, D. (1988) *Biochemistry 27*, 46-52.

Hubbell, W. L., & Altenbach, C. (1994) *Curr. Opin. Struct. Biol. 4*, 566-573.

Knippers, R., & Hoffmann-Berling, H. (1966) *J. Mol. Biol. 21*, 281-292.

Li, Z., Glibowicka, M., Joensson, C., & Deber, C. M. (1993) *J. Biol. Chem. 268*, 4584-4587.

Makino, S., Woolford, J. L. Jr., Tanford, C., & Webster, R. E. (1975) *J. Biol. Chem. 250*, 4327-4332.

Mandal, K., & Chakrabarti, B. (1988) *Biochemistry 27*, 4564-4571.

Marriott, T. B., & Griffith, H. O. (1974) *J. Magn. Reson. 13*, 45-52.

Marsh, D. (1981) in *Membrane Spectroscopy* (Grell, E., ed.) pp. 51-142. Springer-Verlag, Berlin ,Heidelberg, and New York.

Marvin, D. A., Hale, R. D., Nave, C., & Citterich, M. H. (1994) *J. Mol. Biol. 235*, 260-286.

McDonnell, P. A., Shon, K., Kim, Y., & Opella, S. J. (1993) *J. Mol. Biol. 233*, 447-463.

Nozaki, Y., Chamberlain, B. K., Webster, R. E., & Tanford, C. (1976) *Nature 259*, 335-337.

Nozaki, Y., Reynolds, J. A., & Tanford, C. (1978) *Biochemistry 17*, 1239-1246.

Russel, M. (1991) *Mol. Microbiol. 5*, 1607-1613.

Russel, M. (1993) *J. Mol. Biol. 231*, 689-697.

Sanders, J. C., Haris, P. I., Chapman, D., Otto, C., & Hemminga, M. A. (1993) *Biochemistry 32*, 12446-12454.

Sanders, J. C., Van Nuland, N. A. J., Edholm, O., & Hemminga, M. A. (1991) *Biophys. Chem. 41*, 193-202.

Schägger, H., & Von Jagow, G. (1987) *Anal. Biochemistry 166*, 368-379.

Smilowitz, H. (1974) *J.Virol. 13*, 94-99.

Spruijt, R. B., & Hemminga, M. A. (1991) *Biochemistry 30*, 11147-11154.

Spruijt, R. B., Wolfs, C. J. A. M., & Hemminga, M. A. (1989) *Biochemistry 28*, 9158-9165.

Spruijt, R. B., Wolfs, C. J. A. M., Verver, J. W. G., & Hemminga, M. A. (1996) *Biochemistry 35*, 10383-10391.

Stopar, D., Spruijt, R. B., Wolfs, C. J. A. M., & Hemminga, M. A. (1996) *Biochemistry 35*, 15467-15473.

Tanford, C., & Reynolds, J. A. (1976) *Biochim. Biophys. Acta 457*, 133-170.

Williams, K. A., Glibowicka, M., Li, Z., Li, H., Khan, A. R., Chen, Y. M. Y., Wang, J., Marvin, D. A., & Deber, C. M. (1995) *J. Mol. Biol. 252*, 6-14.

Wolkers, W. F., Spruijt, R. B., Kaan, A., Konings, R. N. H., & Hemminga, M. A. (1997) *Biochim. Biophys. Acta 1327*, 5-16.

Woolford, J. L., Jr., Cashman, J. S., & Webster, R. E. (1974) *Virology 58*, 544-560.

Chapter 4

Local Dynamics of the M13 Major Coat Protein in Different Membrane-Mimicking Systems

David Stopar, Ruud B. Spruijt, Cor J.A.M. Wolfs, and Marcus A. Hemminga

Abstract

The local environment of the transmembrane and C-terminal domain of M13 major coat protein was probed by site-directed ESR spin labeling when the protein was introduced into three membrane-mimicking systems, DOPC vesicles, sodium cholate micelles, and SDS micelles. For this purpose, we have inserted unique cysteine residues at specific positions in the transmembrane and C-terminal region, using site-directed mutagenesis. Seven viable mutants with reasonable yield were harvested: A25C, V31C, T36C, G38C, T46C, A49C, and S50C. The mutant coat proteins were indistinguishable from wild type M13 coat protein with respect to their conformational and aggregational properties. The ESR data suggest that the amino acid positions 25 and 46 of the coat protein in DOPC vesicles are located close to the membrane-water interface. In this way the lysines at position 40, 43, and 44 and the phenylalanines at position 42 and 45 act as hydrophilic and hydrophobic anchors, respectively. The ESR spectra of site specific maleimido spin-labeled mutant coat proteins reconstituted into DOPC vesicles, and solubilized in sodium cholate or SDS indicate that the local dynamics of the major coat protein is significantly affected by its structural environment (micellar vs. bilayer), location (aqueous vs. hydrophobic), and lipid/protein ratio. The detergents SDS and sodium cholate sufficiently well solubilise the major coat protein and largely retain its secondary structure elements. However, the results indicate that they have a poorly defined protein-amphiphilic structure and lipid-water interface as compared to bilayers and thus are not a good substitute for lipid bilayers in biophysical studies.

Introduction

M13 is a small filamentous bacteriophage that consists of approximately 2700 copies of the gene VIII product, arranged in a helical, cylinder-like coat along a circular single-stranded DNA (Russel, 1991; Marvin et al., 1994). During infection of *Escherichia coli* cells, bacteriophage M13 leaves its major coat protein in the cytoplasmic membrane. Together with newly synthesised coat proteins, it is used for the assembly of the new phage particles at the membrane-bound assembly site (Smilowitz et al., 1972; Russel, 1991; Hemminga et al., 1993). The primary sequence of the coat protein must be such to allow protein-protein and protein-DNA interactions for the coat protein in the phage, and protein-lipid interactions for the membrane-bound M13 coat protein (Hemminga et al., 1992). The relevant part of the primary sequence of M13 coat protein is shown in Fig. 1.

The secondary structure of the major coat protein has been extensively studied in micellar model systems by various NMR techniques (Henry et al., 1987; Henry & Sykes, 1992; McDonnell et al., 1993; Van de Ven et al., 1993). It is, however, interesting to note that there exists a remarkable discrepancy between the predicted transmembrane domain and the NMR assigned transmembrane helix of the protein in micellar systems (see Fig. 1). Various hydropathy calculations predict different hydrophobic domain stretches ranging from Glu20 to Thr46 depending on the hydropathy scale and subsequent calculational strategies (for an evaluation see Turner & Weiner, 1993). Especially, the membrane-water interface at the C-terminus of the major coat protein is poorly defined, mainly because of the presence of three positively charged lysine residues, which are intercalated between apolar aromatic phenylalanine residues (Turner & Weiner, 1993). Most hydropathy calculations suggest that Phe42 and Phe45 are located in an unfavorable hydrophilic environment. This is unlikely, since aromatic amino acids are often found near the lipid-water interface, where they anchor the protein in the membrane (Deisenhofer et al., 1985; Weiss et al., 1991). The NMR data, on the other hand, suggest a firm α-helix between Tyr24 and Phe45 in SDS micelles leaving only the last four to five amino acids in the C-terminus unstructured (Henry et al., 1987; Henry & Sykes, 1992; McDonnell et al., 1993; Van de Ven et al., 1993). From binding studies, is also known that when a peptide associates with a membrane interface, the probability of secondary structure formation increases drastically, because the interface restricts the degrees of freedom of the peptide (White & Wimley, 1994). Therefore the predicted transmembrane domain in the C-terminal part of the major coat protein may be shifted up to Thr46. When a transbilayer phosphate to phosphate distance of 4.5 nm is taking into account, the membrane could easily accommodate more than 20 amino acid residues (Altenbach et al., 1994).
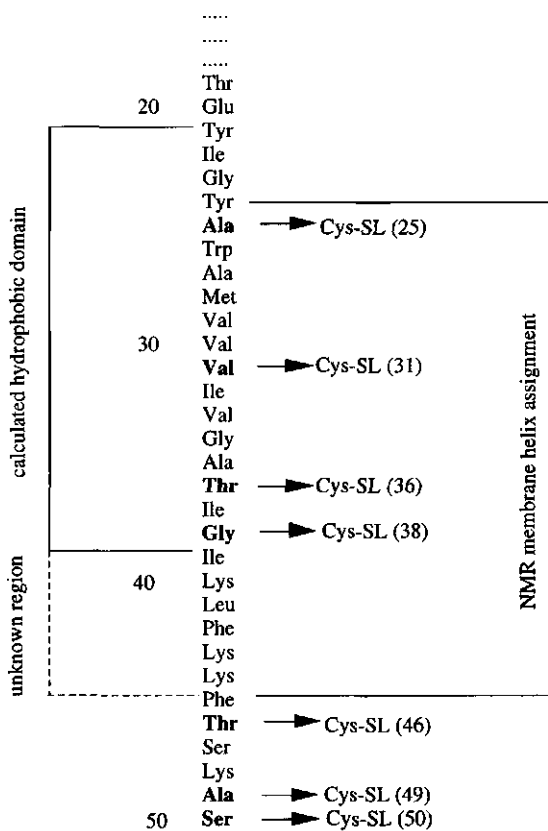
FIGURE 1. Part of primary structure of M13 gene VIII product (major coat protein) with calculated hydrophobic domain and unknown region (dotted line) (Makino et al., 1975) and helix assignment as found from NMR (Chamberlain & Webster, 1978; Brotherus et al., 1981; Cross & Opella, 1985). Bold type amino acid residues are mutated to cysteine residues and used for ESR spin labeling. SL indicates the spin label 3-maleimido proxyl that is used in the spin labeling experiments.

Two widely accepted membrane model systems for biophysical studies are detergent micelles and lipid bilayers. Lipid bilayers are more appropriate to mimic the typical structure of a biological membrane, due to its well characterised structure. Most of the structural determination on the major coat protein, however, has been carried out in micellar systems, mainly in SDS (Cross & Opella, 1980; Henry et al., 1987; Henry & Sykes, 1992; McDonnell et al., 1993; Van de Ven et al., 1993). Therefore, it is interesting to compare the conformational state of the protein in lipids with well described state of the protein in

57

micellar systems. For this reason, a site-directed spin-labeling approach for membrane-embedded M13 coat protein is followed in this paper. A similar approach for the major coat protein has been followed recently by Khan & Deber (1995) and Wolkers et al. (1997).

Analysis of the ESR line shape of the spin-labeled mutants provides direct information about the motional properties of the spin label that reflect the local structure of the protein. Since M13 major coat protein contains no cysteine residues, we have introduced unique cysteine residues at selected position along the protein primary structure. For this substitution the following strategy was chosen: (1) Mutant bacteriophages must be viable; this ensures that the mutation causes a minimal perturbation of the native secondary structure and is thus a good representative of the wild type coat protein; (2) Mutations should be located in different topological domains of the coat protein, *i.e.* membrane-embedded positions as compared to positions in the aqueous phase.

In this paper ESR experiments have been carried out on spin-labeled major coat protein mutants, reconstituted into phospholipid bilayers of DOPC, and solubilized in sodium cholate and SDS micelles. Our data suggest that amino acid 25 and 46 of the coat protein are located close to the membrane-water interface. The local dynamics of the spin-labeled protein is significantly affected by its structure and local environment, and there are marked differences in local dynamics between DOPC and SDS. These results agree with a parallel study carried out by Spruijt et al. (1996), in which cysteine mutants of the M13 coat protein were employed for fluorescent labeling and reactivity studies with DTNB.

Materials and Methods

Chemicals. DOPC, DOPG, CL, sodium cholate and DTNB (Ellman's Reagent) were obtained from Sigma. SDS was purchased from Merck. Mutagenic oligonucleotides were synthesized by Pharmacia Biotech. The spin label 3-maleimido proxyl was obtained from Aldrich Chemical Co. Poly(A) and oligophosphates 15 and 25 in length were purchased from Pharmacia Biotech and Sigma, respectively.

Preparation of cysteine-containing coat protein mutants. Single cysteine-containing major coat protein mutants were prepared as described previously (Spruijt et al., 1996). Mutant bacteriophages were grown to milligram quantities as described previously for wild type bacteriophage M13 (Spruijt et al., 1989). The primary structure of the mutant coat proteins was deduced from the DNA sequence as obtained from automated sequencing.

Solubilisation, labeling, and purification of the major coat protein in SDS and sodium cholate micelles. The SDS-isolated coat proteins were spin labeled with 3-maleimido proxyl

at a spin label to protein ratio of 3:1 (mol/mol) directly after disruption of the bacteriophage in 175 mM SDS, 150 mM NaCl, 10 mM Tris, 0.2 mM EDTA, pH 7.0. The labeling reaction was carried out at 37 °C and was stopped after 60 min by adding an excess of cysteine to the reaction mixture. The mixture was then applied to a Sephacryl S-300 column (3.7 x 65 cm) and eluted with 25 mM SDS, 150 mM NaCl, 10 mM Tris-HCl, and 0.2 mM EDTA, pH 8.0 to separate viral DNA and unbound spin label from the spin labeled coat protein. Fractions with an absorbancy ratio A_{280}/A_{260} greater than 1.5 were collected. Prior to the ESR measurements samples were concentrated by an Amicon stirring cell. The cholate-isolated coat proteins were prepared as described above with SDS replaced by 25 mM sodium cholate. Before storage at 4 °C, sodium cholate was added up to 50 mM to prevent possible protein aggregation. The amount of spin label bound to the coat protein after spin labeling was calculated after determination of the free thiol groups using DTNB.

Reconstitution of the major coat protein in the lipid bilayers. From the desired amount of lipid solution, chloroform was evaporated with nitrogen gas and subsequently dried under vacuum for at least two hours. The lipids were solubilized in a 50 mM sodium cholate buffer (150 mM NaCl, 10 mM Tris-HCl, and 0.2 mM EDTA, pH 8.0) by sonication for 1 min. The spin-labeled protein in 50 mM sodium cholate buffer and phospholipids were mixed to obtain the desired L/P (mol/mol) ratio. To avoid spin-spin interactions the mutant coat protein was diluted 10 times with unlabeled wild-type protein. Reconstitution was carried out by cholate dialyses at room temperature against a 100-fold excess buffer (150 mM NaCl, 10 mM Tris-HCl, 0.2 mM EDTA, pH 8.0) for a total of 48 hours changing the buffer every 12 hours. After dialysis, the samples were concentrated for ESR purposes as described by Sanders et al. (1991). To obtain multilamellar vesicles the samples were freeze-dried and resuspended with distilled water. For the purpose of poly(A) and oligophosphates binding studies, unilamellar vesicles with desired L/P (mol/mol) ratio were prepared by sonication and dialysis as described above and concentrated using ultracentrifugation (Beckman, 3 hours at 45000 RPM). These samples were not freeze-dried. The aggregational and conformational state of samples in the lipid bilayers as well as in SDS and sodium cholate micelles were checked using HPSEC (Spruijt et al., 1989). The L/P ratios and homogeneity in L/P ratios were determined after sample preparation as described previously (Spruijt et al., 1989). CD measurements were performed on a Jobin-Yvon Dichograph Mark V in the wavelength range 190-290 nm as described by Sanders et al. (1993).

Oligonucleotide and oligophosphates binding. For titration with poly(A) and oligophosphates, unilamellar vesicles were prepared as described above. The use of unilamellar vesicles ensures that all the added poly(A) and oligophosphates is able to bind to

the reconstituted coat protein in the vesicles. In the binding experiments, the desired amount of freshly prepared poly(A) or oligophosphates stock solution was added to a constant amount of coat protein reconstituted in vesicles.

ESR studies. Samples containing the labeled major coat protein solubilised in 50 mM sodium cholate buffer or 25 mM SDS buffer and reconstituted in unilamellar or multilamellar lipid vesicles, were filled up to 5 mm with sample in 100 μl glass capillaries and were accommodated within standard 4 mm diameter quartz tubes. ESR measurements were performed on a Bruker ESP 300E ESR spectrometer equipped with a 4103 TM microwave cavity at room temperature. The ESR settings were: 6.38 mW microwave power, 0.1 mT modulation amplitude, 40 ms time constant, 160 s scan time, 10 mT scan width, and 348.5 mT centre field. Up to 200 spectra were accumulated to improve the signal to noise ratio.

Results

Using the strategy described in the introduction, viable mutants with X-Cys substitutions at amino acid positions 25, 31, 33, 36, 38, 46, 47, 49, and 50, were harvested (Spruijt et al., 1996). For the purpose of our study, seven bacteriophage mutants with reasonable yield for biophysical studies (5-25% of wild type yield) were selected and grown to milligram quantities: A25C, V31C, T36C, G38C, T46C, A49C, and S50C. DNA sequence analysis indicated that in addition to the single cysteine residue incorporated at the desired position, the mutants A25C, T36C, G38C, T46C, and A49C have a second spontaneous mutation at amino acid 27: A27S. Mutant V31C has a unique cysteine mutation, while the S50C mutant has a second mutation N12D, which converts this coat protein into a closely related fd major. The efficiency of spin labeling the major coat protein with 3-maleimide proxyl spin label in 100 mM sodium cholate buffer was 50-95% for various mutents. This percentage was generally lower for the SH groups inside the predicted transmembrane domain. The labeling efficiency for the mutants reconstituted in SDS micelles was 10-20% lower as compared to sodium cholate micelles. The spin labeled mutant proteins reconstituted in DOPC vesicles were compared with the wild type M13 coat protein with respect to their homogeneity in L/P ratio, conformation, and aggregation properties. Sucrose density gradient centrifugation showed a single band, indicating that the samples were homogeneous in L/P ratio.
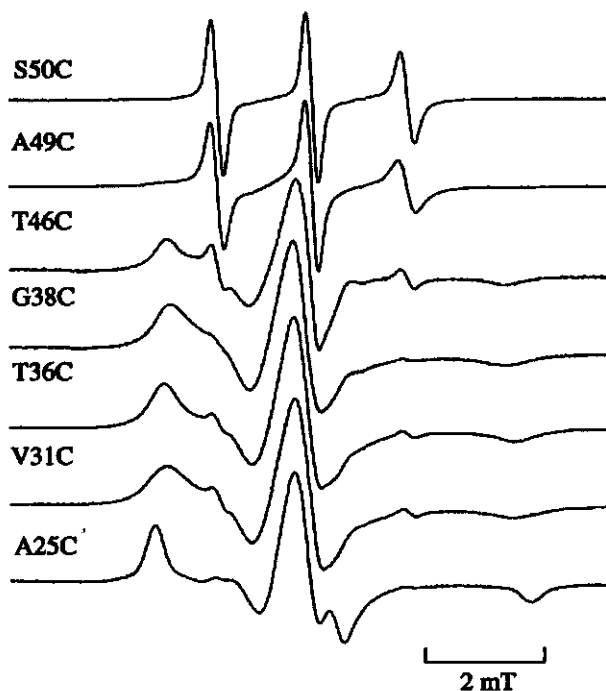
FIGURE 2. ESR spectra of 3-maleimido proxyl site-specific spin-labeled mutant coat proteins at various positions, reconstituted in DOPC multilamellar vesicles at L/P 35 in 150 mM NaCl, 10 mM Tris, and 0.2 mM EDTA at room temperature. Spectral line heights are normalised to each other.

HPSEC elution profiles showed that the spin labeled mutant coat proteins did not differ from the wild type proteins with respect to the aggregational properties. The CD spectra of the spin-labeled mutant proteins in sodium cholate micelles were comparable to those of unlabeled wild type M13 coat protein under the same conditions. Within experimental error the overall secondary structure of the mutant proteins is retained and indicative for an α-helical form (Spruijt & Hemminga, 1991; Sanders et al., 1993). This finding, together with the relatively high viability of the mutants also indicates that the second non-cysteine compensating mutation (A27C or N12D) does not significantly influence the conformation of the mutant coat protein.
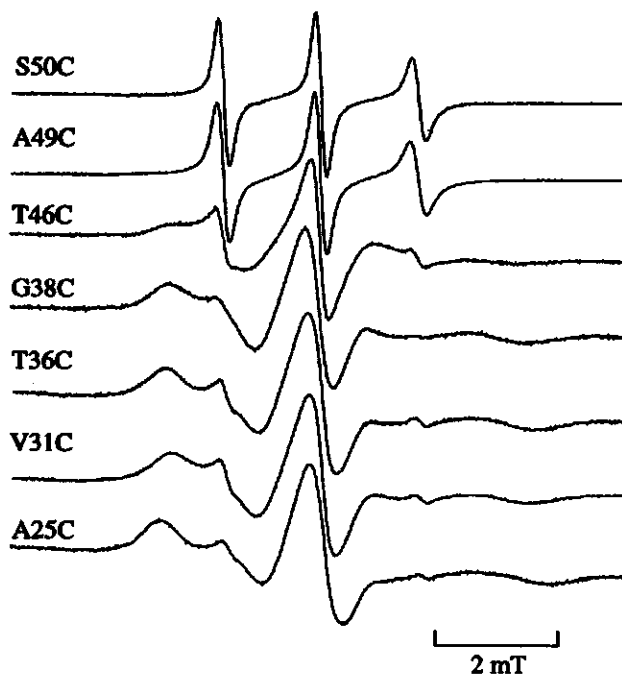
FIGURE 3. ESR spectra of 3-maleimido proxyl site-specific spin-labeled mutant coat proteins at various positions solubilized in 50 mM sodium cholate, 150 mM NaCl, 10 mM Tris, and 0.2 mM EDTA at room temperature. Spectral line heights are normalised to each other.

The ESR spectra of the various spin-labeled coat protein mutants, reconstituted into phospholipid bilayers of DOPC, and solubilized in sodium cholate and SDS are shown in Figs. 2-4, respectively. To characterize the ESR spectra, the rotational correlation time τ_c is used for the spin labels at positions 49 and 50 (see Table 1) that are characteristic for a fast isotropic motion. For the other spin-labeled mutant coat proteins, which have a powderlike appearance, the outer hyperfine splitting $2A_{max}$ is used as a relative measure of spin label mobility (see Fig. 5).

The ESR spectra of spin-labeled mutants that are solubilized in sodium cholate follow the same tendency as found in DOPC. However, the spectra are substantially more broadened, especially for the spin labels at positions 25 and 46. The ESR spectra of spin-labeled mutants that are solubilized in SDS micelles have a strongly reduced outer hyperfine splitting (Fig. 5). It is interesting to note that the spin labels at position 49 and 50, when
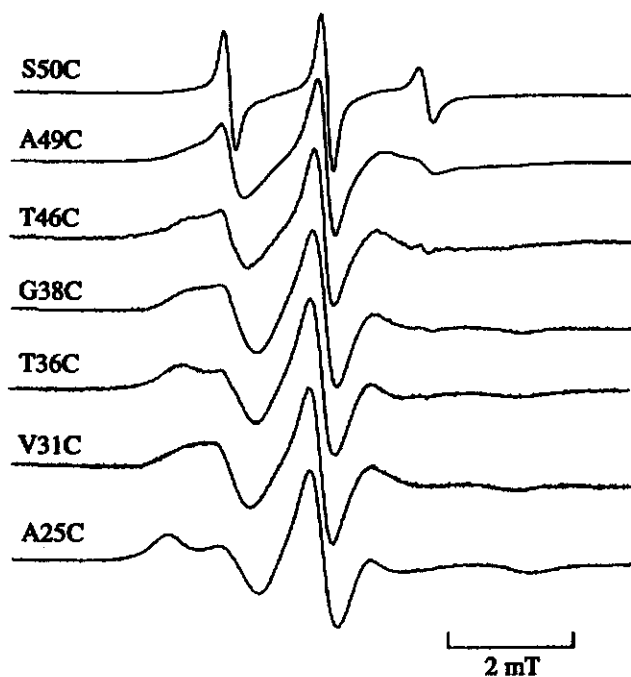
62

FIGURE 4. ESR spectra of 3-maleimido proxyl site-specific spin-labeled mutant coat proteins at various positions dissolved in 25 mM SDS, 150 mM NaCl, 10 mM Tris, and 0.2 mM EDTA at room temperature. Spectral line heights are normalised to each other.

reconstituted in DOPC and sodium cholate, are characteristic for a fast isotropic motion (see also Table 1), but are significantly reduced in mobility when solubilized in SDS micelles. In all model systems studied for the spin label at the position 36, a slightly increased outer hyperfine splitting is observed, indicating a higher local order parameter. This effect can be explained by the presence of the bulky side chains of Val33 and Ile39 one helix turn up and down position 36, respectively. This indicates that the local motion of spin labels attached to proteins can monitor the presence of amino acids, although this effect is small. In all model systems studied the spin label at position 25 has a distinct powder lineshape.

In the ESR spectra in Figs. 2-4, a small additional small spectral contribution with sometimes a large (5.7 mT) or a small (1.6 mT) hyperfine splitting can be observed,

Table 1. Rotational correlation times τ_c of 3-maleimido proxyl labeled mutant major coat protein A49C and S50C at room temperature in various model systems. The τ_c values are calculated from the spectra in Figs. 2-4 according to Marsh (1981).

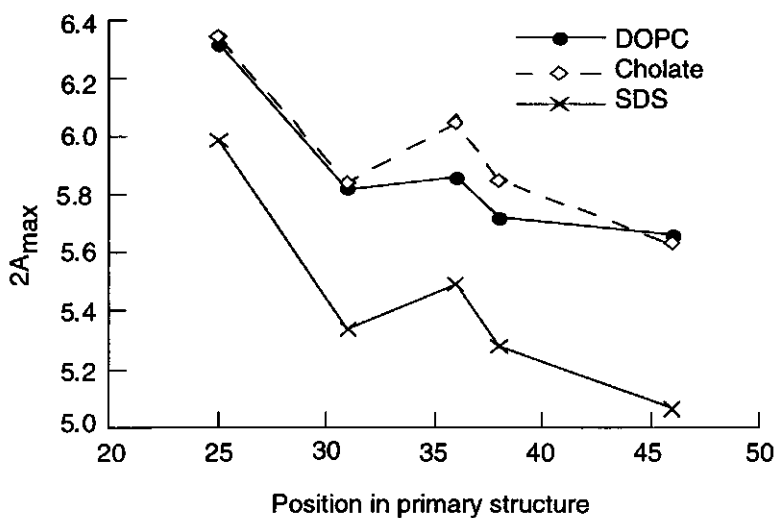| τ_c (ns)	DOPC	sodium cholate	SDS
A49C	0.88	0.55	≈ 10
S50C	0.40	0.41	0.70

FIGURE 5. Outer splitting in mT for the spin label ESR spectra in Figs. 2-4 at the various positions.

depending on the position of labeling. Such spectral components are also observed in samples of spin-labeled wild type M13 coat protein (data not shown), and can be attributed to spin-labeled terminal amino groups and ε-amino groups of lysines of the coat protein. No further attempts were made to subtract these components from the spectra.

To monitor the effect of the L/P ratio on the ESR spectra, the spin-labeled mutant coat proteins G38C, T46C and A49C were reconstituted in DOPC vesicles. The rotational correlation time τ_c was used to characterise the rotational mobility for the spin label at
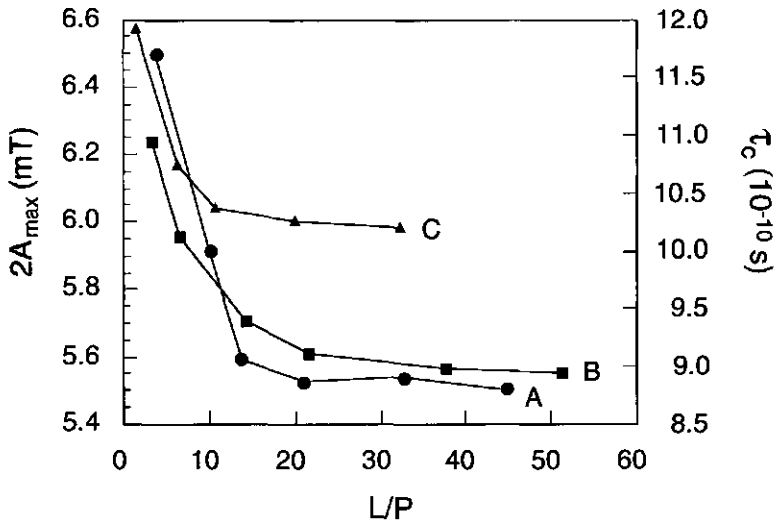
FIGURE 6. Variation of τ_c (right vertical scale) of maleimido spin label attached at position 49 (A), and $2A_{max}$ (left vertical scale) of the spin label attached at position 46 (B) and 38 (C) as a function of the L/P ratio.

position 49. The outer hyperfine splitting $2A_{max}$ was used for the spin labels at positions 38 and 46. Independent of the topological location of the spin label (*i.e.* membrane or aqueous), the same L/P dependence is obtained with a sharp change at an L/P ratio of about 15 (see Fig. 6). The observed decrease of the spin label motion at low L/P ratios can be explained by protein-protein interactions (Sanders et al., 1992). Therefore, all further studies were performed at L/P 20 or higher to avoid direct protein-protein interactions.

Upon reconstitution of the mutant coat proteins G38C, T46C, and A49C, which are expected to be close to the phospholipid head group region and located in the lysine-rich domain of the protein, into phospholipids (L/P > 20) with increasing negative charge: DOPC/DOPG (80/20 mol/mol), DOPC/CL (80/20 mol/mol), DOPG, and DOPG/CL (80/20 mol/mol), there are only small differences in the ESR line shape (data not shown).

Two spin-labeled mutant coat proteins, T46C and A49C, with the spin label located in the lysine-rich C-terminal domain of the protein, which is responsible for DNA binding in the virus particle, were also examined for possible binding effects of negatively charged molecules on their mobility. Spin-labeled mutant coat proteins reconstituted in unilamellar DOPC vesicles (L/P > 20) were titrated with oligophosphates and poly(A). Over a large range of nucleotide to protein ratios from 0 to 60 and NaCl concentrations from 15 to 150 mM, no effects on the spin label mobility could be detected (data not shown).

Discussion

Site-directed ESR spin labeling is used in this paper to probe the local dynamics of the M13 coat protein reconstituted in three membrane-mimicking systems. Seven mutants with relatively good yield were used, that cover the hydrophobic and the C-terminal part of the protein from amino acid position 25 to 50. With respect to the membrane-bound properties, the analysis of the structural and aggregational properties of the mutant coat proteins incorporated in phospholipid systems shows that the mutant proteins are indistinguishable from the wild type M13 coat protein. Thus site-specific mutagenesis results in functional mutant coat proteins with cysteines at locations representative of different topological domains in the major coat protein and a yield high enough to make them suitable for biophysical studies.

M13 coat protein in phospholipid bilayers. The ESR spectra of site-specific spin-labeled mutant coat proteins reconstituted in DOPC vesicles (Fig. 2) are indicative for a large range of molecular motions sensed by the maleimido spin label. The 3-maleimido proxyl spin label, which has a relatively small size and is due to its short linker close to the protein backbone, seems to represent well the different local environments of the protein. The high isotropic flexibility of the spin labels at positions 49 and 50 is in agreement with the absence of a rigid helical structure in this part of the C-terminal region as found by NMR spectroscopy of M13 coat protein solubilised in SDS (Henry & Sykes, 1992; McDonnell et al., 1993; Van de Ven et al., 1993). The isotropic hyperfine splitting is 1.58 mT, which is characteristic for a hydrophilic environment of the two spin labels (Fretten et al., 1980). As is shown in Fig. 6, the spin label at position 49 is sensing the presence of other protein molecules in DOPC bilayers at low L/P ratios. Although this effect is small (the decrease of τ_c is about 20%), this indicates that the mainly segmental motion of the spin label in the terminal protein part is influenced by adjacent termini. However, the packing of the C-termini of M13 coat protein at low L/P is not so dense, that the motion of the spin label is completely blocked.

The spectrum of the spin label attached to a cysteine at positions 31, 36, and 38 is typical for an immobilized spin label with an outer hyperfine splitting $2A_{max}$ of about 5.8 mT (see Fig. 5). This is, however, significantly less than for a rigid limit nitroxide spectrum ($2A_{max} \approx 6.40$ mT), suggesting that some relatively fast, probably anisotropic, motion is taking place. This observation is further confirmed by the large widths of the low and high field peaks in the spectrum. The line shapes are very similar to the spectrum of a phosphatidylcholine C-5 spin label in phospholipid systems with an outer splitting $2A_{max}$ of 5.86 mT and an order parameter of 0.8 (Griffith & Jost, 1976). This similarity indicates that

the anisotropic motion is taking place around the principal z-axis of the maleimido spin label. As has been discussed previously for the analysis of ESR and saturation transfer ESR spectra of maleimido spin labeled coat protein of the plant virus Cowpea Chlorotic Mottle Virus, such an anisotropic motion arises from a local motion of the maleimido spin label about the long axis of the molecule (Vriend et al., 1984; Hemminga & Faber, 1986). Therefore, we interpret the ESR spectrum as a fast wobbling motion of the maleimido spin label at the cysteine within a cone. From the estimated order parameter (≈ 0.8) it can be calculated that the total cone angle is about 40°.

The ESR spectra in Fig. 2 are recorded at an L/P ratio of 35. As is illustrated in Fig. 6, at this L/P ratio, direct protein-protein contacts are expected to give only a small contribution to the reduced motion of the spin label at positions 25, 31, 36, and 38 as compared to the spin label at position 49. Based on transmembrane helix prediction methods, it is well established that residues Ala25 to Gly38 of M13 coat protein are embedded in the hydrophobic part of lipid systems (Kyte & Doolittle, 1982; Turner & Weiner, 1993). Thus the immobilization of the spin label at positions 25 to 38 is in agreement with this concept, because there is a strong increase in local viscosity when going from the aqueous phase to the hydrophobic part of the lipid system. In addition, the presence of anisotropic motion is a strong indication for a reduced local flexibility provided by the presence of a helical protein structure.

It is interesting to note, that although position 46 is close to position 49, and predicted to be in the hydrophilic environment, the line shape of the spin label attached to a cysteine at position 46 is characteristic for an intermediate slow motion ($\tau_c \approx 10^{-8}$ - 10^{-9} s). Clearly, there is a mobility gradient in the C-terminal part of the coat protein reconstituted in DOPC vesicles with a dramatic decrease of local viscosity from position 49 to 46. This can be explained by assuming that the transmembrane domain of the coat protein coincides with the transmembrane helix as assigned by NMR. It was discussed previously in a parallel study using the accessibility of different fluorescence quenchers in fluorescence labeling studies on the major coat protein mutants (Spruijt et al., 1996) that position 46 is located close to the membrane interface. The spin label data are consistent with this conclusion.

A consequence of this finding is that Lys40, Lys43, and Lys44 are buried in the membrane. It is known that due to its long apolar side chain, a lysine can have its α-carbon in the membrane interior, while its positively charged ε-amino group is able to interact with the negatively charged phosphate groups of the phospholipids (Tanford & Reynolds, 1976; Hemminga et al., 1992). This is not unlikely, because of a high molar excess of phosphates in the phospholipid head groups. Since Lys40 is buried deeply in the membrane, distance measurements were carried out on a molecular model of the major coat protein, assuming an α-helical structure from Tyr24 to Thr46 using the computer program Insight II (Biosym

Technologies) on a Silicon Graphics. The bond lengths were kept fixed, while the bond angle between the α, β, and γ carbon of the lysines were allowed to change, without changing the overall structure of the model. These studies indicate that the ε-amino group of Lys40 is able to reach the phosphate groups of the head group region located around Thr46. The ε-amino groups of the side chains of Lys43 and Lys44 can reach the head group region more easily, or could even stick out into the aqueous phase. An interaction with the head group phosphates could also be possible for Lys48, which is present in the aqueous phase, but our results can not confirm this possibility.

The absence of any structural or motional effect of (oligo)phosphates and poly(A) titration on reconstituted spin-labeled M13 coat protein in DOPC is an additional argument for lysines interacting with lipid phosphates. We can not completely exclude weak electrostatic interactions of the C-terminal lysines with DNA in a membrane-bound form, however, they do not manifest themselves in change of the local motion of the protein. This supports the idea that lysines are buried in the lipid head group region, where they can interact with the large molar excess of proximal phosphates.

Another interesting feature of the C-terminal part of M13 coat protein is the presence of two aromatic residues Phe42 and Phe45. It has been described in the literature that aromatic residues play a key role in maintaining a stabile association of the proteins in membrane environment (Deisenhofer et al., 1985; Henderson et al., 1990; Weiss et al., 1991). Phe45, which is next to the 46 position in the phospholipid headgroup region, is also in an unfavorable environment, unless its aromatic side chain is sticking backwards into the membrane interior. Molecular modeling, as described above, shows that the aromatic side chain is probably located in the region of the glycerol moieties of the phospholipids. By combining these conclusions, it turns out that the C-terminal protein part is very well anchored, because the lysine and phenylalanine residues serve as hydrophilic and hydrophobic anchors, respectively. In the case that the protein tends to move up or down along a normal to the membrane surface, either the phenylalanine or the lysine residues would be in an unfavorable environment.

The proposed extension of the transmembrane domain disagrees with the hydrophathy profiles (Makino et al., 1975; Kyte & Doolittle, 1982), which predict that Thr46 is outside the membrane (Fig. 1). This discrepancy arises mainly, because the hydrophathy scales recognize lysine residues to be external to the membrane (Turner & Weiner, 1993).

In comparison with the other ESR lineshapes, the spectrum of the spin label at the position 25 is remarkable. In previous work of our group, it has been discussed that this spectrum arises from an anisotropic motion of the maleimido spin label about the principal z-axis of the nitroxide g-factor and hyperfine tensors with a high order parameter ($S \approx 1$)

(Wolkers et al., 1997). This high value implies that the spin label experiences a strong squeezing effect by its local environment, that reduces the amplitude of its wobbling motion. This squeezing effect is suggested to arise from a turn structure in the coat protein from Glu20 to Gly23 in the membrane-water interface at the N-terminal domain of the major coat protein.

M13 coat protein in detergents. Detergents have been used often to solubilize M13 coat protein for biophysical studies. In fact, all high-resolution NMR work has been carried out with SDS-solubilized coat protein. To make a comparison of the state of the protein in bilayers as compared to well described detergent systems, spin-labeled coat protein mutants were also solubilized in sodium cholate and SDS. Although the spectra in DOPC are following the same tendency as in DOPC they are more broadened (see Fig. 3). The broadening effect is especially strong for the spin label at positions 25 and 46. This broadening is probably due to an increased molecular motion of the protein, as compared to the DOPC bilayer system. This gives rise to an incomplete averaging of the solid state powder components in the line shape. When solubilized in SDS micelles (see Fig. 4), a strong reduction of the outer splittings (Fig. 5) is observed for the spin label at positions 25 to 46, indicating an even more increased molecular motion and reduced order parameter.

In cholate, the molecular motion of the spin label at the C-terminal positions 49 and 50 is only slightly affected as compared to the bilayer system (see Table 1), suggesting a comparable state of the C-terminal part in both systems. However, in SDS the motion of the spin labels at positions 49 and 50 is significantly reduced, suggesting a strongly reduced motion of the C-terminal region. This indicates that SDS is covering the whole C-terminal part of the coat protein as well as the hydrophobic region, without a well-defined boundary as found in a bilayer. This is not surprising when the solubilising properties of the SDS are taken into an account. SDS is a strong amphiphilic molecule, and it is also well known that for a variety of proteins there is a constant binding ratio of the SDS to the protein on a gram to gram basis (Helenius & Simons, 1975). Clearly, this nonspecific covering effect is not present with sodium cholate as a detergent molecule, because the spin labels at positions 49 and 50 are not affected by the presence of the sodium cholate and are located in an aqueous environment. Cholate is a flat hydrophobic molecule and, as can be deduced from the ESR spectra, it is preferentially bound to the hydrophobic parts of the protein. In this respect, sodium cholate better mimics the typical nature of a membrane structure as compared to SDS micelles.

The distinct powder lineshape for the spin label at position 25 in all model systems studied (Figs. 2-4) is remarkable. It has been suggested that the line shape in DOPC bilayers is arising from a reduction of the spin label motion by a specific β-turn structure formed

69

between residues 21 and 23 at the membrane-water interface (Wolkers et al., 1997). Due to this turn the amphiphilic N-terminal helix and the transmembrane helix become almost perpendicular to each other and according to this model, the spin label is squeezed between the two helices. It can be seen from the ESR spectra in the different model systems, that this effect is most pronounced in DOPC, indicating that the bilayer structure stabilizes an L-shaped conformation. The special property of the spin label at position 25 is also seen in the high value of the outer hyperfine splitting (see Fig. 5).

Biological relevance and conclusions. Our data suggest an extension of the predicted transmembrane domain of M13 coat protein towards the C-terminus up to Thr46 in DOPC lipid bilayers, leaving the side chains of Lys40, Lys43, Lys44 and Phe42 and Phe45 at the water-membrane interface. This provides a very good anchoring mechanism for the coat protein, because the lysine and phenylalanine residues serve as hydrophilic and hydrophobic anchors, respectively. The effective neutralisation of lysine ε-NH_2 groups by the high molar excess of the phosphates in proximal head groups may also provide a protection of the lysines in the *E. coli* cytoplasm during virus replication. Although there might be some weak electrostatic interactions between the reconstituted protein and DNA or other negatively charged molecules in the aqueous phase, they will generally exist as independent species. This implies a mechanism in which the coat protein can interact with the DNA only when it is released from the phospholipids. An additional hydrophobic interaction between the major coat proteins could stabilise such a protein-DNA complex in a process which is mediated by the host and virus protein assembly machinery (Russel, 1991).

From the data presented in this paper it can be seen that the local dynamics of the major coat protein is significantly affected by its structural environment (micellar vs. bilayer), location (aqueous vs. hydrophobic), and L/P ratio. Although the detergents SDS and sodium cholate sufficiently well solubilise the coat protein and largely retain its secondary structure elements, they have a poorly defined protein-amphiphilic structure and lipid-water interface as compared to bilayers and thus are not a good substitute for lipid bilayers in biophysical studies.

References

Altenbach, C., Greenhalgh, D. A., Khorana, H. G., & Hubbell, W. L. (1994) *Proc. Natl. Acad. Sci. USA* 91, 1667-1671.

Brotherus, J. R., Griffith, O. H., Brotherus, M. O., Jost, P. C., Silvius, J. R., & Hokin, L. E. (1981) *Biochemistry* 20, 5261-5267.

Chamberlain, B. K., & Webster, R. E. (1978) *J. Bacteriol.* 135, 883-887.

Cross, T. A., & Opella, S. J. (1980) *Biochem. Biophys. Res. Commun.* 92, 478-484.

Cross, T. A., & Opella, S. J. (1985) *J. Mol. Biol.* 182, 367-381.

Deisenhofer, J., Epp, O., Miki, K., Huber, R., & Michel, H. (1985) *Nature* 318, 618-624.

Fretten, P., Morris, S. J., Watts, A., & Marsh, D. (1980) *Biochim. Biophys. Acta* 598, 247-259.

Griffith, H. O., & Jost, P. C. (1976) In *Spin Labeling. Theory and applications* (Berliner, L. J., Ed.) pp. 453-523, Academic Press, New York, San Francisco, London.

Helenius, A., & Simons, K. (1975) *Biochim. Biophys. Acta* 415, 29-79.

Hemminga, M. A., & Faber, A. J. (1986) *J. Magn. Reson.* 66, 1-8.

Hemminga, M. A., Sanders, J. C., & Spruijt, R. B. (1992) In *Progress in Lipid Research* (Sprecher, H., Ed.) Vol 31, pp. 301-333, Pergamon Press, Oxford.

Hemminga, M. A., Sanders, J. C., Wolfs, C. J. A. M., & Spruijt, R. B. (1993) In *Protein-Lipid Interactions* (Watts, A., Ed.) New Comprehensive Biochemistry 25, pp. 191-212, Elsevier, Amsterdam.

Henderson, R., Baldwin, J. M., Ceska, T. A., Zemlin, F., Beckmann, E., & Downing, K. H. (1990) *J. Mol. Biol.* 213, 899-929.

Henry, G. D., & Sykes, B. D. (1992) *Biochemistry* 31, 5284-5297.

Henry, G. D., Weiner, J. H., & Sykes, B. D. (1987) *Biochemistry* 26, 3626-3634.

Khan, A. R., & Deber, C. M. (1995) *Biochem. Biophys. Res. Commun.* 206, 230-237.

Kyte, J., & Doolittle, R. F. (1982) *J. Mol. Biol.* 157, 105-132.

Makino, S., Woolford, J. L., Jr., Tanford, C., & Webster, R. E. (1975) *J. Biol. Chem.* 250, 4327-4332.

Marsh, D. (1981) in *Membrane Spectroscopy. Molecular Biology, Biochemistry and Biophysics* (Grell, E. Ed.) Vol 31, pp 51-142, Springer-Verlag, Berlin, Heidelberg, New York.

Marvin, D. A., Hale, R. D., Nave, C., & Citterich, M. H. (1994) *J. Mol. Biol.* 235, 260-286.

McDonnell, P. A., Shon, K., Kim, Y., & Opella, S. J. (1993) *J. Mol. Biol.* 233, 447-463.

Russel, M. (1991) *Mol. Microbiol.* 5, 1607-1613.

Sanders, J. C., Haris, P. I., Chapman, D., Otto, C., & Hemminga, M. A. (1993) *Biochemistry* 32, 12446-12454.

Sanders, J. C., Ottaviani, M. F., van Hoek, A., Visser, A. J. W. G., & Hemminga, M. A. (1992) *Eur. Biophys. J.* 20, 305-311.

Sanders, J. C., Poile, T. W., Spruijt, R. B., van Nuland, N. A. J., Watts, A., & Hemminga, M. A. (1991) *Biochim. Biophys. Acta* 1066, 102-108.

Smilowitz, H., Carson, J., & Robbins, P. W. (1972) *J. Supramolecular Struct.* 1, 8-18.

Spruijt, R. B., & Hemminga, M. A. (1991) *Biochemistry* 30, 11147-11154.

Spruijt, R. B., Wolfs, C. J. A. M., & Hemminga, M. A. (1989) *Biochemistry* 28, 9158-9165.

Spruijt, R. B., Wolfs, C. J. A. M., Verver, J. W. G., & Hemminga, M. A. (1996) Biochemistry, 35, 10383-10391.

Tanford, C., & Reynolds, J. A. (1976) *Biochim. Biophys. Acta* 457, 133-170.

Turner, R. J., & Weiner, J. H. (1993) *Biochim. Biophys. Acta* 1202, 161-168.

Van de Ven, F. J. M., Van Os, J. W. M., Aelen, J. M. A., Wymenga, S. S., Remerowski, M. L., Konings, R. N. H., & Hilbers, C. W. (1993) *Biochemistry* 32, 8322-8328.

Vriend, G., Schilthuis, J. G., Verduin, B. J. M., & Hemminga, M. A. (1984) *J. Magn. Reson.* 58, 421-427.

Weiss, M. S., Abele, U., Weckesser, J., Welte, W., Schiltz, E., & Schulz, G. E. (1991) *Science* 254, 1627-1630.

White, S. H., & Wimley, W. C. (1994) *Curr. Opin. Struct. Biol.* 4, 79-86.

Wolkers, W.F., Spruijt, R.B., Kaan, A. Konings, R.N.H., & Hemminga, M.A. (1997) *Biochim. Biophys. Acta 1327*, 5-16.

Chapter 5

Membrane Location of Spin-Labeled M13 Major Coat Protein Mutants Determined by Paramagnetic Relaxation Agents

David Stopar, Kitty A.J. Jansen, Tibor Páli, Derek Marsh, and Marcus A. Hemminga

Abstract

Mutants of the M13 bacteriophage major coat protein containing single cysteine replacements (A25C, V31C, T36C, G38C, T46C, and A49C) in the hydrophobic and C-terminal domains were purified from viable phage. These were used for site-directed spin labeling to determine the location and assembly of the major coat protein incorporated in bilayer membranes of dioleoylphosphatidylcholine. The membrane location of the spin-labeled cysteine residues was studied with molecular oxygen and Ni^{2+} ions as paramagnetic relaxation agents preferentially confined to the hydrophobic and aqueous regions, respectively, by using progressive-saturation electron spin resonance (ESR) spectroscopy. The section of the protein around Thr36 is situated at the center of the membrane. Residue Thr46 is placed at the membrane surface in the phospholipid head group region with a short C-terminal section, including Ala49, extending into the aqueous phase. Residue Ala25 is then positioned consistently in the head group region of the apposing lipid monolayer leaflet. These positional assignments are consistent with the observed mobilities of the spin-labeled groups. The outer hyperfine splittings in the ESR spectra decrease from the N-terminal to the C-terminal of the hydrophobic section (residues 25-46), and then drop abruptly in the aqueous phase (residue 49). Additionally, the strong immobilization and low oxygen accessibility of residue 25 are attributed to steric restriction at the hinge region between the transmembrane and N-terminal amphipathic helices. Sequence-specific modulations of the ESR parameters are also observed. Relatively low oxygen accessibilities in the hydrophobic region suggest intermolecular associations of the transmembrane helices, in agreement with saturation transfer ESR studies of the overall protein mobility. Relaxation enhancements additionally reveal a Ni^{2+} binding site in the N-terminal domain that is consistent with a surface orientation of the amphipathic helix.

Introduction

The major coat protein of bacteriophage M13 exists, prior to phage assembly, as a small monotopic integral protein in the plasma membrane of the *Escherichia coli* host cell. The major coat protein has a hydrophobic stretch of 20 amino acids, flanked by an acidic N-terminal region located in the periplasm and a basic C-terminal region located in the cytoplasm (Asbeck et al., 1969). The overall secondary structure of the protein is α-helical with a turn structure between Gly23 and Glu20. This specific β-turn connects the transmembrane helix with an amphipathic N-terminal helix. Although the secondary structure of the protein is well characterized (McDonnell et al., 1993; Van de Ven et al., 1993), the location of the secondary structural elements relative to the lipid bilayer is poorly identified. In this paper, the emphasis is placed on the membrane location of the transbilayer helix and of the C-terminal domain of the protein, where the presence of four positively charged lysines intercalated between hydrophobic residues complicates the positioning relative to the membrane-water interface (Turner & Weiner, 1993).

To obtain information on the location of the membrane-bound form of the major coat protein and in particular of the C-terminal domain, a series of site-specific cysteine mutants were prepared for studies using electron spin resonance (ESR) spectroscopy. Such an approach allows site-directed spin-labeling at specific residue attachment sites (Altenbach et al., 1989). Care is required, however, in the design of the mutations in order to avoid nonfunctional proteins. Mutations of the M13 major coat protein prepared here did not include replacement of any charged or aromatic residues which apparently causes lethal mutations (Marvin et al., 1994). Selection for viable mutant bacteriophages ensured the choice of functional mutant major coat proteins. Purified mutant major coat proteins were spin-labeled and incorporated in phospholipid bilayers as model integral membrane proteins.

The position of the spin-label on the protein in the membrane-bound form was determined from the interaction of the nitroxide label with paramagnetic relaxation agents by using progressive saturation ESR spectroscopy (Páli et al., 1993; Snel et al., 1994). Combination with site-directed spin labelling generally allows one to obtain detailed information on the secondary and tertiary protein structure (Hubbell et al., 1996). The relaxation agents, molecular oxygen and paramagnetic ions, were used earlier to determine the location and immersion depth in the membrane of specific spin-labelled sites in bacteriorhodopsin, apocytochrome *c* and cytochrome *c* (Altenbach et al., 1990, 1994; Snel et al., 1994). Changes in the nitroxide spin-lattice relaxation rates on interaction with fast-relaxing paramagnetic species are a measure of their accessibility or distance of closest

approach to the nitroxide group (Páli et al., 1992). Oxygen dissolves preferentially in the hydrophobic core of the membrane, whereas uncomplexed paramagnetic ions are restricted mainly to the aqueous phase (Subczynski & Hyde, 1983, 1984). A relatively low accessibility to oxygen is, however, not entirely diagnostic for the spin label location, because it may arise either from exposure of the label to the aqueous phase or from the label being buried in the interior of the protein (Altenbach et al., 1990). In the later case, a range of values may be expected depending on the protein environment. Thus, a combination of relaxation data from both oxygen and a paramagnetic ion is required for unambiguous interpretation in terms of the protein topography (Marsh, 1994).

In the present work, the location of the spin-labelled M13 coat protein cysteine mutants was determined with Ni^{2+} ions and oxygen as relaxation agents in lipid bilayers of dioleoylphosphatidylcholine. This was calibrated by using similar measurements on specific positionally spin-labelled lipids (n-PCSL and TS) in the same lipid bilayer system.

Materials and Methods

Materials. DOPC was obtained from Avanti Polar Lipids (Birmingham, AL). Spin-labelled phosphatidylcholine derivatives (n-PCSL) were synthesized from the corresponding stearic analogues (n-SASL) specifically spin-labelled at different positions in the *sn*-2 chain as described previously (Marsh & Watts, 1982). The tempol ester of stearic acid (TS) spin label was obtained from Molecular Probes (Eugene, OR). 5-Maleimidoproxyl (5-MSL) and DTNB (Ellman's reagent) were obtained from Sigma (St. Louis, MO).

Lipid Vesicle Preparation. Lipid vesicles were prepared by dissolving 1 mg of DOPC and 1 mol % spin-labelled lipid in chloroform/methanol (2:1, v/v) solvent. To prevent peroxidation of the unsaturated lipid chains, 0.1 mol % butylated hydroxytoluene was added to the lipid solution. The solvent was evaporated with nitrogen gas, and residual traces of solvent were removed by drying under vacuum overnight. Lipids were hydrated with 100 µL of oxygen-saturated buffer (150 mM NaCl, 10 mM Tris-HCl, pH 7.0), or deoxygenated buffer containing 0, 5, 10, 25, or 50 mM $NiCl_2$, by vortex mixing at room temperature.

Major Coat Protein Spin-Labeling. Six M13 major coat protein cysteine mutants (A25C, V31C, T36C, G38C, T46C, and A49C) with a yield high enough for ESR purposes were grown and purified from phage as described previously (Spruijt et al., 1989; Stopar et al., 1996). Major coat protein mutants were spin labelled with 5-Maleimidoproxyl spin label (5-

75

MSL), directly after bacteriophage disruption. Typically 5-10 mg of bacteriophage was suspended in 100 mM sodium cholate, 150 mM NaCl, 10 mM Tris-HCl, pH 7.0, with subsequent addition of 2.5 % (v/v) chloroform. The mixture was incubated at 37 °C for 10 min with occasional mixing. To remove chloroform, the mixture was flushed with nitrogen gas until a clear nonopalescent suspension was obtained. To this suspension was added a 3-fold molar excess of 5-MSL spin label, and the mixture was incubated for 30 min at 37 °C. The reaction was stopped by addition of excess cysteine. The mixture was applied to a HiPrep 16/60 Sephacryl S-300 High Resolution column (Pharmacia, Uppsala, Sweden), that was eluted with 25 mM sodium cholate, 150 mM NaCl and 10 mM Tris-HCl, pH 7.0, to separate the major coat protein from DNA and free spin label. Fractions with an A_{280}/A_{260} absorbance ratio higher than 1.4 were collected and concentrated by Amicon filtration. Before storage at 4 °C, sodium cholate was added to a final concentration of 50 mM.

Labeling Efficiency. The extent of spin labelling was determined by using the reaction with DTNB to assay remaining free sulfydryl groups. A bacteriophage suspension (2 mg/mL) was disrupted, and an aliquot was labelled as described above in 100 mM Na-cholate, 150 mM NaCl, 10 mM Tris-HCl, pH 7.0. The control unlabelled sample was disrupted in the same buffer and incubated for 30 min at 37 °C. To determine the amount of free cysteine groups after spin labelling, 100 μL of DTNB stock solution (4 mg/mL in sodium phosphate buffer, pH 8.0) was added to 900 μL of spin-labelled or control unlabelled major coat protein suspension and incubated for 15 min at room temperature. The degree of labeling of the wild-type protein has been discussed in an earlier paper (Stopar et al., 1996) and is not significant compared to the specific labeling under the conditions used (30 min, pH 7.0). The absorption at 412 nm was determined for the spin-labelled mutant and control samples, and the percentage of labelled SH groups relative to the control sample was calculated.

Coat Protein Reconstitution in Lipid Vesicles. Incorporation of the spin-labelled major coat protein mutants into DOPC vesicles was performed from dispersions in sodium cholate as described earlier (Spruijt et al., 1989), with the following modifications. Lipid vesicles were prepared by dissolving the desired amount of DOPC in chloroform/methanol (2:1, v/v). To prevent lipid peroxidation 0.1 % (mol/mol) butylated hydroxytoluene was added to the solution. The solvent was evaporated with a stream of nitrogen gas, and the samples were dried under vacuum overnight to remove residual traces of the solvent. The lipids were solubilized in 50 mM Na-cholate buffer (150 mM NaCl, 10 mM Tris-HCl, pH 7.0) by sonication for 1 min (Sonifier cell disrupter, Model W185, Heat Systems-Ultrasonics Inc.). The desired amount of spin-labelled mutant major coat protein was added to give a lipid/protein molar ratio of 50 (L/P 50). Dialysis was performed at room temperature against

76

a 100-fold excess of deoxygenated buffer (150 mM NaCl, 10 mM Tris-HCl, pH 7.0). The dialysis buffer was changed 4 times every 12 hours. After dialysis, the proteoliposome suspension either was adjusted to the desired $NiCl_2$ concentration (0, 0.5, 1, 2.5, 5, 10, 15, or 25 mM $NiCl_2$, 150 mM NaCl, 10 mM Tris-HCl, pH 7.0) in deoxygenated buffer or was saturated with oxygen. The proteoliposomes were concentrated by centrifugation (Beckman L7-55 ultracentrifuge, 45 000 RPM, 2.5 hours, 10 °C). To ensure accessibility of Ni^{2+} to all lipid membrane surfaces, the samples containing various concentrations of $NiCl_2$ were freeze-dried and then resuspended in a volume of distilled water equal to that of the original dispersion before preparing the samples for ESR measurements. Freeze-drying and resuspension did not alter the spectra in the absence of Ni^{2+} or oxygen as compared to the non-freeze-dried samples (data not shown).

The aggregation state of the major coat protein mutants in the reconstituted membrane samples was checked by using high-performance size exclusion-chromatography (HPSEC) (Spruijt et al., 1989). The L/P ratios and homogeneity of the samples were determined directly after sample preparation as described previously (Spruijt et al., 1989).

ESR Spectroscopy. Membrane dispersions were loaded into glass capillaries (i.d. 1 mm), flushed with oxygen or argon as required, and were pelleted at 12 000 RPM for 10 min in a Biofuge A. Excess supernatant was removed from the pellets in the ESR capillaries to obtain samples 5 mm in length. This avoids inhomogeneities of the microwave and modulation fields in the ESR cavity (Fajer & Marsh, 1982). The sample capillary was flushed with either argon or oxygen and sealed with a fine-wire thermocouple inserted directly into the sample. ESR spectra were recorded on a Varian Century Line Series 9 GHz spectrometer equipped with a nitrogen gas-flow temperature regulation system. The spectrometer was interfaced to an IBM PC for digital data collection. The sample capillaries were accommodated within standard 4 mm quartz ESR tubes containing light silicone oil for thermal stability. Conventional first harmonic, in-phase, absorption spectra were recorded at a modulation frequency of 100 kHz and modulation amplitude of 0.05 mT, and microwave amplitudes ranging from 0.0002 to 0.06 mT for progressive saturation measurements. The microwave amplitudes were measured as described in Fajer and Marsh (1982). Low-power conventional ESR spectra were recorded at a subsaturating microwave amplitude of $B_1 =$ 8.3 μT for line shape analysis. ST-ESR spectra were recorded in the second harmonic, 90° out-of-phase absorption mode at a modulation frequency of 50 kHz, a modulation amplitude of 0.5 mT, and an average microwave field $<B_1^2>^{1/2}$ of 0.025 mT, according to the standardized protocol for dealing with cavity Q variations and field inhomogeneities (Fajer & Marsh, 1982; Hemminga et al., 1984). The phase was set using the self-null method (Marsh, 1981) at a subsaturating microwave field. Effective rotational correlation times

77

were determined from the diagnostic line height ratios in the ST-ESR spectra, as described in Horváth and Marsh (1983). First and second integrals of ST-ESR and conventional ESR spectra, respectively, were determined after a base line correction.

Evaluation of Relaxation Rates. For labels with anisotropic line shapes (5- and 9-PCSL and all spin-labelled mutants except A49C), convolutions of Lorentzian and Gaussian functions, i.e., Voigt absorption line shapes, were fitted simultaneously to the low- and high-field wings of the low- and high-field peaks in the low-power unsaturated conventional ESR spectra, after the center of each line was determined. Fitting parameters were the Lorentzian line width and vertical normalization for the two lines, and a common Gaussian line width. This procedure corrects for the inhomogeneous line broadening, yielding the homogeneous (i.e., Lorentzian) line widths for both lines (Bales, 1989). For labels with isotropic line shapes (TS, 14-PCSL, and spin-labelled mutant A49C), the low-power conventional ESR spectra were first integrated with respect to magnetic field and then fitted to a sum of three Voigt absorption line shapes. The Lorentzian line widths were used to calculate the spin-spin relaxation times T_{2L}, T_{2C} and T_{2H} for the low-field, central, and high-field hyperfine manifolds, respectively. For the anisotropic line shapes, it was assumed that $T_{2C} \approx T_{2L}$.

In the progressive saturation experiments, the second integral of the first-derivative absorption spectra (i.e., the spectral intensity of absorption), I, was determined as a function of the microwave amplitude, B_1. These values were fitted to the following dependence on B_1:

$$I(B_1) = I_0 B_1 \left[\frac{1}{\sqrt{1 + \gamma^2 B_1^2 T_1 T_{2L}}} + \frac{1}{\sqrt{1 + \gamma^2 B_1^2 T_1 T_{2C}}} + \frac{1}{\sqrt{1 + \gamma^2 B_1^2 T_1 T_{2H}}} \right] \qquad (1)$$

where T_{2L}, T_{2C}, and T_{2H} were the spin-spin relaxation times determined from the linewidths and γ is the electron gyromagnetic ratio (Páli et al., 1993). The two fitting parameters were the spin-lattice relaxation time, T_1, and a common normalization factor, I_0. Equation (1) describes the saturation of the integrated intensity of the three hyperfine components in the absence of cross-relaxation, nuclear relaxation, and spin-exchange processes (Marsh, 1995a,b). The above procedure results in determinations of T_1 that are far less sensitive to inhomogeneous broadening than are standard amplitude or line width saturation techniques for measuring $T_1 T_2$ products (Páli et al., 1993).

Accessibility Parameters. In the presence of a fast-relaxing paramagnetic species, the spin-lattice relaxation rate, $1/T_1$, of the spin label is enhanced by an amount depending on the concentration, c, of the fast-relaxing species (Snel & Marsh, 1993):

$$1/T_1 = 1/T_1^o + k_{RL} c \qquad (2)$$

Here T_1^o is the value of T_1 for c = 0, and k_{RL} is an accessibility parameter that depends on the diffusion coefficient and cross section for collision of the relaxing agents in the case of Heisenberg spin exchange, and on the distance of closest approach to the spin label in the case of magnetic dipole-dipole interactions (Marsh, 1994).

In the case of molecular oxygen, the accessibility parameter is defined as the difference in the T_1 relaxation rate for the nitroxide group in the presence (p) and in the absence (o) of a paramagnetic species:

$$\text{accessibility parameter} = 1/T_1^p - 1/T_1^o \tag{3}$$

For oxygen, the exchange interaction with spin labels is assumed to be diffusion-controlled, and is determined by the local concentration of oxygen in the vicinity of the spin label (Subczynski & Hyde, 1984).

Results

The mutant coat proteins were indistinguishable from the wild-type protein with respect to their aggregational state and conformational state in reconstituted systems, as has been described previously (Stopar et al., 1996).The HPSEC elution profiles indicated that all the mutant proteins, except for mutant G38C, were in an α-helical oligomeric form, with no β-sheet polymeric form. The mutant G38C had a tendency to form β-sheet polymers under the experimental conditions used for reconstitution (up to 50 % β-sheet conformation). For all cysteine mutants, the formation of S-S bridged dimers immediately after phage disruption was less than 5 %. The spin-labelling efficiency in 100 mM Na-cholate buffer was 90 % (± 5 %) for the mutant coat protein A25C, 88 % (± 5 %) for the mutant V31C, 50 % (± 5 %) for the mutant T36C, 77 % (± 5 %) for the mutant G38C, 93 % (± 5 %) for the mutant T46C, and 97 % (± 2.5 %) for the mutant A49C. The residue positions 36 and 38 are significantly less accessible for alkylation by the maleimide spin label than are the other positions.

The conventional ESR spectra of the various 5-MSL spin-labelled coat protein mutants, incorporated in DOPC bilayers at L/P 50 mol/mol, are given in Fig. 1. The spectra are characteristic of one of two different motional regimes sensed by the different spin labels: fast for the spin-labelled A49C mutant or slow for the spin-labelled T46C, G38C, T36C,
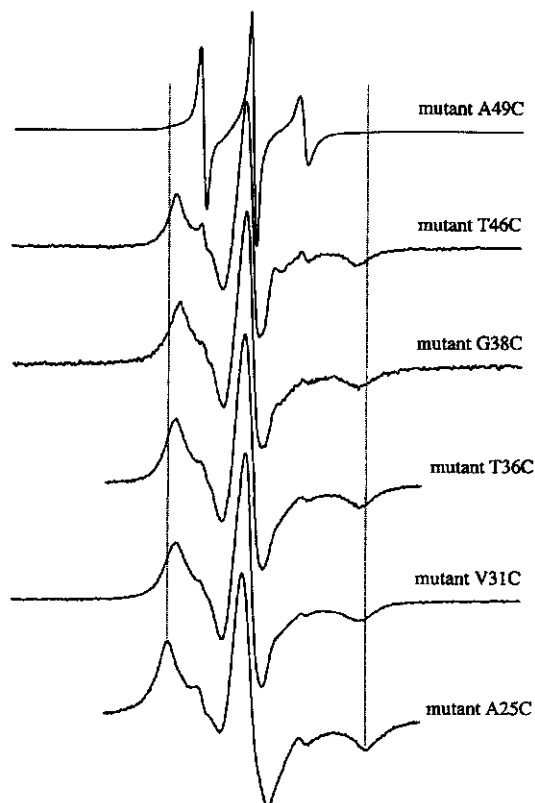
FIGURE 1: Conventional ESR spectra of spin-labelled major coat protein mutants in DOPC bilayers at a lipid/protein ratio 50 mol/mol. Spectra are normalised to the same central line height. The temperature of the samples is 20 °C. Total scan width is 16 mT for the spin-labelled mutants A49C, T46C, G38C, and V31C and 10 mT for the spin-labelled mutant coat proteins T36C and A25C.

V31C, and A25C mutants. This is consistent with an extramembranous location of residue 49 and a membrane location of the other residues, as will be discussed below. The outer hyperfine splitting in the spectra of the nitroxide radicals varies along the protein primary sequence, but the overall shape of the spectra is not influenced by the presence of $NiCl_2$ or oxygen relaxation agents. The positional dependence of the outer hyperfine splitting, $2A_{max}$, for those labels that give immobilized ESR spectra is presented in Fig. 2. Overall, the outer hyperfine splitting decreases on going from the N-terminal to the C-terminal in this section of the protein (dashed line in Fig. 2 and figure legend), but with a local
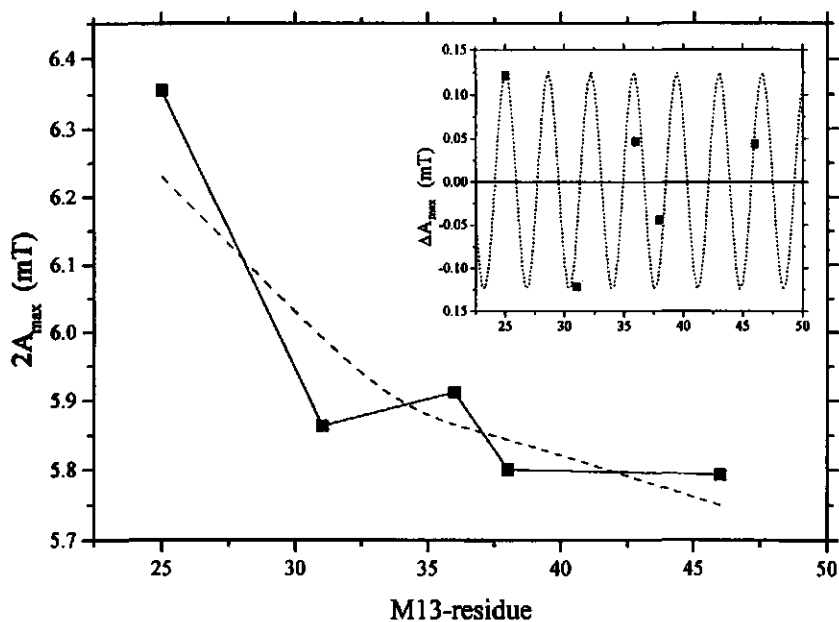
80

FIGURE 2: Dependence of the outer hyperfine splitting, $2A_{max}$, on spin-labelled residue position for cysteine mutants of the M13 major coat protein in DOPC bilayers at 20 °C. The dashed line connects the mean splittings between successive measurement points. The inset shows the deviation of A_{max} from the local mean value, with an α-helical periodicity superimposed (dotted line).

sequence-specific periodicity superimposed (see inset to Fig. 2). Although the total number of measurement points is limited by the requirement that all cysteine mutants used should assemble in viable phage there clearly is not a monotonic or symmetrical dependence on sequence position, hence indicating local perturbations in residue mobility.

ST-ESR spectra of the 5-MSL spin-labelled major coat protein mutants in DOPC bilayers at L/P 50 mol/mol are given in Fig. 3. With the exception of the mutant A49C, which displays fast motion on the conventional ESR time scale, the spectra are mostly characteristic of relatively rapid motion on the slower ST-ESR time scale (Thomas et al., 1976). The effective rotational correlation time for the spin-labelled major coat protein mutant A25C estimated from calibrations of the diagnostic spectral line height ratios lies
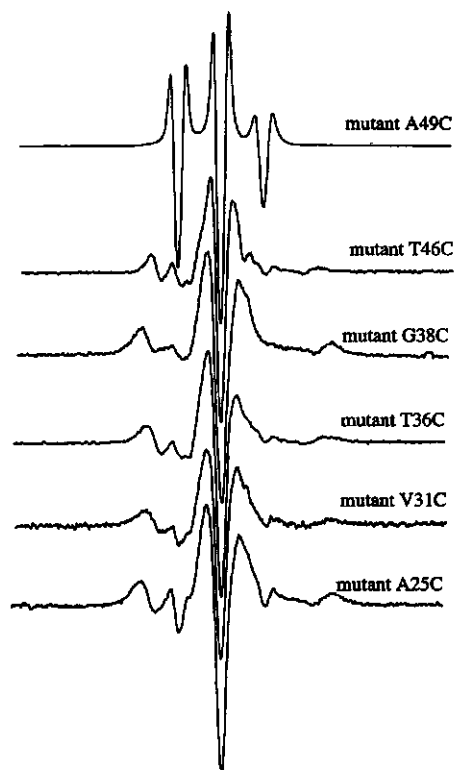
FIGURE 3: Saturation transfer ESR spectra of spin-labelled major coat protein mutants in DOPC bilayers at a lipid to protein ratio of 50 mol/mol. The temperature of the samples is 20 °C. Total scan width is 16 mT.

between 5 and approximately 10-20 μs for the low-field and high-field regions, respectively (Horváth & Marsh, 1983; Marsh, 1992).This is the mutant that displays little segmental motion on the conventional ESR time scale (see Figs. 1 and 2) and therefore is most likely to reflect the overall rotational motion of the whole protein. The effective rotational correlation is defined in terms of isotropically rotating calibration systems.

The T_1 relaxation enhancement by Ni^{2+} ions of spin-labelled mutants, incorporated in DOPC vesicles at L/P 50 mol/mol, is given in Fig. 4. All samples were deoxygenated. Effective spin-lattice relaxation times, T_1, were obtained from progressive saturation experiments with increasing microwave power, together with line width measurements, as described
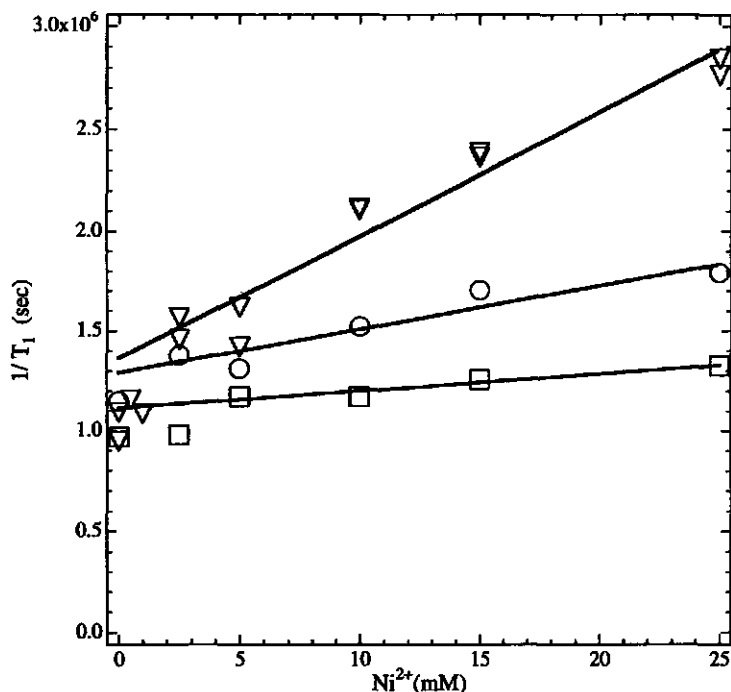
under

FIGURE 4: Dependence of the reciprocal T_1 relaxation times of the spin-labelled major coat protein mutants reconstituted in DOPC bilayers at 20 °C on bulk Ni^{2+} concentration in the aqueous phase. The solid lines represent linear regressions in the concentration range 2.5-25 mM Ni^{2+}. Data are given for three representative spin-labelled mutants: A49C (triangles), V31C (circles), and G38C (squares).

under Materials and Methods. The T_1 relaxation rate is found to be directly proportional to the Ni^{2+} ion concentration for all the different spin-labelled mutants in the concentration range 2.5-50 mM $NiCl_2$ (cf. eq 2). The slopes of the concentration dependence of the relaxation rate in Fig. 4 are a measure of the accessibility to aqueous Ni^{2+} ions, or their distance of closest approach, for the different spin-labelled mutant major coat proteins. The relaxation enhancements by Ni^{2+} ions at low concentrations (<2.5 mM) will be considered later. Relaxation enhancements were also determined for samples saturated with oxygen (in the absence of $NiCl_2$), and the accessibilities of the different spin-labelled mutants to oxygen were calculated according to eq 3.

The accessibilities both to oxygen and to Ni^{2+} ions that were determined from the relaxation enhancements are given in Fig. 5 for the various spin-labelled major coat protein mutants
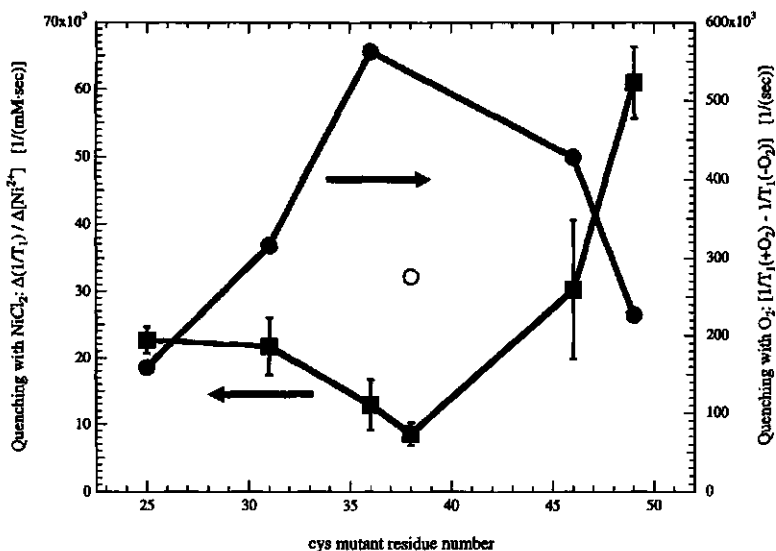
83

FIGURE 5: Dependence on label position of the relaxation enhancements by oxygen (circles) and by Ni^{2+} (squares) of the spin-labelled major coat protein mutants in DOPC bilayers. The left-hand ordinate (squares) gives the gradient of the increase in spin-label T_1 relaxation rate with respect to Ni^{2+} concentration. The right-hand ordinate (circles) gives the difference in spin label T_1 relaxation rate for samples saturated with oxygen and deoxygenated samples. The G38C mutant shows a tendency to aggregate, and its accessibility to oxygen is given by the open circle.

incorporated in DOPC bilayers at L/P 50 mol/mol. The cysteine mutants studied span the hydrophobic as well as the C-terminal domain of the major coat protein. The relaxation enhancement by aqueous Ni^{2+} ions decreases from position 25 to position 38 and then increases steeply to position 49. It should be noted that for spin-labelled residues embedded in the membrane, the relaxation enhancement induced by aqueous Ni^{2+} ions does not represent a direct accessibility but rather a distance-dependent, through-space effect of magnetic dipole interactions (Páli et al., 1992). The results with aqueous Ni^{2+} ions are in contrast to the accessibility to oxygen dissolved in the hydrophobic interior of the membrane. The relaxation enhancement induced by molecular oxygen increases from position 25 to position 36 and then decreases toward position 49. The maximum accessibility to oxygen at position 36 corresponds to the minimum relaxation enhancement by Ni^{2+} ions which occurs around positions 36 and 38. This suggests that this region
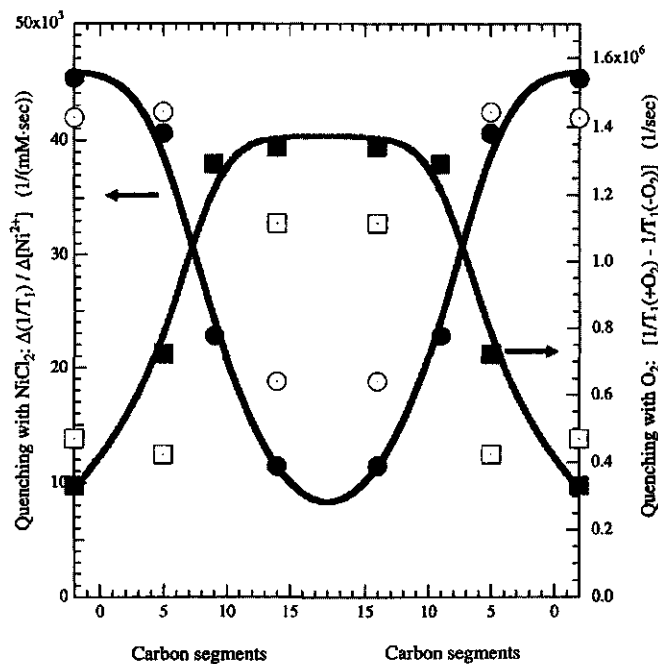
84

FIGURE 6: Dependence on label position of the relaxation enhancement by oxygen (filled squares) and by Ni^{2+} (filled circles) for the lipid head group spin label (TS) and for spin-labelled phospholipid acyl chains (5-PCSL, 9-PCSL, 14-PCSL) in DOPC bilayers. The relaxation enhancement of spin-labelled lipids in DOPC bilayers containing unlabelled major coat protein by oxygen is indicated by open circles and by aqueous Ni^{2+} by open squares.

corresponds to the center of the bilayer membrane. The asymmetry in the distribution of relaxation enhancements induced by Ni^{2+}, which is strongest in the case of residue 25, suggests that none of the labelled residues on the N-terminal side of the protein (from residue 25 onward) are directly exposed to the aqueous phase. The irregularity in the distribution of accessibility to oxygen, relative to the overall profile, may partly be attributed to sequence/secondary structure-specific effects.

To calibrate the positional dependence of the relaxation enhancements obtained from the spin-labelled protein, comparable experiments were performed with spin-labelled lipids in the presence of oxygen or NiCl$_2$. The relaxation enhancements for a lipid head group spin label (TS) and for phospholipids spin-labelled in the chain (5-PCSL, 9-PCSL, 14-PCSL)
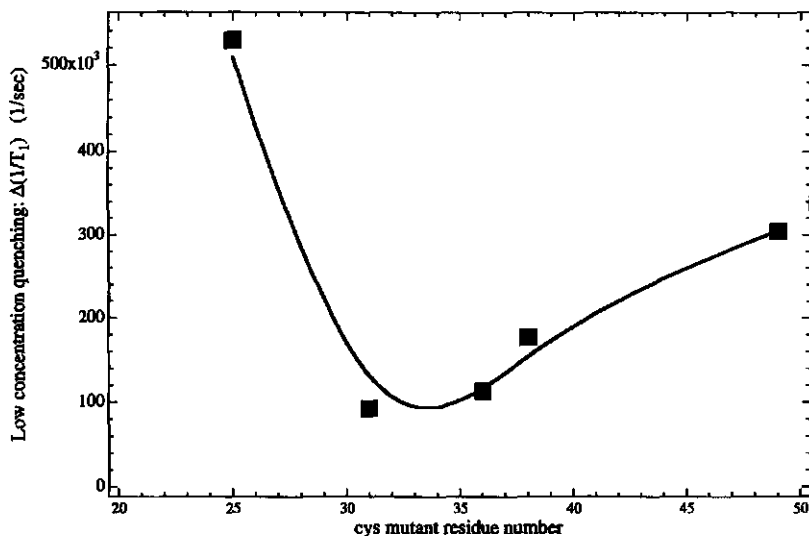
85

FIGURE 7: Difference in relaxation rates, $\Delta(1/T_1)$, between the linear regression intercepts of the relaxation dependence at high $NiCl_2$ concentrations (2.5-25 mM) and at low $NiCl_2$ concentrations (0-2.5 mM) for different spin-labelled mutant major coat proteins at 20 °C in DOPC bilayers.

determined in DOPC bilayers with and without the unlabelled major coat protein are given in Figure 6. The relaxation enhancement of the phospholipid spin labels by both oxygen and aqueous Ni^{2+} ions is modified somewhat by insertion of the major coat protein in the bilayer, but the overall positional profiles remain qualitatively the same. The decrease in relaxation enhancement by oxygen of the chain-labelled lipids is probably caused by a decreased solubility of oxygen in the hydrophobic interior of the protein-containing bilayers. This correlates with the decreased chain mobility evidenced by the spectra of the chain-labelled lipids in the presence of protein (data not shown). From Fig. 6, it can be seen that the relaxation enhancement by oxygen or by aqueous Ni^{2+} is increasing or decreasing monotonically as a function of the distance from the lipid head group phosphate region. The effect of oxygen is relatively low in the aqueous phase and in the phospholipid head group region, but increases toward the center of the membrane. This is consistent with the known preference of oxygen to dissolve in the hydrocarbon phase. Compared to oxygen, the relaxation enhancement by aqueous Ni^{2+} ions shows qualitatively the inverse profile with position of the spin labels in the membrane. Large enhancements induced by Ni^{2+} ions are observed for spin labels at the membrane surface in the lipid head group region. These then decrease rapidly with depth in the membrane for the chain-labelled lipids because of the

86

diminishing dipolar interactions with Ni^{2+} ions confined to the aqueous phase. Because the bilayers are symmetrical and the n-PCSL spin labels are uniformly distributed, the relaxation enhancements by both oxygen and Ni^{2+} ions represent both halves of the bilayer and are plotted relative to both surfaces of the bilayer in Fig. 6.

The relaxation enhancements by aqueous Ni^{2+} ions that are given in Fig. 5 were determined for high $NiCl_2$ concentrations (>2.5 mM). However, the concentration dependence was biphasic with a different dependence of the relaxation enhancement by Ni^{2+} ions in the low concentration range of 0-2.5 mM $NiCl_2$ (see Fig. 4). This initial relaxation enhancement at low Ni^{2+} ion concentrations is also dependent on the position of the spin-labelled cysteine. The high efficiency of this relaxation enhancement almost certainly arises from binding of Ni^{2+} ions to a specific site on the protein. No biphasic behavior upon $NiCl_2$ titration was observed with the spin-labelled TS or n-PCSL lipids (data not shown). The relaxation enhancement of the spin-labelled mutant proteins at low Ni^{2+} concentrations is given in Fig. 7. Plotted is the total relaxation enhancement in the low concentration region which is obtained from the difference between the relaxation rate in the absence of $NiCl_2$ and the extrapolated value at zero concentration from the linear regression of the dependence in the high concentration regime. The effect at low Ni^{2+} concentrations is most pronounced for the spin-labelled A25C mutant and sharply decreases for the spin-labelled mutants V31C, T36C, and G38C with an increase again toward the C-terminus.

Discussion

The location of spin-labelled site-directed mutants of the M13 major coat protein reconstituted into DOPC vesicles has been investigated directly by determining the accessibility of the spin-labelled sites to molecular oxygen and to cationic Ni^{2+} ions. In the latter case, a decreasing distance-dependent relaxation enhancement is expected for spin-labelled residues that are embedded in the membrane. The major coat protein mutants were selected to be regularly spaced along the lipid-exposed transmembrane protein surface, almost completely traversing the bilayer.

From the profiles of relaxation enhancement by both oxygen and Ni^{2+} ions (Fig. 5), it can be seen that the spin-labelled residue T36C is located near the center of the bilayer. The spin-labelled mutants V31C and G38C are clearly located in the hydrophobic core of the membrane. There is also little doubt about the aqueous location of the spin label on the A49C mutant, due to its high mobility on the time scale of conventional ESR, the high isotropic hyperfine splitting (1.59 mT), and the respective relaxation enhancements by both

oxygen and aqueous Ni^{2+} ions. Such a transmembrane profile is also in agreement with the efficiency of spin-labelling for which the lowest accessibility for alkylation of SH groups by 5-MSL is found with the mutants V31C, T36C, and G38C.

Previously, it was suggested that the transmembrane domain extends toward the C-terminus up to Thr46 (Stopar et al., 1996), leaving the α-carbon of the lysine side chains in the membrane, while the ϵ-amino groups are interacting with the phosphates of the lipid head groups. The nitroxide spin label covalently attached to the mutant coat protein T46C has a reduced relaxation enhancement by Ni^{2+} ions as compared to A49C, and a significantly increased oxygen accessibility. Relatively high relaxation enhancement by Ni^{2+} does not permit this residue to be buried in the membrane. The rather high oxygen accessibility of this mutant and the reduced mobility on the conventional ESR time scale; on the other hand, suggest that the spin label attached to T46C is located in a more hydrophobic environment. The accessibility to both polar and apolar relaxants would thus qualitatively locate the spin label at T46C in the lipid head group region. The exact location of the membrane-water interface in the C-terminal domain of the major coat protein, however, is further complicated by four positively charged lysines intercalated between apolar residues. The relatively high oxygen accessibility could possibly be provided by the glycerol moiety of the lipid head group and the surrounding strongly hydrophobic phenylalanines and leucine residues in the α-helical conformation of the protein. Such a location of the T46C residue is further supported by an independent study using the accessibility of fluorescence-labeled M13 major coat proteins to different fluorescence quenchers (Spruijt et al., 1996).

The relaxation enhancement profiles for both oxygen and Ni^{2+} ions exhibit an asymmetric distribution across the membrane toward position 25 (Fig. 5). Additionally, the positional profile of the mobility of the spin-labelled residues that is given in Fig. 2 is highly asymmetric. This is not altogether surprising when the asymmetric structure of the major coat protein is taken into account (see Fig. 8). The major coat protein in the membrane-bound form consists of two connected helices: a transmembrane and an amphipathic helix that are oriented perpendicular to one another (Nambudripad et al., 1991; Williams et al., 1996). Thermodynamically, the most probable location for the amphipathic helix is aligned along the membrane surface (White & Wimley, 1994). This orientation would determine the position of the interface in the N-terminal section of the transmembrane helix. The spin label at position 25 is highly immobilized, which may be because it is squeezed between the two helices in the lipid head group region, as has already been proposed (Stopar et al., 1996). Alternatively, the trend to increasing side-chain mobility toward the C-terminal (Fig. 2) could suggest that the N-terminal end of the transmembrane helix is preferentially anchored by the surface association of the amphipathic helix to which it is attached. Relaxation
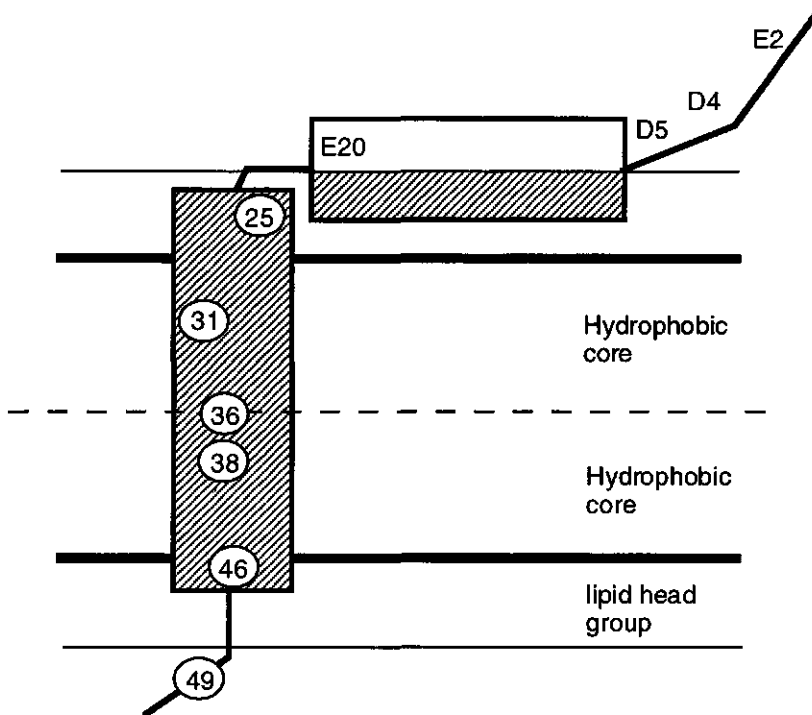
FIGURE 8: Location of the M13 major coat protein in a phospholipid bilayer. The two boxed regions represent a transmembrane helix and an amphiphilic helix aligned along the membrane surface. The residues that were changed to cysteine and spin labelled are indicated by numbered circles. The positions of the amino acids with spin-labeled side chains are indicated in the amphipathic helix and in the N-terminus. The solid horizontal lines indicate the approximate boundaries of the lipid polar head groups in the bilayer. The dashed line indicates the center of the bilayer.

enhancement of the spin-labelled A25C mutant by aqueous Ni^{2+} is low, which would locate this residue inside the membrane. However, the low accessibility of this residue to oxygen suggests that it cannot be buried deep in the hydrophobic core. The low oxygen accessibility may arise partly because the spin label on mutant A25C is spatially constrained between the two helices in the polar head group region. The Ni^{2+} ion distribution on this side of the bilayer may also be complicated by the presence of the charged amphipathic helix at the membrane surface as indicated by low Ni^{2+} concentration relaxation enhancement. The two different mechanisms of spin relaxation enhancement on interaction with fast-relaxing Ni^{2+}

89

ions at low Ni^{2+} concentration and high Ni^{2+} concentration, respectively, may not be directly comparable. High efficiency of relaxation for low Ni^{2+} concentration is attributed to binding of Ni^{2+} ions to the protein, on the other hand, Ni^{2+} ions in the bulk phase are responsible for the high Ni^{2+} concentration relaxation. The bulk Ni^{2+} ion distribution on the spin labeled A25C mutant coat protein side of the bilayers, however, is complex as discussed above. The exclusion of the bulk Ni^{2+} ions is the main reason for the low apparent accessibility at higher Ni^{2+} concentrations. It is clear from the low accessibility to bulk Ni^{2+} ions, however, that this spin label cannot be located in the aqueous phase, but it is likely to be positioned in the membrane interfacial region.

The nitroxide spin label covalently attached to the mutant coat protein G38C shows the smallest relaxation enhancement by Ni^{2+} ions, which is consistent with its location in the hydrophobic core. It is notable, however, that the oxygen accessibility is rather low. This mutant shows a tendency to aggregate by partially forming β-sheet structures. It is therefore possible that oxygen is excluded from collisions with those spin labels that are tightly packed within the protein aggregate [cf. Altenbach et al. (1990)]. Overall, the asymmetry in the profile of oxygen accessibility (Fig. 5) may arise to some extent from local sequence-specific effects such as are evident in the modulation of the increasing side-chain mobility from the N- to the C-terminal in Fig. 2. Comparison of these two figures suggests that a locally low mobility (i.e., high value of A_{max}) correlates with a high value of oxygen accessibility and vice-versa. This alternation in ΔA_{max} and $\Delta(1/T_1)$ has a roughly helical periodicity, and examination of a helical wheel reveals clustering of large and hydrophobic side chains close to the face containing spin labels with high values of A_{max} and oxygen-induced relaxation enhancements. The one exception to this is the low oxygen accessibility of spin-labelled mutant A25C, for which other possible origins have already been discussed.

In general, the relaxation enhancements of the spin-labelled major coat protein mutants by oxygen are lower than those for the calibration set of spin-labelled phospholipids in the hydrophobic region. The two spin-labelled systems may not be comparable directly in quantitative terms because of the higher mobility of the spin-labelled lipids. However, the 2-fold difference in efficiency of oxygen-induced relaxation suggests that the spin-labelled coat proteins may be associated to some extent in the lipid membranes, hence reducing the accessibility to oxygen. Effective rotation correlation times estimated from isotropic calibrations of the ST-ESR spectra for the mutant that shows the least mobility on the conventional ESR time scale (A25C) are in the region of 5-15 μs. The correlation times for uniaxial rotation, $\tau_{R//}$, are maximally half this value, assuming that the most probable orientation of the spin label is perpendicular to the rotation axis (Marsh & Horváth, 1989).

Hydrodynamic calculations, however, suggest rotational correlation times of $\tau_{R//} \sim 0.1\text{-}0.2$ μs for a transmembrane α-helical monomer with membrane viscosities in the range 2.5-5 P (Marsh & Horváth, 1989). Although the rotational diffusion will be further hindered by the surface interactions of the amphipathic N-terminal helix (Wolkers et al., 1997), this comparison suggests that a limited reversible association of the transmembrane helices does occur.

The very efficient relaxation induced by the spin-labelled mutants at low Ni^{2+} concentrations (Fig. 4) strongly suggests specific binding of Ni^{2+} to the protein. The enhancement is greatest for the A25C mutant (see Fig. 7), which indicates that the metal ion site is situated in the N-terminal domain. There are five negative charges in the major coat protein: four in the N-terminal arm, Glu2, Asp4, Asp5, Glu20, and one at the terminal COOH group. These may act as binding sites for the positively charged Ni^{2+} ions. Estimates of the distance of these sites from the spin label by using the Solomon-Bloembergen equation [see. e.g., Marsh (1992); Páli et al. (1992)] give values of ca. 11 Å for the spin label on mutant A25C and ca. 15 Å for the spin label on mutant G31C. This would favor Glu20 as being one of the residues associated with Ni^{2+} ion binding. The relatively large enhancement found for the spin-labelled mutant A49C (Fig. 7) probably arises from a random transmembrane orientation of the coat protein in the reconstituted membrane. This could allow the C-terminal to come into close proximity at the membrane surface with the N-terminal domain of an adjacent protein.

Conclusions

The location of the site-specific major coat protein mutant agents in the phospholipid bilayer, as determined by paramagnetic relaxation, is indicated schematically in Fig. 8. Amino acid residues 25 and 46 are located in the lipid head group region at the membrane-water interface. A short part of the C-terminus (three to four amino acid residues) extends into the aqueous phase. This transmembrane topography is in agreement with a parallel study on fluorescence-labelled major coat protein mutants (Spruijt et al., 1996). Such a membrane location inevitably leaves the α-carbons of Lys40, Lys43, and Lys44 in the membrane interior. The distance between residues 25 and 46 is 31.5 Å in an α-helical conformation, which is compatible with the thickness of a DOPC bilayer of 36 Å as measured by X-ray diffraction (Gruner et al., 1988). The location of the Ni^{2+} binding site in the N-terminal amphipathic helix positions this at the membrane surface. Local sequence-specific effects are consistent with the α-helical structure. The lower oxygen accessibility for protein membrane spin-labels compared with the spin-labeled lipids suggests a

reversible hydrophobic association of the proteins in the membrane.

References

Altenbach, C., Flitsch, L. S., Khorana, G. H., & Hubbell, W. L. (1989) *Biochemistry 28*, 7806-7812.

Altenbach, C., Marti, T., Khorana, H. G., & Hubbell, W. L. (1990) *Science 248*, 1088-1092.

Altenbach, C., Greenhalgh, D. A., Khorana, H. G., & Hubbell, W. L. (1994) *Proc. Natl. Acad. Sci. U.S.A . 91*, 1667-1671.

Asbeck, F., Beyreuther, K., Kohler, H., Wettstein, G., & Braunitzer, G. (1969) *Physiol. Chem. 350*, 1047.

Bales, B. L. (1989) in *Biological Magnetic Resonance-Spin Labeling Theory and Applications* (Berliner, L.J., & Reuben, J., Eds.) pp 77-130, Plenum Press, New York and London.

Fajer, P., & Marsh, D. (1982) *J. Magn. Reson. 49*, 212-224.

Gruner, S. M., Tate, M. W., Kirk, G. L., So, P. T. C., Turner, D. C., Keane, D. T., Tilcock, C. P. S., & Cullis, P. R. (1988) *Biochemistry 27*, 2853-2866.

Hemminga, M. A., De Jager, P. A., Marsh, D., & Fajer, P. (1984) *J. Magn. Reson. 59*, 160-163.

Horváth, L. I., & Marsh, D. (1983) *J. Magn. Reson. 54*, 363-373.

Hubbell, W. L., Mchaourab, H. S., Altenbach, C., & Lietzow, M. A. (1996) *Structure 4*, 779-783.

Marsh, D. (1981) Mol. Biol. Biochem and Biophys., *31* 51-142.

Marsh, D. (1992) *Appl. Magn. Reson. 3*, 53-65.

Marsh, D. (1994) in *Electron Spin Resonance, Specialist Periodical Reports* (Atherton, N. M., Davies, M. J., & Gilbert, B. C., Eds.) Vol. 14, pp 166-202, The Royal Society of Chemistry, Cambridge.

Marsh, D. (1995a) *Spectrochim. Acta A51*, L1-L6.

Marsh, D. (1995b) *J. Magn. Reson. A114*, 248-254.

Marsh, D., & Horváth, L. I. (1989) in *Advanced EPR. Applications in Biology and Biochemistry* (Hoff, A. J., Ed.) pp 707-752, Elsevier, Amsterdam.

Marsh, D., & Watts, A. (1982) in *Lipid-Protein Interactions* (Jost, P. C., & Griffith, O. H., Eds.) Vol. 2, pp 53-156, Wiley-Interscience, New York.

Marvin, D. A., Hale, R. D., Nave, C., & Citterich, M. H. (1994) *J. Mol. Biol. 235*, 260-286.

McDonnell, P. A., Shon, K., Kim, Y., & Opella, S. J. (1993) *J. Mol. Biol. 233*, 447-463.

Nambudripad, R., Stark, W., Opella, S. J., & Makowski, L. (1991) *Science 252*, 1305-1308.

Páli, T., Bartucci, R., Horváth, L. I., & Marsh, D. (1992) *Biophys. J. 61*, 1595-1602.

Páli, T., Horváth, L. I., & Marsh, D. (1993) *J. Magn. Reson. A54*, 363-373.

Snel, M. M. E., & Marsh, D. (1993) *Biochim. Biophys. Acta 1150*, 155-161.

Snel, M. M. E., De Kruijff, B., & Marsh, D. (1994) *Biochemistry 33*, 11150-11157.

Spruijt, R. B., Wolfs, C. J. A. M., & Hemminga, M. A. (1989) *Biochemistry 28*, 9159-9165.

Spruijt, R. B., Wolfs, C. J. A. M., Verver, J. W. G., & Hemminga, M. A. (1996) *Biochemistry 35*, 10383-10391.

Stopar, D., Spruijt, R. B., Wolfs, C. J. A. M., & Hemminga, M. A. (1996) *Biochemistry 35*, 15467-15473.

Subczynski, W. K., & Hyde, J. S. (1983) *Biophys. J. 41*, 283-286.

Subczynski, W. K. & Hyde, J. S. (1984) *Biophys. J. 45*, 743-748.

Thomas, D. D., Dalton, L. R., & Hyde, J. S. (1976) *J. Chem. Phys. 65*, 3006-3024.

Turner, R. J., & Weiner, J. H. (1993) *Biochim. Biophys. Acta 1202*, 161-168.

Van de Ven, F. J. M., Van Os, J. W. M., Aelen, J. M. A., Wymenga, S. S., Ramerowski, M. L., Konings, R. N. H., & Hilbers, C. W. (1993) *Biochemistry 32*, 8322-8328.

White, S. H., & Wimley, W. C. (1994) *Curr. Opin. Struct. Biol. 4*, 79-86.

Williams, K. A., Farrow, N., Deber, C. M., & Kay, L. E. (1996) *Biochemistry 35*, 5145-5157.

Wolkers, W. F., Spruijt, R. B., Kaan, A., Konings, R. N. H., & Hemminga, M. A. (1997) *Biochim. Biophys. Acta 1327*, 5-16.

Chapter 6

Summarizing Discussion

During the infection process the major coat protein of bacteriophage M13 is reconstituted in the cytoplasmic membrane of the *Echerichia coli*. To specifically monitor the local structural changes and changes in the environment of the major coat protein that allow the protein reconstitution in a membrane environment, a set of cysteine site-specific mutants of the major coat protein was produced for spin and/or fluorescence labeling.

The general features of phage particle disassembly, whereby the phage coat is inserted in the cytoplasmic membrane and DNA is released in the cytoplasm, are well documented. The molecular details of this process are described in chapter 2, using spin or fluorescence labeled mutant phage particles, disrupted in different membrane-mimicking systems. The very tight phage particle structure was disrupted only with the strong ionic detergents SDS and CTAB, but was not affected by either lipids or nonionic detergents. On the other hand, upon a chloroform-induced transformation of the filamentous phage particle to the S-form, the major coat protein was completely solubilized with both ionic and nonionic detergents, as well as with lipids. It is a remarkable finding that the major coat protein can change its conformation to accommodate three distinctly different environments: phage filament, S-form, and membrane bound form. The results also indicate that during conversion from filament phage to S-form and subsequently to a membrane bound-form, the protein undergoes pronounced changes in environment, and in response the α-helical content decreases, and the local structure changes dramatically.

The tight architecture of the virus coat reveals that in order to get optimal DNA binding and hydrophobic interactions along the filament long axis, the neighbouring proteins are shifted relative to each other for 1.6 nm, forming a "structural dimer". Because the "structural dimer" is not disrupted during solubilization with sodium cholate, a weak detergent, the hydrophobic interactions between proteins in the "structural dimer" could be studied (chapter 3). The ESR spectra of spin-labeled A49C major coat protein mutant clearly show the presence of a second strongly immobilized component in the "structural dimer", which was absent from the spectra only when the pH of the samples was increased from pH 7.0 to pH 10.0. This was an irreversible step suggesting a major structural change resulting in the "structural dimer" disruption. The same type of protein behavior was observed when the protein dimer was reconstituted in lipid bilayers. The results show that the major coat

95

protein monomer is stable in a membrane environment, and does not have a tendency to aggregate. Since the major coat protein has to aggregate to form a protective coat around viral DNA, these results indicate that lipids should be removed first at the assembly site, before the major coat protein can aggregate in a new virus coat.

The pertinent questions once the major coat protein is reconstituted in different membrane mimicking environments are: how does the major coat protein structure accommodate to different membrane environments, and is the protein structure in the micelles representative for the structure in lipid bilayers. Because technical limitations of high-resolution NMR or X-ray crystallography do not permit one to compare the major coat protein structure in micellar and lipid bilayer model systems, site-directed spin labeling ESR spectroscopy was employed in chapter 4. To allow a stable association with different membrane-mimicking systems, the local structure of the major coat protein changed significantly, but surprisingly the major structural elements such as α-helix content was largely retained. The results also indicate that the transmembrane domain of the major coat protein in the lipid bilayers was shifted toward the C-terminus of the protein up to Thr46. This means that almost the full length of the C-terminus is embedded in the bilayer.

A direct consequence of this finding is that the positively charged Lys40, Lys43 and Lys44 are buried in the membrane. To test this finding, a detailed location of the spin-labeled major coat protein mutants reconstituted in lipid bilayers was determined by paramagnetic relaxation agents (chapter 5). The section of the major coat protein around Thr36 is situated in the centre of the membrane. Amino acid residues 25 and 46 are located in the lipid head group region at the water-membrane interface, with only a short part of the C-terminus (three to four amino acid residues) extending into the aqueous phase. This transmembrane topology inevitably leaves the α-carbons of Lys40, Lys43 and Lys44 in the membrane interior, while the ϵ-amino group of the lysine side chains probably interacts with the large excess of phosphates in the lipid head groups.

Tentative Model

The results obtained in this thesis can be summarised in the following tentative model, describing distinct conformational states of the major coat protein of bacteriophage M13, caused by adaptation to different environments, during the infection process. It is assumed in the following simple model that changes in protein environment alone, are able to trigger structural changes.

(1)   (2)   (3)

N-terminus

C-terminus
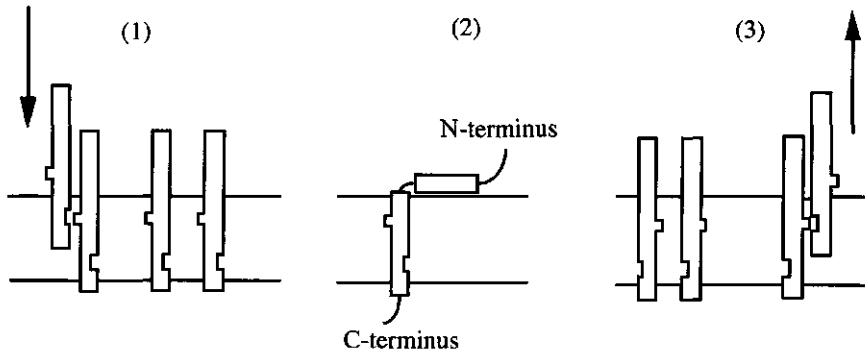
Schematic model of the involvement of the coat protein in virus assembly and disassembly: (1) *Disassembly of the phage particle*; to get an optimal protein-lipid interaction, the disassembling virus particle moves in steps of 1.6 nm into the plane of the membrane as indicated by the arrow. The step of 1.6 nm is equal to a distance between neighbouring proteins in the structural dimer. The major coat protein forms almost a continuos α-helix in the phage particle. Knobs and holes represent protein-protein interactions in the phage particle. The two horizontal lines indicate the headgroup boundaries of the lipid bilayer. (2) *Membrane-bound form of the major coat protein*; the protein undergoes a major structural change from a single continuos helix in the phage particle to a transmembrane helix and an amphiphatic helix. The C and N-terminus are not structured. (3) *Assembly of the new phage particle*; extrusion of the newly phage through the membrane and addition of the coat protein is regulated in such a way that the extruding phage moves 1.6 nm out of the plane of the membrane before the next coat protein is added. This allows optimal side-chain interlocking between neighbouring proteins in the virus particle.

The major coat protein in the phage particle makes a stable coat cylinder around the DNA. The protein in the filament phage particle forms a continuos helix aligned approximately along the filamentous axis. When major coat protein is brought into contact with the cytoplasmic membrane it is, due to the inherent instability of the phage coat in the presence of amphiphiles, solubilized in the membrane, presumably without an extra requirement of host energy. This is probably taking place in a stepwise manner, whereby the disassembling virus particle moves 1.6 nm into the plane of the membrane, a distance between neighbouring proteins in the phage particle, as depicted in a schematic model. This provides optimal hydrophobic interactions between the protein and the host membrane for protein solubilization. Complete solubilization of the protein in the membrane is probably enhanced by locally increased pH values. The major coat protein is solubilized in the cytoplasmic membrane as a monomer with two helices; a transmembrane helix and an

97

amphiphatic helix that are perpendicular to each other, and connected by a short flexible loop. The amphiphatic helix determines the protein position at one side of the membrane, while the lysines and phenylalanines serve as hydrophilic and hydrophobic anchors, respectively, at the other side of the bilayer. In addition, the effective neutralization of the lysines ε-amino groups by the high molar excess of phosphates in the proximal lipid head groups provides a protection of the lysine charges during storage in the cytoplasmic membrane. The major coat protein, however, can interact with the viral DNA when it is released from the phospholipids by the virus assembly machinery. Such a lipid free protein monomer interacts electrostatically with the viral DNA, and hydrophobically with the coat protein previously added to the elongating phage particle. During this process the transition from two helices in the membrane bound form to a single helix in the virus particle is taking place. To obtain the final side-chain interlocking in the virus particle, extrusion of the newly phage through the membrane and addition of the coat protein must be correlated in such a way that the extruding phage moves 1.6 nm out of the plane of the membrane before the next coat protein is added.

Summary

This thesis describes the results of a spectroscopic study of the major coat protein of bacteriophage M13. During the infection process this protein is incorporated into the cytoplasmic membrane of *Escherichia coli* host cells. To specifically monitor the local structural changes and changes in the environment of the protein upon membrane insertion, a set of cysteine site-specific mutants of protein was produced for the purpose of ESR spin labeling and fluorescence spectroscopy. These spectroscopic techniques, in combination with CD spectroscopy, are particularly suitable for comparison of protein structural changes in different membrane model systems. The spectroscopic experiments indicate that the very tight structure of the phage particle was disrupted only with strong ionic detergents, such as SDS and CTAB. However the phage structure was not affected by either lipids or nonionic detergents. On the other hand, after a chloroform-induced transformation of the filamentous phage particle into the S-form, the major coat protein was completely solubilized under these conditions. Upon solubilization of the phage particle in sodium cholate at low pH, a protein "structural dimer" appeared to be the most stable aggregate. This structural dimer, in which the protein subunits that are slightly shifted with respect to each other, is proposed to play a key role in the assembly and disassembly of the phage particle *in vivo*. However, when completely solubilized in the membrane, the major coat protein is stable in a monomer state, and does not have a tendency to aggregate. Site-directed ESR spin labeling was found to be a useful technique to compare the protein structure and topology in micellar and lipid bilayer model systems. To allow a stable association with different membrane model systems, the local structure of the major coat protein changed significantly, but surprisingly the major structural elements, such as the α-helix content, are largely retained. The detailed topology of the major coat protein in lipid bilayers was determined by using Ni^{2+} quenchers with the spin-labeled mutants. The results show that the part of the major coat protein around amino acid residue Thr36 is situated in the centre of the membrane. Amino acid residues 25 and 46 are located in the lipid head group region at the two water-membrane interfaces, with only a short part of the C-terminus (three to four amino acid residues) extending into the aqueous phase. This transmembrane topology leaves the α-carbons of Lys40, Lys43, and Lys44 in the membrane interior, while the ϵ-amino groups of the lysine side chains probably interact with the large excess of phosphates in the lipid head groups. Since the major coat protein has to aggregate to form a protective coat around viral DNA, these results indicate that lipids should be removed first at the assembly site, before the major coat protein can interact with DNA to form a new virus coat.

Samenvatting

Dit proefschrift beschrijft de resultaten van een spectroscopische studie van het mantel-eiwit van de bacteriofaag M13. Tijdens de infectieprocessen wordt dit eiwit geïncorporeerd in het cytoplasmatische membraan van de *Escherichia coli* gastheercellen. Om specifiek de lokale structuur en veranderingen in de omgeving van het eiwit te volgen tijdens membraan-insertie, is via plaatsgerichte mutagenese een serie cysteïnemutanten van het eiwit gemaakt voor de toepassing van ESR-spinlabeling en fluorescentiespectroscopie. Deze spectroscopi-sche technieken zijn, in combinatie met circulair dichroïsmespectroscopie, bijzonder geschikt om de structuurveranderingen van het eiwit in verschillende membraanmodelsys-temen te vergelijken. De spectroscopische experimenten geven aan dat de zeer compacte structuur van het faagdeeltje door sterke ionische detergentia, zoals SDS en CTAB, uiteen kan worden gescheurd. De faagstructuur wordt echter niet aangetast door lipiden of niet-ionische detergentia. In tegenstelling tot het voorgaande wordt het manteleiwit volledig gesolubiliseerd onder deze condities na een chloroformgeïnduceerde overgang van het faagdeeltje in de S-vorm. Na solubilisatie van het faagdeeltje bij lage pH in natriumcholaat wordt een "structureel dimeer" gevormd als het meest stabiele aggregaat. Dit dimeer, waarin de eiwitsubeenheden enigszins ten opzichte van elkaar zijn verschoven, speelt een sleutelrol in de assemblage en disassemblage van het faagdeeltje *in vivo*. Echter, een stabiele monomeertoestand van het eiwit is aanwezig, zonder neiging tot aggregatie, wanneer het manteleiwit volledig in het membraan is gesolubiliseerd. Plaatsgerichte ESR-spinlabeling blijkt een geschikte techniek om de eiwitstructuur en -topologie in micellaire en lipidemodel-systemen te vergelijken. De lokale structuur van het manteleiwit verandert aanzienlijk om een stabiele vereniging met verschillende membraanmodelsystemen mogelijk te maken, maar het is verassend dat de grote structuurelementen, zoals de α-helixstructuur, in grote mate behouden blijven. De gedetailleerde topologie van het manteleiwit in lipidedubbellagen werd bepaald door gebruik te maken van Ni^{2+}-ionen met de gespinlabelde mutanten. De resultaten laten zien dat het deel van het manteleiwit rond aminozuurresidu Thr36 is gesitueerd in het midden van het membraan. De aminozuurresiduen 25 en 46 zijn gelokaliseerd in het gebied van de lipidekopgroepen in de twee water-membraangrensvlak-ken, met slechts een klein deel van de C-terminus (drie tot vier aminozuurresiduen) dat uit-steekt in de waterfase. In deze transmembraantopologie zitten de α-koolstofatomen van Lys40, Lys43 en Lys44 binnenin het membraan, terwijl de ϵ-aminogroepen van de lysinezijketens waarschijnlijk een interactie aangaan met de grote overmaat van fosfaten in de lipidekopgroepen. Omdat het manteleiwit moet kunnen aggregeren om een beschermende mantel te vormen om het virale DNA, geven deze resultaten aan dat de lipiden eerst van de assemblageplaats verwijderd moeten worden, voordat het manteleiwit een interactie aan kan gaan met het DNA voor de vorming van een nieuwe virusmantel.

Curriculum vitae

David Stopar was born on 14 May 1967 in Sempeter pri Novi Gorici, Slovenia. In 1992 he graduated in agriculture at the Ljubljana University, Slovenia. In 1995 he received his MSc degree in microbiology at the Ljubljana University, Slovenia. From 1995 to 1997 he carried out his PhD study at the Department of Molecular Physics at the Wageningen Agricultural University, The Netherlands. From September 1997 he works as a researcher at Ljubljana University, Slovenia.